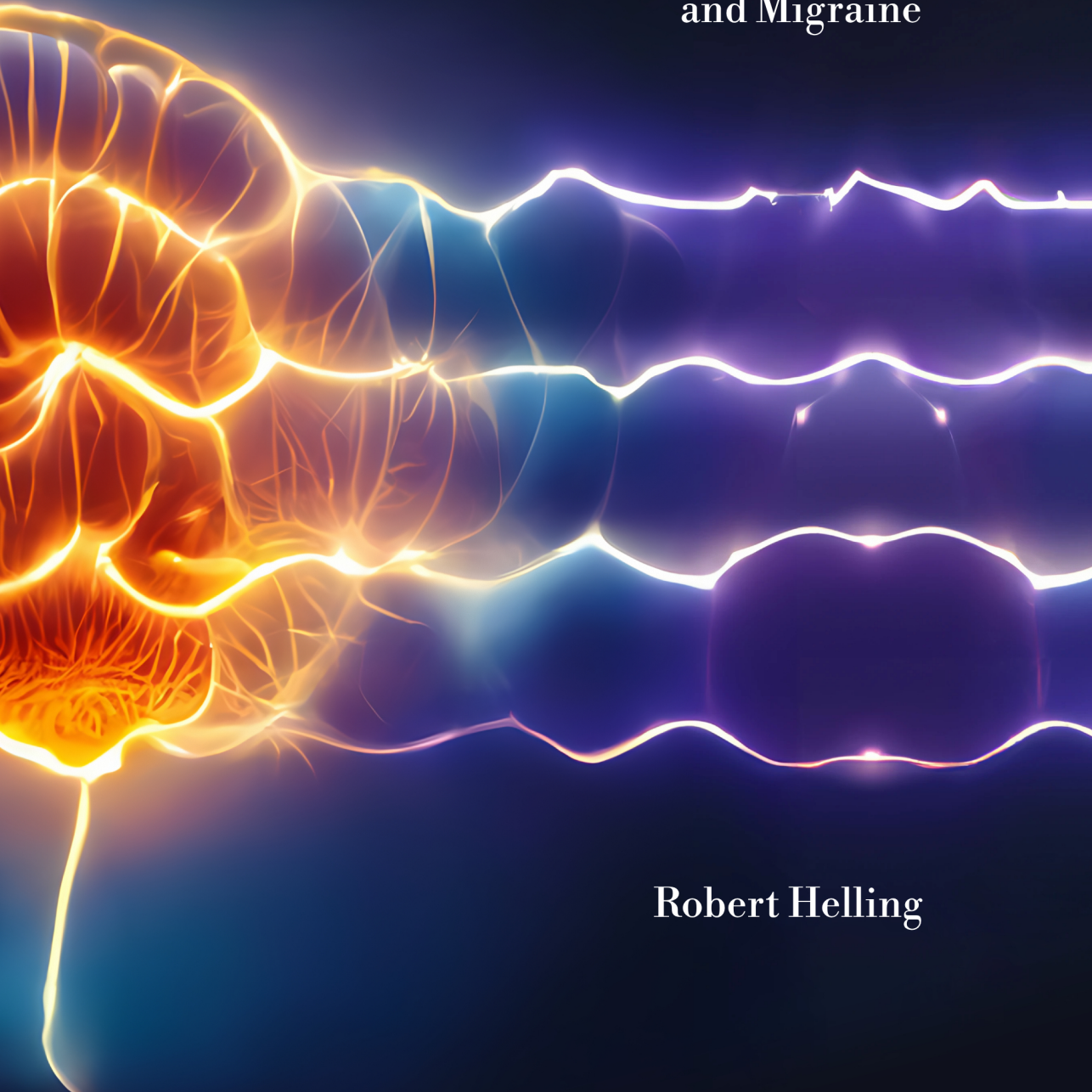


# Brainwaves and Breakdowns

Tracking Brain Dynamics in Epilepsy  
and Migraine



Robert Helling



# Brainwaves and Breakdowns - Tracking Brain Dynamics in Epilepsy and Migraine

Robert Martijn Helling

© Robert Helling, 2023

All rights reserved. No part of this publication may be reproduced or transmitted in any form or by any means, without permission in writing from the copyright holder. The copyright of the articles that have been accepted for publication or that have already been published, has been transferred to the respective journals.

The research in this thesis was performed at Stichting Epilepsie Instellingen Nederland, Heemstede, The Netherlands.

This work is funded by the ‘Christelijke Vereniging voor de Verpleging van Lijders aan Epilepsie’. Chapter 6 is funded by an unrestricted grant of EISAI, the manufacturer of perampanel. Chapter 7 is funded by grants of the Dutch National Epilepsy Fund (EpilepsieNL) and Health Holland [Project number: 15/10]; and the Netherlands Organization for Health Research and Development (ZonMW) [Brain@home, Project number: 114025101].

Printed by: ProefschriftMaken

ISBN: 978-94-6469-490-1

Design and layout: Robert Helling

Cover: © Midjourney, 2022, image adapted for this thesis and used under the Creative Commons Attribution-Noncommercial 4.0 International License (CC BY-NC 4.0).

A catalogue record is available from the Utrecht University Library.

# **Brainwaves and Breakdowns – Tracking Brain Dynamics in Epilepsy and Migraine**

**Hersengolven en Verstoringen – Volgen van de  
Hersendynamiek in Epilepsie en Migraine**

(met een samenvatting in het Nederlands)

## **Proefschrift**

ter verkrijging van de graad van doctor aan de Universiteit Utrecht  
op gezag van de rector magnificus, prof.dr. H.R.B.M. Kummeling,  
ingevolge het besluit van het college voor promoties  
in het openbaar te verdedigen op  
dinsdag 12 september 2023 des middags te 2.15 uur

door

Robert Martijn Helling

geboren op 23 november 1988 te Amsterdam

**Promotor:**

Prof. dr. ir. M.A. Viergever

**Copromotoren:**

Dr. G.H. Visser

Dr. S.N. Kalitzin

**Beoordelingscommissie:**

Prof. dr. R.M. Dijkhuizen

Prof. dr. S.A. van Gils

Prof. dr. A.M.J.M. van den Maagdenberg

Prof. dr. N.F. Ramsey

Prof. dr. G.J.M. Zijlmans

Dit proefschrift werd (mede) mogelijk gemaakt met financiële steun van de Christelijke Vereniging voor de Verpleging van Lijders aan Epilepsie.

# Contents

<b>Chapter 1</b>	General introduction	7
<b>Chapter 2</b>	Gap junctions as common cause of high-frequency oscillations and epileptic seizures in a computational cascade of neuronal mass and compartmental modelling	21
<b>Chapter 3</b>	Expert system for pharmacological epilepsy treatment prognosis and optimal medication dose prescription	47
<b>Chapter 4</b>	TMS-evoked EEG potentials demonstrate altered cortical excitability in migraine with aura	63
<b>Chapter 5</b>	Phase clustering in transcranial magnetic stimulation-evoked EEG responses in genetic generalized epilepsy and migraine	95
<b>Chapter 6</b>	Cortical excitability before and after long-term perampanel treatment for epilepsy	127
<b>Chapter 7</b>	Tracking cortical excitability dynamics with transcranial magnetic stimulation in focal epilepsy	147
<b>Chapter 8</b>	General discussion	171
	List of acronyms	186
	List of definitions	190
	Summary and Appendices	
	Summary	196
	Nederlandse samenvatting   Dutch summary	200
	List of publications	206
	Dankwoord   Acknowledgements	207
	Biography	209



# Chapter 1

General introduction



## 1.1 Epilepsy and migraine

The brain is a highly complex network of connections between 10 billion neurons and about 60 trillion synapses that mediate communication between neurons through neurotransmitters.<sup>1</sup> All these interneuronal connections can be regarded as components in a complex system of circuits that are the substrate of voluntary and automatic behaviour, including cognition, visceral regulation, emotion, and abstract reasoning.

Epilepsy is a common and disabling brain condition characterized by a lasting susceptibility to spontaneous epileptic seizures.<sup>2,3</sup> With a prevalence of more than 50 million people worldwide, it's one of the most prevalent neurological disorders.<sup>4</sup> Epileptic seizures are sudden transient events where normal brain functioning is disrupted through abnormal, excessive and hypersynchronous neuronal activity.<sup>5</sup> The abnormal seizure activity stops effective communication between involved brain regions and networks. The highly stereotypical clinical and electroencephalographic (EEG) manifestations that are observed in seizures reflect the cortical areas and networks of the brain affected by the seizure activity. Clinical manifestations may include impaired awareness, changes in cognitive function (e.g. memory loss) and behaviour, as well as abnormal motor and sensory function.<sup>6</sup> These seizures occur seemingly randomly and in many people with epilepsy long periods may pass without any symptoms.<sup>2</sup> Both the physical and psychosocial consequences associated with unpredictable seizures can have major impact on everyday activities and quality of life.<sup>7,8</sup> The study of the physiology and underlying biological mechanisms of these synchronized events is crucial for understanding the causes of epilepsy and developing effective treatments.

Migraine is a type of brain disorder that affects around 1.3 billion people worldwide.<sup>9</sup> It is more common in women than in men, occurring 3 to 4 times more frequently in women. Migraine attacks are characterized by severe, throbbing, unilateral headaches that can last for 4 to 72 hours, often accompanied by symptoms such as nausea, vomiting, and sensitivity to sensory stimuli.<sup>10</sup> In some cases, individuals with migraines may also experience an aura, which is a temporary neurological symptom that can involve visual, tactile,

motor, or speech disturbances.<sup>11</sup> Auras may occur before or after a headache, or may occur without a headache at all. There is strong evidence for an association between migraine and epilepsy.<sup>12</sup> This finding is consistent with the growing understanding that migraines and epilepsy often occur together (a phenomenon known as comorbidity or multi-morbidity).

## 1.2 Treatment of epilepsy

Reducing the frequency of seizures is essential in the treatment of epilepsy.<sup>13</sup> The primary choice for treatment is anti-seizure medication (ASM). ASMs control epilepsy— either directly or indirectly – by decreasing the amount of excitation, or increasing the amount of inhibition within cortical networks.<sup>14</sup> Approximately 47% of all people with newly diagnosed epilepsy will become seizure free with the first prescribed ASM, and about 63% of people with epilepsy have remission of seizures within the first five years of treatment with the first and subsequent drugs.<sup>15</sup> If the first drug is ineffective at eliminating seizures, the likelihood of remission of seizures in subsequent trials decreases significantly to about 10%, with a further reduction in likelihood of remission with each subsequent drug or combination of drugs.<sup>16</sup> An estimated 20-30% of people with epilepsy do not become seizure free on ASMs and are considered people with refractory epilepsy.<sup>17</sup> This makes epilepsy notoriously difficult to treat and imposes a huge burden on society. Overall, the treatment of epilepsy remains a challenging endeavour, with many patients not responding to initial treatment and a significant decrease in the likelihood of seizure freedom with each subsequent trial of medication.

Despite insight into the underlying biological mechanisms and processes during a seizure,<sup>18–20</sup> there is a large knowledge gap regarding disease monitoring and evaluating treatment response. The initial diagnosis of epilepsy relies almost exclusively on medical history obtained from the patient and from witnesses. The choice for type of ASM and dose finding within a subject is a matter of trial and error, using the seizure diary as a feedback mechanism to determine treatment success. The EEG can be used to monitor cortical activity in the search for epileptiform activity - such as interictal epileptiform discharges

(IEDs) - which can help to accurately diagnose and classify the type of epilepsy.<sup>21,22</sup> The sensitivity and specificity of the EEG however, was recently estimated at approximately 17.4% and 94.7% respectively,<sup>23</sup> indicating that short term monitoring with the EEG can easily miss the transient events by pure chance. Some patients require multiple diagnostic EEGs to capture a single IED, but in 10% of patients multiple recordings do not provide the required information sufficient for diagnosis.<sup>16</sup> Even in the much more elaborate and time-consuming presurgical evaluation, seizure events crucial for delineating the seizure onset zone may not occur. To summarize, diagnosis and treatment of people with refractory epilepsy requires a lot of effort and involves procedures that can take a long time and require patience.

### 1.3 System dynamics and bistable systems

The normal functioning of cortical networks critically depends on a finely tuned level of cortical excitability,<sup>24,25</sup> which is the transient responsiveness to sudden stimuli or steady-state response to ongoing input.<sup>14</sup> If the level of excitability is too low, the brain may not be able to adequately process incoming information and function properly. On the other hand, if the level of excitability is too high, the brain may become overactive and prone to seizures and other abnormal activity. The neuronal state of part of the cortex might be shaped by current ongoing activity as well as by activity of other neuronal structures that project into the given area. A comprehensive understanding of cortical excitability and how to monitor it is crucial for understanding both normal and pathological brain function.<sup>26,27</sup>

Computational models are a valuable tool for testing various dynamic scenarios and gaining insight into the dynamics of epileptic seizures.<sup>28,29</sup> These models must accurately represent phenomena at different levels of biological organization. However, there is always a trade-off between the level of detail included in the model, its computational feasibility, and the interpretability of its results. Compartmental models are detailed models that simulate a small network of neurons at a microscopic level, incorporating the electrophysiology of individual neurons and the synaptic connections between them.<sup>30,31</sup> Neuronal mass models (NMMs), on the other hand, simulate the behaviour of populations

of cells at a more macroscopic level and are effective in describing brain rhythms as measured by the EEG.<sup>28</sup> Given a macroscopic architecture that describes the overall connectivity between populations, it is possible to simulate the steady-state dynamics of the system. Depending on the parameters of the model and its initial conditions, different types of behaviour can be observed. The model can be in a steady state, representing normal behaviour, or in a limit cycle, representing an epileptic seizure or ictal state.<sup>28,29</sup> Additionally, the system can have a third state where both types of behaviour exist, the bistability region. Due to internal noise fluctuations within the system or external perturbations applied to it, the behaviour of the model can alternate between the steady state and limit cycle. By varying one or more control parameters, the impact of these fluctuations and perturbations on system behaviour can be explored. This allows computational models to be used for investigating, predicting, and even controlling the behaviour of complex systems.<sup>32</sup>

A stable equilibrium losing its stability - as a slowly varying control parameter passes some critical value (tipping point) - may cause a sudden and significant change in a system, known as a critical transition.<sup>33</sup> A system close to a tipping point can exhibit certain dynamic characteristics. As a system approaches a critical transition, it becomes increasingly sensitive to perturbations and shows a slower recovery from them. This phenomenon, known as critical slowing down, can be used as a marker for seizure susceptibility.<sup>34</sup> By investigating a system's response to perturbations, it is possible to determine if it is undergoing critical slowing down and approaching a critical transition. This information can provide valuable insight into the dynamics of the system and the likelihood of a critical transition occurring.

## 1.4 Transcranial Magnetic Stimulation

Transcranial magnetic stimulation (TMS) is a technique used to directly stimulate the cortex of the brain in a non-invasive manner.<sup>35</sup> A TMS device consists of a stimulator – essentially a large bank of powerful capacitors capable of holding a strong electrical charge – and a coil – a series of coils of copper wire encased in a plastic shell. When the device is discharged, charge very briefly flows through the coil. This change in electric potential produces a very short-lasting,

but very strong magnetic field on the order of 1-2 Tesla. When a TMS coil is discharged in the vicinity of nerve tissue, the short last-lasting magnetic field can induce action potentials in the underlying tissue. The depolarization of the underlying tissue depends on several factors such as the distance between coil and tissue, the angle of the coil relative to the axon, and the specific geometry of the coil. The induced magnetic field depends on the coil configuration, a single coil results in a relatively diffuse magnetic field underneath the coil. Two coils in a figure-of-eight configuration creates a 'hotspot' where the induced magnetic field is strongest below the midpoint of the coil. This type of coil generally is used to focally stimulate a region of neocortex.

TMS has opened the possibility to assess cortical excitability safely and non-invasively in humans. The effect of TMS is most frequently assessed by stimulating the motor system while assessing the induced contraction of the target muscle with the electromyogram (EMG).<sup>36,37</sup> The muscle twitch is quantified by its electrical response - the motor evoked potential (MEP). In the context of studies of motor cortex excitability TMS is often applied in single stimuli (single pulse TMS; spTMS), or in pairs of stimuli (paired pulse TMS; ppTMS) where a conditioning stimulus and test stimulus are given with a short time interval in-between.<sup>37,38</sup> The resting motor threshold (rMT) is defined as the minimal stimulation intensity required to produce an MEP response with a peak to peak amplitude above a certain threshold.<sup>39</sup> The rMT is generally considered as a measure of global excitability of the corticospinal system. Many types of ASMs either directly or indirectly influence membrane excitability of motor neurons. ASMs that block the voltage gated sodium channels, or open the potassium channels, are known to increase rMT. The combination of pairs of stimuli with ppTMS has been shown to be a useful tool for examining underlying excitatory and inhibitory circuits. The conditioning stimulus typically enhances or attenuates the evoked response of the test stimulus – thought to reflect the magnitude of regional inhibitory or excitatory neurons - depending on the interstimulus interval (ISI). The ratio of the conditioned response to the unconditioned response is typically used as the outcome measure. Overall, TMS has provided a valuable tool for safely and non-invasively assessing motor cortex excitability through the use of spTMS and ppTMS.

Measuring the neuronal activity elicited by TMS with EEG is a relative new modality of functional brain mapping.<sup>14,40</sup> Multichannel EEG mapping of cortical responses to TMS and multi-modal stimulation experiments showed that TMS-evoked EEG responses can be reliably recorded over the whole scalp, and that the TMS-EEG technique is suitable for detection of subtle changes in cortical excitability. The TMS-evoked EEG potential (TEP), which is the response averaged over a large number of trials, has a distinctive pattern of positive and negative deflections occurring between 10-400 ms after TMS stimulation.<sup>41</sup> One field in which the TEP has gained traction is the field of pharmaco-EEG.<sup>42-44</sup> Single dose pharmaco-EEG studies involve the administration of a single dose of a drug to a participant and comparing the measurement pre- and post- intake. These studies are useful for examining the acute effects of a drug on brain activity. Single dose pharmaco-EEG studies are used to evaluate the safety and effectiveness of new drugs, as well as to gain insight into their mechanisms of action.<sup>45</sup> By comparing the brain activity of participants before and after drug administration, researchers can identify changes in brain activity that may be related to the drug's effects. Single dose pharmaco-EEG studies are also useful for identifying potential side effects of a drug, as changes in brain activity may be indicative of adverse effects.

## **1.5 The role of Transcranial Magnetic Stimulation in the evaluation of epilepsy**

TMS is of particular interest in the study of epilepsy, as abnormal excitability is at the heart of the disease. It has been used to study cortical excitability,<sup>46</sup> and explore changes in excitation and inhibition in relation to seizures.<sup>47</sup> It has shown promise as a potential tool for evaluating seizure susceptibility and response to treatment. Studies using TMS-EMG have generally found that people with epilepsy have higher baseline measures of cortical excitability compared to healthy controls, and that a positive response to antiepileptic medication is associated with a reduction in motor cortex excitability.<sup>48-50</sup> These results suggest an association between achieving seizure freedom and a significant reduction in measures of cortical excitability, with a normalization towards the healthy control group. It should be noted that most of the research in this field has been

conducted by a single research group, and there is limited literature on the reproducibility of their findings.

TMS-EEG has been used to study the activation patterns in people with epilepsy.<sup>50,51</sup> One study assessed the applicability of TMS-EEG as a tool for differentiating people with genetic generalized epilepsy from controls and responders from non-responders.<sup>52</sup> However, research in this area is still in the early stages, and further studies are needed to fully understand the utility of TMS-EEG in the evaluation of epilepsy. There have not yet been longitudinal studies in people with epilepsy where TMS was combined with EEG to evaluate long-term effects of ASM treatment.

## 1.6 Thesis outline

In this thesis we present the results of seven studies, each designed to explore and/or investigate potential biomarkers of epilepsy and migraine.

In **Chapters 2 and 3**, we investigate the epileptogenicity of computational models with connected excitatory and inhibitory neuronal populations while varying either the connectivity between the populations (nodes) or their properties as control parameters. In **Chapter 2**, we use a cascade of different types of computational models to better understand the relationship between two epileptic phenomena – HFOs and seizures. We show that the addition of gap junctions can generate HFOs in the microscopic compartmental model, while simultaneously shifting the operational point of the higher-level NMM - from a steady state - into bistable behaviour that can autonomously generate seizures. In **Chapter 3**, we continue with a combined clinical and modelling study and we assess epileptogenicity within people with epilepsy from resting state EEG measurements using the aggregated functional connectivity as a critically important measure that reflects the E:I balance. We demonstrate that it is possible to assess the epileptogenicity of the stimulated networks with high accuracy from the MFC measure inferred from RS-EEG segments. The methodology was validated in a small dataset, which included responders, non-responders and negative responders to ASM treatment.

In the next four chapters, we explore the use of perturbations, such as photic stimulation and direct cortical activation with TMS, in the paroxysmal disorders of epilepsy and migraine. **Chapter 4** focusses on exploring spTMS time-amplitude responses in people with migraine, another paroxysmal disorder, when compared with matched healthy controls to better understand migraine pathophysiology and its comorbidity with epilepsy. This study provides evidence of altered cortical responses in-between attacks in people with migraine with aura. Peak amplitude differences and reduced response consistency are in line with reduced cortical inhibition and expand observations on cortical excitability from earlier migraine studies using more indirect measurements. **Chapter 5** is focused on analytic quantification of the spTMS and photic stimulation evoked responses using phase clustering in people with JME, migraine, and healthy controls. We show that rPCI elicited by TMS and photic stimulation was increased in those with JME on and off medication compared with controls but not in those with migraine with aura. In **Chapter 6**, we present the results of a longitudinal study where people with refractory epilepsy were measured with TMS - in combination with EMG and EEG - and were followed for 6 months after starting with adjuvant non-competitive AMPA-receptor agonist perampanel. After introduction of perampanel, right hemisphere rMT increased significantly. Left hemisphere rMT showed no difference when compared to pre-treatment levels. Notwithstanding the rMT changes, adjuvant perampanel therapy had no significant effects on TMS-evoked EEG peak amplitudes or latencies. In **Chapter 7**, we report the results of serial within-subject measurements in people with epilepsy admitted for presurgical evaluation to the epilepsy monitoring unit (EMU). We show that the occurrence of seizures and the tapering of ASMs had distinct effects on various TMS-EMG measures of excitability.

Finally, in **Chapter 8**, we will conclude with a general discussion of the findings within a wider context.

## References

1. Kandel, E. R., Schwartz, J. H. & Jessell, T. M. Principles of Neural Science, fourth addition. *McGraw-Hill Co.* (2000).
2. Fisher, R. S. *et al.* ILAE Official Report: A practical clinical definition of epilepsy. *Epilepsia* **55**, 475–482 (2014).
3. Fisher, R. S. *et al.* Epileptic seizures and epilepsy: Definitions proposed by the International League Against Epilepsy (ILAE) and the International Bureau for Epilepsy (IBE). *Epilepsia* vol. 46 470–472 (2005).
4. Fiest, K. M. *et al.* Prevalence and incidence of epilepsy. *Neurology* vol. 88 296–303 (2017).
5. Berg, A. T. *et al.* Revised terminology and concepts for organization of seizures and epilepsies: Report of the ILAE Commission on Classification and Terminology, 2005–2009. *Epilepsia* **51**, 676–685 (2010).
6. Thijs, R. D., Surges, R., O'Brien, T. J. & Sander, J. W. Epilepsy in adults. *The Lancet* vol. 393 689–701 (2019).
7. Mula, M. & Sander, J. W. Psychosocial aspects of epilepsy: a wider approach. *BJPsych Open* **2**, 270–274 (2016).
8. Quintas, R. *et al.* Psychosocial difficulties in people with epilepsy: A systematic review of literature from 2005 until 2010. *Epilepsy and Behavior* vol. 25 60–67 (2012).
9. Erratum: Global, regional, and national incidence, prevalence, and years lived with disability for 354 diseases and injuries for 195 countries and territories, 1990–2017: a systematic analysis for the Global Burden of Disease Study 2017 (*The Lancet* (2018) 392(10159) (1789–1858), (S0140673618322797), (10.1016/S0140-6736(18)32279-7)). *The Lancet* (2019)
10. Olesen, J. Headache Classification Committee of the International Headache Society (IHS) The International Classification of Headache Disorders, 3rd edition. *Cephalalgia* (2018) doi:10.1177/0333102417738202.
11. Goadsby, P. J. & Holland, P. R. An Update: Pathophysiology of Migraine. *Neurologic Clinics* (2019) doi:10.1016/j.ncl.2019.07.008.
12. Bauer, P. R., Tolner, E. A., Keezer, M. R., Ferrari, M. D. & Sander, J. W. Headache in people with epilepsy. *Nature Reviews Neurology* (2021).
13. Huerta, P. T. & Volpe, B. T. Transcranial magnetic stimulation, synaptic plasticity and network oscillations. *J. Neuroeng. Rehabil.* **6**, 7 (2009).
14. Bauer, P. R., Kalitzin, S., Zijlmans, M., Sander, J. W. & Visser, G. H. Cortical excitability as a potential clinical marker of epilepsy: A review of the clinical application of transcranial magnetic stimulation. *Int. J. Neural Syst.* **24**, 1430001 (2014).
15. Kwan, P. & Brodie, M. J. Early Identification of Refractory Epilepsy. *N. Engl. J. Med.* **342**, 314–319 (2000).
16. Rosenow, F., Klein, K. M. & Hamer, H. M. Non-invasive EEG evaluation in epilepsy diagnosis. *Expert Review of Neurotherapeutics* vol. 15 425–444 (2015).

17. Rugg-Gunn, F., Sander, J. & Smalls, J. *Epilepsy 2011. From Science to Society. A practical guide to epilepsy. 13th Epilepsy Teaching Weekend, 23-25 September 2011, St. Anne's College, Oxford* (2011).
18. Bal, T. & McCormick, D. A. What stops synchronized thalamocortical oscillations? *Neuron* **17**, 297–308 (1996).
19. Destexhe, A., Babloyantz, A. & Sejnowski, T. J. Ionic mechanisms for intrinsic slow oscillations in thalamic relay neurons. *Biophys. J.* **65**, 1538–1552 (1993).
20. McCormick, D. A. *et al.* Persistent Cortical Activity: Mechanisms of Generation and Effects on Neuronal Excitability. *Cereb. Cortex* **13**, 1219–1231 (2003).
21. De Curtis, M. & Avanzini, G. Interictal spikes in focal epileptogenesis. *Progress in Neurobiology* vol. 63 541–567 (2001).
22. Staley, K. J. & Dudek, F. E. Interictal Spikes and Epileptogenesis. *Epilepsy Curr.* **6**, 199–202 (2006).
23. Bouma, H. K., Labos, C., Gore, G. C., Wolfson, C. & Keezer, M. R. The diagnostic accuracy of routine electroencephalography after a first unprovoked seizure. *European Journal of Neurology* vol. 23 455–463 (2016).
24. Jefferys, J. G. R. Advances in understanding basic mechanisms of epilepsy and seizures. *Seizure* **19**, 638–646 (2010).
25. Avoli, M. & de Curtis, M. GABAergic synchronization in the limbic system and its role in the generation of epileptiform activity. *Progress in Neurobiology* vol. 95 104–132 (2011).
26. Rogawski, M. A. Common pathophysiological mechanisms in migraine and epilepsy. *Arch. Neurol.* **65**, 709–714 (2008).
27. Mantegazza, M. & Cestè, S. Pathophysiological mechanisms of migraine and epilepsy: Similarities and differences. *Neuroscience Letters* vol. 667 92–102 (2018).
28. Suffczynski, P., Kalitzin, S. & Lopes Da Silva, F. H. Dynamics of non-convulsive epileptic phenomena modeled by a bistable neuronal network. *Neuroscience* **126**, 467–484 (2004).
29. Jirsa, V. K., Stacey, W. C., Quilichini, P. P., Ivanov, A. I. & Bernard, C. On the nature of seizure dynamics. *Brain* **137**, 2210–2230 (2014).
30. Huxley, A. F. Hodgkin and the action potential 1935-1952. *J. Physiol.* **538**, 2 (2002).
31. Méla, X. & Petersen, K. *Dynamical properties of the Pascal adic transformation. Ergodic Theory and Dynamical Systems* vol. 25 (2005).
32. Koppert, M., Kalitzin, S., Velis, D., Da Silva, F. L. & Viergever, M. A. Reactive control of epileptiform discharges in realistic computational neuronal models with bistability. *Int. J. Neural Syst.* **23**, 121102031948003 (2013).
33. Dakos, V., Carpenter, S. R., van Nes, E. H. & Scheffer, M. Resilience indicators: Prospects and limitations for early warnings of regime shifts. *Philos. Trans. R. Soc. B Biol. Sci.* **370**, 1–10 (2015).
34. Maturana, M. I. *et al.* Critical slowing down as a biomarker for seizure susceptibility. *Nat. Commun.* **11**, (2020).

35. Barker, A. T., Jalinous, R. & Freeston, I. L. Non-Invasive Magnetic Stimulation of Human Motor Cortex. *The Lancet* vol. 325 1106–1107 (1985).
36. Kobayashi, M. & Pascual-Leone, A. Transcranial magnetic stimulation in neurology. *Lancet Neurol.* **2**, 145–156 (2003).
37. Kujirai, T. *et al.* Corticocortical inhibition in human motor cortex. *J. Physiol.* **471**, 501–519 (1993).
38. Valls-Solé, J., Pascual-Leone, A., Wassermann, E. M. & Hallett, M. Human motor evoked responses to paired transcranial magnetic stimuli. *Electroencephalogr. Clin. Neurophysiol. Evoked Potentials* **85**, 355–364 (1992).
39. Theodore, W. H. Transcranial Magnetic Stimulation in Epilepsy. *Epilepsy Curr.* **3**, 191–197 (2003).
40. Ilmoniemi, R. J. & Kičić, D. Methodology for combined TMS and EEG. *Brain Topogr.* **22**, 233–248 (2010).
41. Ilmoniemi, R. J. *et al.* Neuronal responses to magnetic stimulation reveal cortical reactivity and connectivity. *Neuroreport* **8**, 3537–3540 (1997).
42. Ziemann, U. *et al.* TMS and drugs revisited 2014. *Clin. Neurophysiol.* **126**, 1847–1868 (2015).
43. Premoli, I. *et al.* TMS-EEG signatures of GABAergic neurotransmission in the human cortex. *J. Neurosci.* **34**, 5603–5612 (2014).
44. Conde, V. *et al.* The non-transcranial TMS-evoked potential is an inherent source of ambiguity in TMS-EEG studies. *Neuroimage* **185**, 300–312 (2019).
45. Premoli, I. *et al.* TMS-EEG and TMS-EMG to assess the pharmacodynamic profile of a novel potassium channel opener (XEN1101) on human cortical excitability. *Brain Stimul.* **12**, 459 (2019).
46. Badawy, R. A. B., Curatolo, J. M., Newton, M., Berkovic, S. F. & Macdonell, R. A. L. Changes in cortical excitability differentiate generalized and focal epilepsy. *Ann. Neurol.* **61**, 324–331 (2007).
47. Badawy, R., MacDonell, R., Jackson, G. & Berkovic, S. The peri-ictal state: Cortical excitability changes within 24 h of a seizure. *Brain* **132**, 1013–1021 (2009).
48. Badawy, R. A. B., Macdonell, R. A. L., Berkovic, S. F., Newton, M. R. & Jackson, G. D. Predicting seizure control: Cortical excitability and antiepileptic medication. *Ann. Neurol.* **67**, 64–73 (2010).
49. Badawy, R. A. B., Jackson, G. D., Berkovic, S. F. & MacDonell, R. A. L. Cortical excitability and refractory epilepsy: A three-year longitudinal transcranial magnetic stimulation study. *Int. J. Neural Syst.* **23**, (2013).
50. de Goede, A. A., ter Braack, E. M. & van Putten, M. J. A. M. Single and paired pulse transcranial magnetic stimulation in drug naïve epilepsy. *Clin. Neurophysiol.* **127**, 3140–3155 (2016).
51. ter Braack, E. M., Koopman, A. W. E. & van Putten, M. J. A. M. Early TMS evoked potentials in epilepsy: A pilot study. *Clin. Neurophysiol.* **127**, 3025–3032 (2016).
52. Kimiskidis, V. K. *et al.* TMS combined with EEG in genetic generalized epilepsy: A phase II diagnostic accuracy study. *Clin. Neurophysiol.* **128**, 367–381 (2017).



## Chapter 2

Gap junctions as common cause of high-frequency oscillations and epileptic seizures in a computational cascade of neuronal mass and compartmental modelling

Based on:

**Helling RM**, Koppert MMJ, Visser GH, Kalitzin SN. Gap junctions as common cause of high-frequency oscillations and epileptic seizures in a computational cascade of neuronal mass and compartmental modeling. *International Journal of Neural Systems*. 2015;25(6):1550021.

DOI: 10.1142/S0129065715500215

## **Abstract**

High frequency oscillations (HFO) appear to be a promising marker for delineating the seizure onset zone (SOZ) in patients with localization related epilepsy. It remains, however, a purely observational phenomenon and no common mechanism has been proposed to relate HFOs and seizure generation. In this work we show that a cascade of two computational models, one on detailed compartmental scale and a second one on neural mass scale can explain both the autonomous generation of HFOs and the presence of epileptic seizures as emergent properties. To this end we introduce axonal–axonal gap junctions on a microscopic level and explore their impact on the higher level neural mass model (NMM). We show that the addition of gap junctions can generate HFOs and simultaneously shift the operational point of the NMM from a steady state network into bistable behaviour that can autonomously generate epileptic seizures. The epileptic properties of the system, or the probability to generate epileptic type of activity, increases gradually with the increase of the density of axonal–axonal gap junctions. We further demonstrate that ad hoc HFO detectors used in previous studies are applicable to our simulated data.

## 2.1 Introduction

Epilepsy is a condition in which periods of normal brain functioning are interrupted by intermittent periods of synchronized oscillatory behaviour, i.e. epileptic seizures. The physiology of these synchronized events and the underlying biological mechanisms have been studied in great detail.<sup>1-3</sup> However, the dynamics of transitions to and from these pathological states are not yet fully understood.

High frequency oscillations (HFOs) in cortical neurons are synchronized network oscillations of more than 80 Hz that last for about 100 ms, although definitions vary. While they were first described as physiological oscillations related to memory consolidation in rodents,<sup>4,5</sup> and later in human mesial temporal structures,<sup>6,7</sup> they recently emerged as a new marker for epileptic areas<sup>8</sup>. These pathological ripples occur in epilepsy patients and appear to indicate a propensity of cortical tissue to originate in seizures.<sup>9-11</sup> In physiological situations, firing of a single neuron results in recruitment of interconnected neurons and synchronous firing of action potentials. In pathological situations with changes on a molecular, functional, and morphological level this synchronous firing can be disturbed which may result in HFOs. Considering the speed at which the action potential propagates, any synchronizing mechanisms must synchronize activity within 2–5 ms. The most likely candidates of biological mechanisms behind HFO generation are: (1) electrotonic coupling via gap junctions,<sup>12-15</sup> (2) ephaptic interactions,<sup>16,17</sup> or (3) fast synaptic transmission.<sup>18</sup> It should be emphasized that while there is a correlation between resection of tissue with HFOs and good surgical outcome,<sup>19</sup> i.e. seizure freedom, there is as of yet no causal relationship between the occurrence of HFOs and epileptic seizures.

Computational models are a valuable tool for testing various dynamic scenarios to gain insight into the dynamics of epileptic seizures.<sup>20</sup> Neuronal mass models (NMMs) simulate the behaviour of populations of cells on macroscopic level and are very successful in describing brain rhythms as measured with an electroencephalogram (EEG). Such models can lead to predictions of various emergent dynamical properties of neuronal networks, such as the autonomous

generation of epileptic type of behavior.<sup>21,22</sup> However, modelling of neuronal systems is always limited by the selection of appropriate level of complexity. While the synaptic current is explicitly modelled in NMMs, ion channel electrophysiology is not taken into account. Using realistic parameter values for the GABA and AMPA types of synapses results in a model that only accounts for low frequency oscillations of up to about 20 Hz. The presence of higher frequencies requires inclusion of more complex mechanisms, i.e. the ion channel electrophysiology.

In this study, we aim to investigate the relation between HFO presence in the system dynamics and the ability of the system to generate behaviour resembling epileptic seizures. To study phenomenology at different scales of complexity, we introduce the concept of cascade modelling where two (or in general more) levels of detail or complexity are simultaneously considered. In particular, we investigate the effect of axonal–axonal gap junctions as a common mechanism causing oscillatory behaviour on a microscopic level in a compartmental model with Hodgkin–Huxley type of dynamics and the generation of epileptic seizures at a macroscopic level in an NMM. To this end we use a cascade of two models, one describing the biological reality at ion channel level and another, a NMM that represents the neuronal lump scale of organization. The link between the two scales is provided by inferring parameters of the NMM from the simulations of the detailed, compartmental model as illustrated in Fig. 1. Furthermore, we investigate whether two ad hoc developed HFO detector algorithms, the relative phase clustering index (rPCI) and the autoregressive residual (ARR), could detect the simulated HFOs and whether the detector indices in any way correlate to the state of the axonal network.

## 2.2 Methods

In this work, we use two types of computational neuronal models. A detailed, microscopic model, where individual neurons and connection between these neurons are modelled, and a macroscopic model, where neuronal populations of specific cell types and connections between these populations are described. The parameters of both models are based on known experimental data.<sup>23</sup>

### 2.2.1 Microscopic compartmental model

The microscopic compartmental model consists of a network of 50 axons coupled with gap junctions, illustrated in Fig. 2. Each axon consists of 10 single connected compartments. The single cell compartments are modelled with a Hodgkin–Huxley type of dynamics with voltage gated  $Na^+$  and  $K^+$ -channels and leak currents.<sup>24</sup> For simplicity, the same parameters were chosen for all compartments. The current flowing through the membrane of compartment  $k$  is described by:

$$C_m \frac{dV^k}{dt} = -\sum I_{ion}^k - \sum I_{ext}^k \quad (1)$$

where  $C_m$  is the membrane capacitance,  $V^k$  is the transmembrane potential,  $I_{ion}^k$  is the total ionic membrane current, and  $I_{ext}^k$  the total external current. The total ionic current is written as:

$$\begin{aligned} \sum I_{ion}^k = & \overline{g}_{Na} m^3 h (V^k - E_{Na}) + \overline{g}_K n^4 (V^k - E_K) \\ & - g_{leak} (V^k - E_{leak}) \end{aligned} \quad (2)$$

where  $\overline{g}_{Na}$  and  $\overline{g}_K$  are the maximum value of the conductance of sodium and potassium, respectively.  $g_{leak}$  is the conductance of the leakage current.  $E_{Na}$ ,  $E_K$  and  $E_{leak}$  are the sodium, potassium, and leakage reversal potentials, respectively. It should be noted that the reversal potentials are the source of noise in our

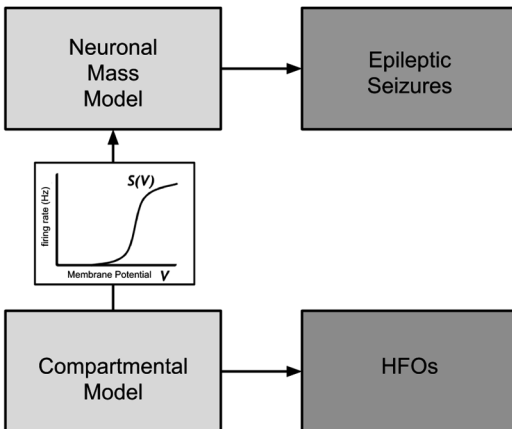


**Fig. 1.** Overview of the cascade modelling approach to connect phenomenology at different scales connected by the firing rate curve, where the firing rate  $S(V)$  is illustrated for various value of the membrane potential  $V$ . On the microscopic scale the addition of gap junctions in the compartmental model gives rise to HFOs, while in the macroscopic NMM this leads to the autonomous generation of epileptic seizures.

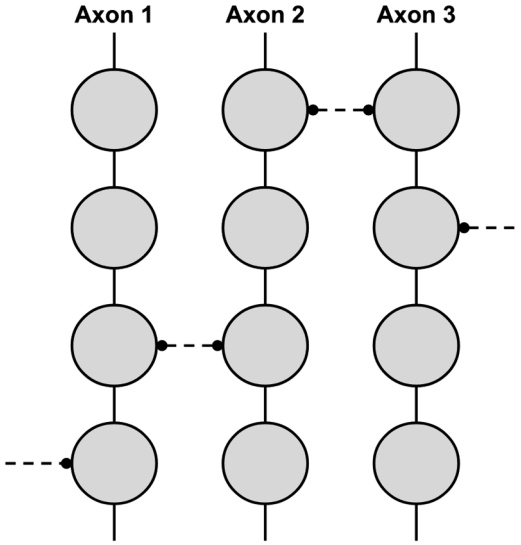


**Fig. 2.** Schematic overview of part of the network of the microscopic model. The total network consists of 50 axons. Each axon consists of 10 single connected compartments. The axons are interconnected via gap junctions, as indicated by the dashed lines. It should be noted that any compartment of any axon can be connected to any other compartment of another axon.

system, where they could deviate from their assigned value. For example the sodium reversal potential was given by  $E_{\text{Noise}}(t) = E_{\text{Na}} + \psi(t)$ , where  $E_{\text{Noise}}(t)$  is the reversal potential of sodium varying in time due to  $\psi(t)$ , which is a randomly generated signal that emulates shifts in the Nernst potential due to ionic concentration differences. The used parameter values are shown in Table 1.

The dimensionless quantities  $m$ ,  $h$ , and  $n$  describe the membrane state variables, which are associated with sodium channel activation, sodium channel inactivation, and potassium channel activation. A second differential equation defines the evolution of the membrane state variables  $m$ ,  $h$ , and  $n$ . Let  $z^k$  be one of the dimensionless state variables  $m$ ,  $h$ , or  $n$  in compartment  $k$ . The evolution of the state variable is then given by:

$$\frac{dz^k}{dt} = \alpha^z(V^k) \cdot (1 - z^k) - \beta^z(V^k) \cdot z^k, \quad (3)$$

Where  $\alpha^z$  and  $\beta^z$  are rate functions for that state variable  $z^k$ , and are given in Table 2. The total external current  $I_{\text{ext}}$  is given by:

$$\sum I_{\text{ext}}^k = I_{\text{inj}}^k + \sum_l \gamma_{l,k}(V_l - V_k) \quad (4)$$

where  $k$  and  $l$  are the indices of different compartments,  $I_{inj}$  represents the injected current, and  $\gamma$  is the coupling conductance between different connected compartments. The product of the coupling conductance with the potential difference is summed over all compartments connected to compartment  $k$ . It should be noted that only the first compartment of each axon receives the injected input current in the simulations.

The injected current,  $I_{inj}$ , can serve as different types of input in our simulations. It can be a pulse generator which represents a short injected current to depolarize a compartment, but it can also represent dendritic input from other neurons or a continuous injected current. In the latter case,  $I_{inj}$  is defined as:

$$I_{inj}^k = g_{inj} (V^k - V_{inj}), \quad (5)$$

where  $g_{inj}$  is the injected current conductivity and  $V_{inj}$  the injected current reversal potential.

Networks were generated with random gap junction connectivity, subject to two constraints: (i) total number of gap junctions formed by any axon is less than five, and (ii) one single axonal compartment can only have one gap junction. The first restriction is made in order to avoid extreme distributions of the gap junctions. The second restriction, while not essential, is made since a compartment with two gap junctions can always be split into two compartments with each having a single gap junction. To construct such a network, first the

**Table 1.** Parameter values for the microscopic Hodgkin-Huxley compartmental model.

Parameter	Value
$g_{Na}$	120 mS/cm <sup>2</sup>
$g_K$	36 mS/cm <sup>2</sup>
$g_{leak}$	0.3 mS/cm <sup>2</sup>
$g_{inj}$	0.3 mS/cm <sup>2</sup>
$E_{Na}$	50 mV
$E_K$	-77 mV
$E_{leak}$	-54.38 mV
$C_m$	1 $\mu F cm^2$
$\gamma_{axon}$	0.5 mS/cm <sup>2</sup>
$\gamma_{gap}$	3.5 mS/cm <sup>2</sup>

average number of junctions formed on each axon is specified, called the connectivity  $C_{junctions}$  (ranging from 0 to 3.0). The total number of gap junctions to be inserted into the network is defined as:

$$N_{junctions} = C_{junctions} \frac{N_{axons}}{2}, \quad (6)$$

with  $N_{axons}$  the total number of axons in the network. Pairs of cells were generated using a pseudo-random number generator, and were discarded if constraints (i) and (ii) were not met. The connectivity  $C_{junctions}$  of the network was set 0, 0.5, 1, 1.5, 2, and 3 for the different simulations.

Five different randomly connected networks for each level of the gap junction densities were generated. For each of these networks (30 in total) we simulated the output from 50 different initial conditions, corresponding to initial activation of each individual of the 50 somatic compartments. As a result 1500 simulated trials were performed, 250 for each gap junction density level. In each simulation, the averaged signal was used to compute the corresponding quantifier, the ARR or the rPCI. The firing rate curve was determined by stimulating the first compartment of all axons with an injected current as described by Eq. (5), which represents the dendral input current for various levels of injected current reversal potential  $V_{inj}$  ranging from  $-40$  mV up to  $25$  mV in steps of  $5$  mV. For all levels of  $V_{inj}$  the amount of spikes in a set time interval were averaged for each realized network topology and connectivity  $C$ .

**Table 2.** Rate functions for the membrane state variables  $m$ ,  $h$ , and  $n$ .

Parameter	Rate function
$\alpha_m$	$\frac{9.1(V + 40)}{1 - e^{-(V+40)/10}}$
$\beta_m$	$4e^{-(V+65)/18}$
$\alpha_h$	$0.07e^{-(V+65)/20}$
$\beta_h$	$\frac{1}{1 + e^{-(V+35)/10}}$
$\alpha_n$	$\frac{0.01(V + 55)}{1 - e^{-V/(+55)/10}}$
$\beta_n$	$0.125e^{-(V+65)/80}$

### 2.2.2 Macroscopic neuronal mass model

NMMs are successful in describing brain rhythms as observed in macroscopic measurements such as the EEG. Every individual unit in a NMM represents a specific lump of interconnected neuronal populations. A NMM produces the average activity, i.e. firing rates, for each population of neurons which generates postsynaptic currents based on incoming signals. These currents are integrated and contribute to the mean membrane potential of the neuronal population. The macroscopic NMM or lumped model used has been described in detail in previous work, where a complete description of the model can be found.<sup>22</sup> A lumped model consisting of two cell types, a pyramidal cell population and an interneuron population was used as illustrated by Fig. 3. The evolution of the transmembrane potential is described by the following general equation:

$$C_m \frac{dV^{(i)}}{dt} = -\sum I_{syn}^{(i)} - g_{leak} (V^{(i)} - V_{leak}^{(i)}), \quad (7)$$

$$i = \{PY, IN\}$$

with synaptic currents:

$$I_{syn}^{(i)} = g_{syn}^{(i)} (V^{(i)} - V_{syn}^{(i)}) \quad (8)$$

In Eqs. (7) and (8),  $C_m$  is the membrane capacitance,  $V$  the membrane potential,  $g_{leak}$  the leak current conductance,  $g_{syn}$  the synaptic current conductance, and  $V_{leak}$  and  $V_{syn}$  the reversal potentials of the leak current and synaptic current, respectively. PY stands for pyramidal cell and IN for interneuron. The output of each model population, interpreted as the collective firing rate, is usually described by a sigmoid function with offset  $V_0$  and slope (gain)  $\mu$ :

$$S(t) = \sigma(V(t)); \quad (9)$$

$$\sigma(V) = S_0 \left( 1 - \frac{1}{1 + e^{\mu(V_0 - V)}} \right) \quad (10)$$

However, with the cascading modelling approach, the firing rate curves acquired from the detailed model were embedded into the macroscopic model, modifying the standard sigmoidal function. The dynamics of the synaptic current conductance are described by the following equations:

$$\frac{d^2}{dt^2}g(t) + \frac{2}{\tau} \frac{d}{dt}g(t) + \frac{1}{\tau^2}g(t) = H(t) \quad (11)$$

$$g_{syn}(t) = G_{syn}^{max} \quad (12)$$

where  $G_{syn}^{max}$  is the maximum synaptic conductance,  $H(t)$  is the synaptic input and  $\eta(t) = \zeta(t)\theta(t)$  with  $\theta(t)$  the Heaviside step function, and  $\zeta(t)$  is a randomly generated signal that emulates postsynaptic noise. The dynamic variable  $g(t)$  can be considered to represent the concentration of the neurotransmitter near the postsynaptic membrane.

The output of the model is the average membrane potential of the PY cell population. This model is autonomous in the sense that its dynamics can generate an epileptic type of oscillatory behaviour with no input from outside except for a certain amount of postsynaptic noise. Seizure generation is controlled by the strength of the pyramidal-to-pyramidal feedback loop. Depending on the parameter initial conditions, the model can display different types of behaviour. The model can be in a steady state which represents normal behaviour, or in a limit cycle which represents an epileptic seizure or ictal state. Additionally, the system can have a third state where both types of behavior exist, the bistability region. Due to internal noise or external perturbations in the

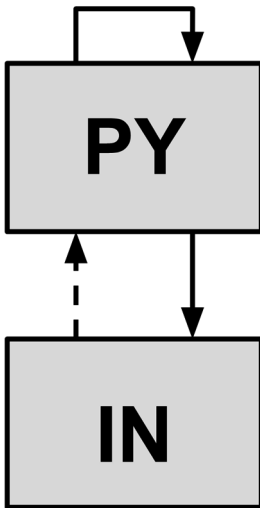


**Fig. 3.** Schematic overview of the NMM with an excitatory pyramidal cell (PY) population and an inhibitory interneuron (IN) population. The solid arrows show excitatory connections and the dashed arrow is an inhibitory connection.

system, the behaviour of the model can alternate between the steady state and limit cycle. Simulations were performed to determine the phase space of the system for each gap junction density level by slowly increasing and decreasing the self-coupling coefficient. The noise level was set to zero to prevent noise-induced changes.

### *2.2.3 Cascade modelling*

Modelling of neuronal systems is always limited by the selection of appropriate level of detail. Therefore, we have adopted the concept of cascade modelling where two (or in general more) levels of complexity are simultaneously considered. The challenge addressed in this paragraph is two find links between the different levels of modelling. This concept of cascade modelling is illustrated in Fig. 1, where the firing rate curve is used as the link between the microscopic compartmental model where HFOs can be generated, and the macroscopic NMM where autonomous generation of epileptic seizures can occur. With the cascade modelling approach, we investigate the effects of the gap junction density on the single cell firing rate in the compartmental model, which is mapped to a NMM as variation in slope and threshold of the transfer function from the cell population membrane potential to the firing rate. Using the cascade modelling approach, the average single neuron firing rate curves acquired from the detailed model are embedded into the macroscopic NMM as the collective firing rates of the population. The average firing rate curve of the compartmental model without gap junctions was mapped to the sigmoidal curve in Eq. (10) of the NMM. The following equation shows the translation function used:

$$\sigma_{NMM}(V) = a \cdot \sigma_{comp}(c(V + b)) \quad (13)$$

where  $\sigma_{NMM}$  is the scaled and translated sigmoidal function, and  $\sigma_{comp}$  is the piecewise cubic hermite interpolated polynomial curve of the average single neuron firing rate, ranging from  $-40$  to  $20$  mV. The shifting and scaling parameters  $a$ ,  $b$ , and  $c$  are selected according to best match (minimal square difference) between the original sigmoidal function as described by Eq. (9) and the translated sigmoidal function with no gap junctions. These parameters were subsequently used for all gap junction densities in order to obtain the gap

junction induced deformed collective population firing rate function for the pyramidal cell population in the NMM.

Simulations of the model are performed using Simulink Version 7.8 (Mathworks Inc. Natick, MA, USA); Matlab Version R2011b (7.13.0.564) (Mathworks Inc. Natick, MA, USA) is used for data analysis.

*Ictality.* Methods used to determine the systems likelihood to seizure normally encompass determination of the beginning and end of a seizure and are based on predefined thresholds. In recent work, the autocovariance of the pyramidal cell population membrane is used to determine the system's ictality.<sup>25</sup> The first order of the autocovariance peak represents the steady state behaviour, and the second-order peak paroxysmal behaviour. The ictality of the system is now defined as:

$$J = \frac{P_2}{P_1}, \quad (14)$$

where  $P_1$  and  $P_2$  are the height of the first- and second-order peak, respectively. If the ictality of the system is low, the ictality index will be close to zero. Conversely, if the amount of paroxysmal behavior is high, the ictality index will be close to one. To examine the influence of the gap junction density on the ictality of the system, 10 min of simulated EEG data was generated with the NMM for each level of the gap junction density as indicated above. The self-coupling parameter of the NMM was set in such a way that with increasing gap junction density the system migrates from only showing steady state behaviour, through a bistable region, and finally into a region where only limit cycle behaviour is elicited. The self-coupling coefficient is set at 1.65, which is at a level within the bistability zone where it is able to cause a transition from one state to another, if such transition exists in the dynamics of the system. The noise is set to 0.04, which determines the probability of transitions. If it is too low, longer stimulation runs (waiting for a fluctuation of the right magnitude) in order to accumulate statistics would be needed. Extremely high values of the noise will cause much more transitions from normal to ictal type of states but the distinction between these two states will become obscured. Detailed analysis of

the noise influence of the system transitions is published in the work of Koppert et al.<sup>22</sup>

#### *Ad hoc derived HFO detector testing.*

To test whether HFO detector algorithms are applicable to the simulated data, the microscopic compartmental model HFO bursts triggered by stimulation of the network were overlapped on macroscopic EEG data acquired from the NMM. Two different HFO detection algorithms were used. The first detection algorithm is the rPCI as proposed by Kalitzin et al.<sup>26</sup> The concept behind the rPCI is that perturbing the brain dynamics through external stimulation can yield a measure for the presence or absence of a possible epileptic state and the risk of transition to such a state. The rPCI is a measure of a time-variant propensity of the system to phase-lock its response to an external stimulus.

The second detection algorithm used is the ARR, a novel algorithm proposed by Geertsema et al.<sup>27</sup> The ARR uses the nonlinear features, i.e. the residual error, after an autoregressive (AR) model fit as HFO detection method. Windows with HFOs in the seizure onset zone (SOZ) have a higher residual signal variation after AR modelling than EEG windows with HFOs from a channel outside the SOZ. In this algorithm, the data acquired from the microscopic compartmental model overlapped with macroscopic EEG data acquired from the NMM was divided into windows of 40 ms with 50% overlap. Next, three-pole AR models were estimated, thereby obtaining the residual signal variation.

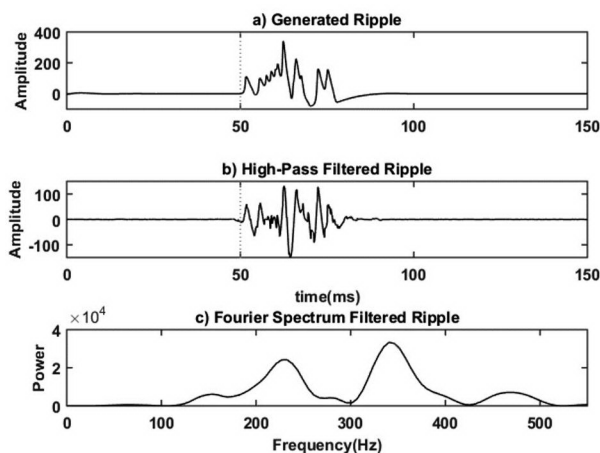


**Fig. 4.** Example of a generated ripple of one of the randomly generated network realizations (a). The network of cells is stimulated at 50 ms with a short injected current pulse of 1ms indicated by the dotted line. After Huang bandpass filtering from 150 to 500 Hz, an HFO emerges (b). Fourier analysis of the Huang filtered data shows dominant frequency peaks at 230, 340, and 460 Hz for this ripple (c).

## 2.3 Results

### 2.3.1 Microscopic compartmental model

*Network response and HFO-like behaviour.* Figure 4 shows an example of a generated ripple of one of the randomly generated network realizations. After bandpass filtering from 150 to 500 Hz, an HFO emerges lasting for about 50 ms. A Huang filter was used which is a filter specifically designed to keep the morphology of the signal intact. Fourier analysis of the Huang filtered data, shows dominant frequency peaks at 195, 255 and 305 Hz. Figure 5 shows the population or network response after single neuron firing due to an injected current pulse for

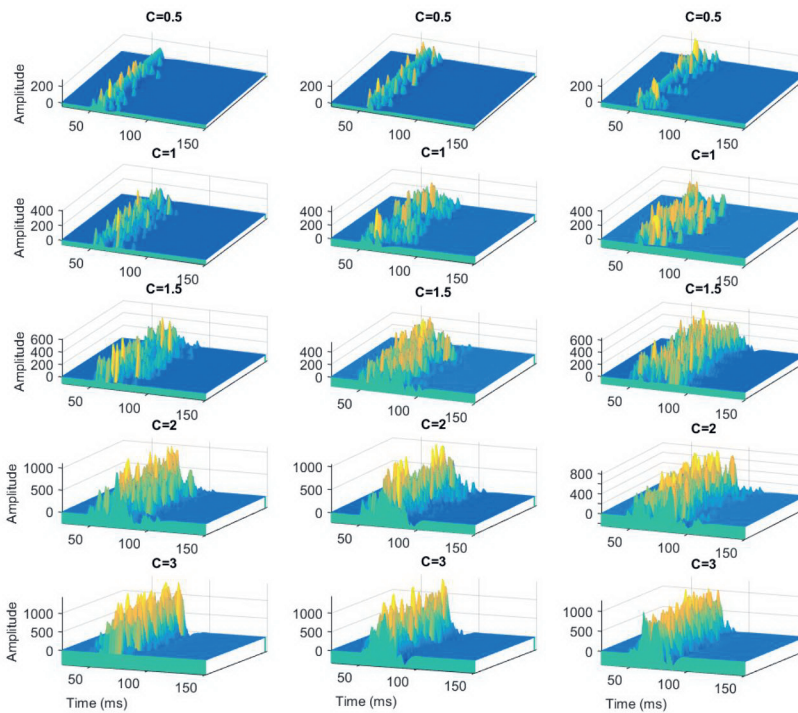


**Fig. 5.** In this figure each row of frames represents one gap junction density level while the individual frames in each row correspond to the different network topologies. In each frame 50 traces, simulated from the 50 initial conditions, are plotted together. At 50 ms a current pulse is injected into the system. The Y -axes are the summed amplitude over the last compartments of the axons in the network.

every neuron in the network. For each fixed topology, increasing the connectivity  $C_{junctions}$  results in an increase in duration and amplitude of the ripple-like behavior due to recruitment of interconnected cells via gap junctions. With a connectivity  $C_{junctions}$  of 0.5 the average duration is about 25 ms, while a connectivity  $C_{junctions}$  of 2.0 results in an average network response of about 70 ms. Further increasing of the gap junction density leads to the synchronous firing of all the compartments which results in the formation of a large spike complex. There, the fast oscillatory HFO-like behaviour is superimposed on a slow-wave ‘carrier’ component further shown in Fig. 6.

*Sigmoidal current firing-rate curve.* Figure 7 shows the average firing rate curves for each gap junction density. The firing rate curve shifts to the left with increasing gap junction density. The slope of the curve changes at various points of the curve due to the increased gap junction density. Not shown are the fitted firing rate curves after translation using Eq. (13). The used parameters for the translation were a vertical scaling parameter  $a$  of 0.76, a horizontal shift  $b$  of  $-20.5$ , and a horizontal scaling parameter  $c$  of 2.13 which gave the smallest fitting error (minimal square difference).

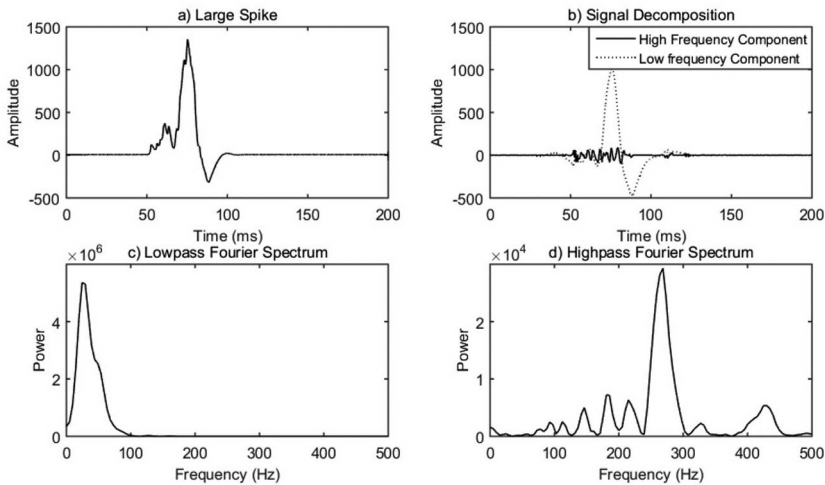


**Fig. 6.** Example of the slow-wave ‘Carrier’ phenomenon for high gap junction densities (a), where a high frequency component is superimposed on a slow-wave (b). The Fourier spectrum of both components are shown in the bottom row (c and d).

## 2.3.2 Macroscopic neuronal mass model

*Space deformation and emergent bistability: Seizure generating scenario.* In Fig. 8, the amplitude of the oscillations in the system is mapped as a function of the self-coupling coefficient in a system without noise. These are the results of dual runs, with gradual increases and decreases of the coupling constant. Low self-coupling coefficients result in steady state behaviour, representing normal background

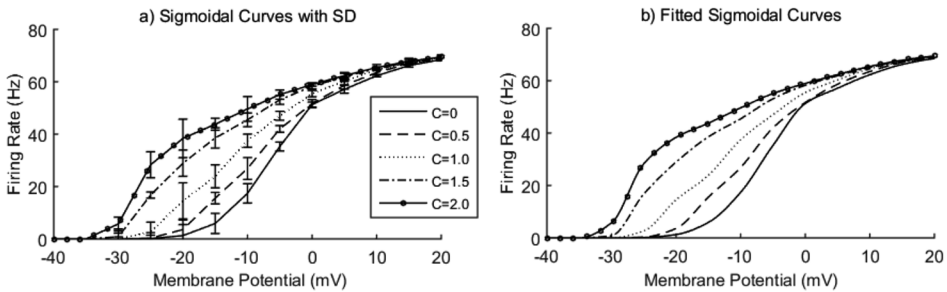


**Fig. 7.** Average firing rate curves for different connectivity's  $C$  of the network as a function of the membrane potential. The standard deviations for the original curves are shown in the top row (a), while the fitted curves are shown the bottom row (b).

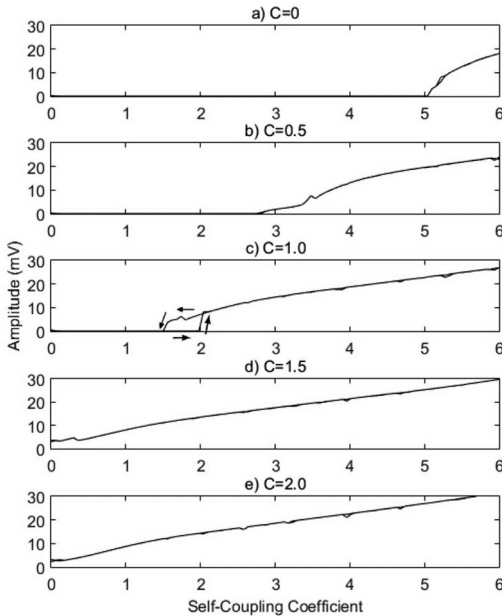


**Fig. 8.** Amplitude of the membrane potential oscillations of the pyramidal cell population as a function of the self-coupling coefficient for different levels of  $C$ . These are the results of dual runs, with gradually increasing and decreasing coupling constant. The arrows (shown only for the hysteresis part in (c)) indicate the direction of change in the self-coupling coefficient.

EEG. When increasing the self-coupling coefficient, the system will eventually transit to a limit cycle due to excessive excitation. For the system with zero connectivity, the transition to limit cycle type of behaviour takes place at a self-coupling coefficient of about 5. Increasing the connectivity of the system causes the system to elicit limit cycle type of behaviour for smaller self-coupling coefficients. For a connectivity  $C_{junctions}$  of the system of 0.5 limit cycle type of behaviour emerges at a self-coupling coefficient of about 2.8. When gap junction density is increased enough, bistable behaviour emerges as shown in Fig. 8(c), where both states are present simultaneously. Further increasing of the gap junction density results in a system that always generates limit cycle type of behaviour as is shown in the last two plots.

*Ictality.* The systems ictality for different levels of gap junction density are shown in Fig. 9. With increasing connectivity of the system, the NMM systems ictality steadily increases from 0.32 with no gap junction connectivity in the system, indicative of a low seizureiness of the system, up to 0.91 with a connectivity of 2, indicative of high seizureiness of the system.

*Adhoc derived HFO detector testing.* Figures 10 and 11 show the statistics for the ARR and rPCI, respectively, where each frame represents the results of a given level of gap junction density. The box plot represents the distribution of the rPCI and ARR for the different random network realizations. Both indices steadily increase in value with increasing gap junction density. The rPCI increases from 0.33 with no gap junctions up to 0.52 with a connectivity of 3, while the ARR increases from 1.01 with no gap junction connectivity up to 6.43 with a

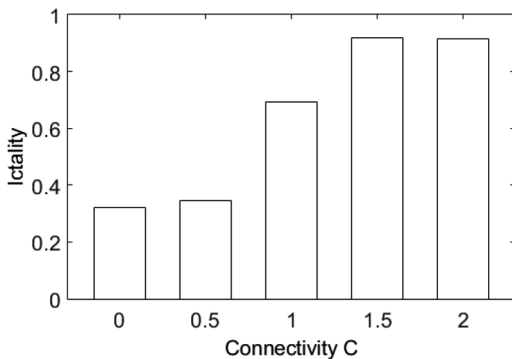


**Fig. 9.** Ictality for different levels of gap junction density, i.e. connectivity parameter  $C$ . The ictality of the system increases with increasing gap junction density.

connectivity of 3. The ARR seems to better distinguish between the different levels of connectivity of the network, with a much more pronounced difference between the values of the index for different levels of connectivity  $C$ .

## 2.4 Discussion

Computational models are a useful mathematical tool to study the behaviour of single neurons or networks of neurons. While microscopic compartmental models take ion electrophysiology into account, they tend to become computationally time consuming with increasing network size. NMMs on the other hand afford a straightforward approach to modelling the activity of populations of neurons. They deal with increasing complexity by assuming that the state of a cell population can be approximated using very few state variables. Given a macroscopic architecture, describing the overall connectivity between populations, it is possible to simulate the steady state dynamics of the system or even the transient response to a perturbation of extrinsic input or connectivity. Consequently, NMMs are useful and despite their relative simplicity, they can exhibit complex dynamical behaviour reminiscent of the real brain.

This study demonstrates that microscopic features such as gap junctions, channel mutations and biological or molecular mechanisms can be embedded in a cascade of models to connect phenomenology at different scales. In particular, axonal–axonal gap junctions can produce HFO-like type of activity and be responsible for emergent bistability leading to autonomous generation of seizures. Single neuron firing results in fast recruitment of interconnected cells by gap junctions, resulting in HFO-like desynchronous firing of the population of neurons. The addition of gap junctions in a axonal network leads to changes in the average firing rate of a single axon. When these changes in the firing rate curve are embedded into the collective population firing rate of the higher order NMM, it resulted in phase space deformations with emergent bistability. While the transformation parameters used for embedding the realizations of the average firing rate curves into the NMM transform the curve at the lower and upper end beyond realistic values, the model is still successful because it operates on a small part of the firing rate curve. In this cascade of models, gap junctions

are a common cause for both HFO-like behaviour and epileptic seizures. The NMMs likelihood to seizure, defined by the autocovariance peaks in the ictality index, increases with an increase in the gap junction density or connectivity  $C_{junctions}$  of the network as was shown in Fig. 9. This demonstrates that the changes in the embedded population firing rate curve due to an increase in gap junction density results in a shift in the operational working point of the system.

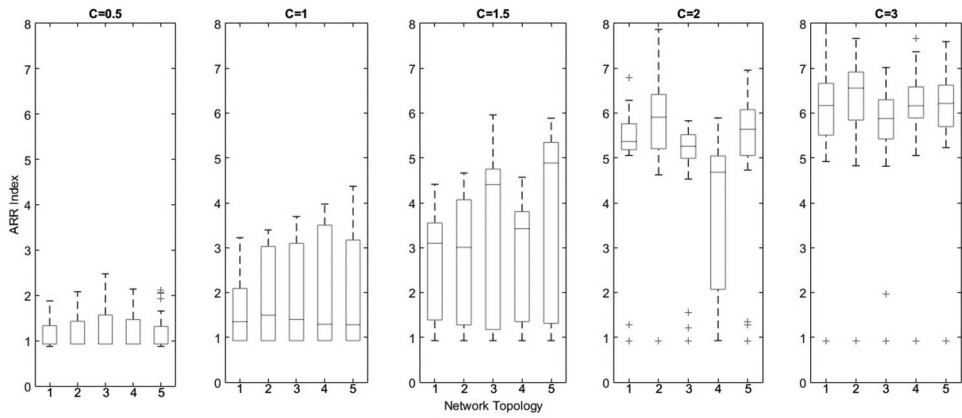


**Fig. 10.** Results of the ARR HFO detector. Each frame represents the result of a given level of gap junction connectivity (given above the frame). The horizontal axes indicate the five different random network realizations. The box plots represent the ARR distribution over the 50 initial conditions.

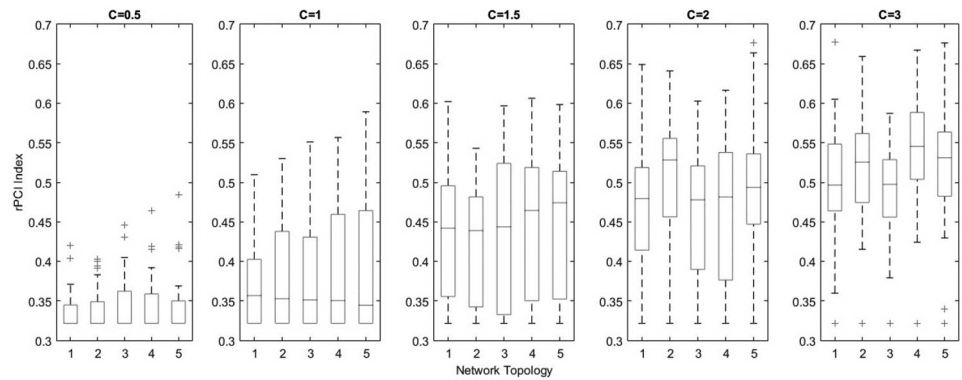


**Fig. 11.** Results of the rPCI HFO detector. Each frame represents the result of a given level of gap junction connectivity (given above the frame). The horizontal axes indicate the five different random network realizations. The box plots represent the rPCI distribution over the fifty initial conditions.

These changes lead to an increase in epileptic type of behaviour and thus an increase in the ictality of the system. Similar increases can be found in the ad hoc HFO detector indices for the different connectivity levels. These modelling results imply that both the rPCI and ARR seem to be good methods to capture the ictality or state of a neuronal network. Further investigation is required to elucidate whether these indices can give clinically useful information about the brain state of a patient. In addition to the results presented in this study, we note that models can help developing new dedicated HFO detectors. We observe from Fig. 5 that for higher gap junction densities the HFOs are superimposed with a slow-wave “carrier” component that can be used to identify this specific phenomenon. This is an emergent property of the model due to desynchronous firing of a highly connected network population. HFOs superimposed on slow-waves have been shown to occur during direct electrical stimulations in epilepsy patients.<sup>28</sup>

To make a parallel with our previous NMM studies, we note that in our previous work, the bistability control parameter was either the external input to the pyramidal population,<sup>21</sup> or the excitatory self-coupling between the pyramidal populations.<sup>22</sup> In this work, we demonstrate that similar control properties can be realized by (nonparametric) deformations of the sigmoid response function induced in turn by the gap junction density, i.e. connectivity parameter  $G_{junctions}$ .

Phenomena associated with different scales of biological organization have to be modelled adequately by different models. In fact every model is a compromise between the amount of details incorporated, computational feasibility, and interpretability of the results. In earlier work, it was shown that for large scale phenomena even the NMM can be simplified and reduced to a simple analytical model that still carries the essential features of seizure generation.<sup>29,30</sup> In the same spirit, here we use a cascade, or an ordered pair of models at two different scales of organization. The link is established by embedding the output of the detailed model into the collective model (the NMM). In this way, we believe the dichotomy of detailed computationally complex models versus comprehensive — but lacking full realism — models can be resolved.

#### 2.4.1 *Clinical perspective*

In epilepsy surgery, resection of tissue with pathological HFOs are a predictor for good surgical outcome.<sup>19</sup> This potentially diagnostic and predictive value of HFOs suggest that they should be taken into account for clinical evaluations. However, the overlap of physiological and pathological ripple frequency bands makes it hard to distinguish the ripples on the basis of frequency band analysis alone. A recent study showed that not only the amount of HFOs but conjointly the HFO pattern is an important feature for the interpretation of HFOs in epileptic patients.<sup>31</sup> Ripples occurring in an oscillatory background may be suggestive of physiological activity, while those ripples occurring on a flat background reflect epileptic activity. In our study, the epileptic HFOs are desynchronous, transient bursts of population spikes which is compliant with the above empiric findings observation that oscillations as paroxysmal events should rather occur from a quiet baseline than continuous oscillatory activity. This transient desynchronous population burst mechanism behind HFO generation has been suggested in previous work.<sup>32</sup> Another recent phenomenological study uses detection of intermittent bursts of nonharmonic HFOs which appear to be associated with the pro-epileptic potential of the neuronal tissue.<sup>27</sup> The ad hoc detector developed there is based on the temporal variation of the signal ARR and was tested to be consistent with our simulated HFO signals.

Recent research has shown that HFOs can be detected with scalp EEG measurements which require the EEG to be sampled at a frequency above the usual 200 or 500 Hz.<sup>33-35</sup> However, the fact that HFOs tend to be spatially localized, low in amplitude, in combination with the low-pass filtering properties of the skull make it a challenge to successfully capture them on the scalp EEG measurements. This microscopic compartmental model predicts that perturbing a neuronal network with increased gap junction density through external stimulation such as TMS or electrical stimulation can generate evoked HFOs. TMS has been shown to modulate epileptiform discharges in epilepsy patients.<sup>36</sup> While evoked HFOs have been recorded in intracranial EEG measurements, there is to date no convincing evidence that TMS-evoked HFOs can be recorded using scalp-EEG recordings. Our modelling results suggest that the two ad hoc developed HFO detectors, but in particular the ARR ad hoc HFO detection method should be able to successfully capture evoked HFOs. Such

measurements could give clinically relevant information about the brain state of the patient, where a decrease in the frequency of (induced or spontaneous) HFOs after application of an anti-epileptic drug can be predictive for the efficiency of that anti-epileptic drug in seizure suppression.

#### 2.4.2 *Model considerations*

In both the microscopic and higher order model, most parameters are assumed to be constant. This is not likely to be true in real neurons. The multistability theory with autonomous transitions however does not preclude the involvement of other mechanisms such as parameter-based bifurcations. The results of the microscopic compartmental model in this work are limited to the Hodgkin–Huxley type of neurons, and may not be generalizable to other types of models. Furthermore, we assume that axonal–axonal gap junctions are (one of) the underlying mechanism(s) behind the generation of HFO activity. While a few studies have shown evidence of connexions (the functional unit of gap junctions) between axons, there is little evidence of functional axonal–axonal gap junctions in neurons.<sup>37</sup> Most of the support comes from computational models, in particular those of Traub et al.<sup>14,15</sup> However, we do not rely on empirical or experimental findings for proving the existence of axonal–axonal gap junctions. Our model study, along with other computational studies, deduces the role of axonal electrical connections in causing both HFO bursts and epileptic type of behavior. We postulate that alternative biological substrates, such as dendral-axonal gap junctions, can be instrumental for explaining gamma range of oscillatory behaviour and possibly its relation to epilepsy, but further investigation is required.

One study showed that a high gap junction density was associated with suppression of the firing rate for low stimulation inputs due to reduced input resistance of the model neurons and, therefore, enforced fast relaxation of subthreshold excitation.<sup>38</sup> In our study, the gap junction network topology was randomly generated but restricted to constraints that avoid extremely inhomogeneous distributions, which may have reduced the effect of this phenomenon. Without these constrictions, there may be instances of network configurations where the gap junction density is higher in one part of the network than in others. While such a construct offers the possibility to introduce

sub-systems of higher epileptogenic properties, possibly presenting models of SOZs, such networks with strong inhomogeneity were beyond the envelope of this research.

Finally, we comment on the source of stochasticity in the microscopic model. In our model, the reversal potentials in the detailed model are presumed to incorporate additive stochastic noise, as opposed to the more commonly used conductance fluctuations. This was done in order to avoid negative conductance when a large fluctuation occurs and allows for the use of simple normal distributions instead of fixed flat range ones or restricted (to positive values) normal distributions. The two variables (the transmembrane potential and the conductance) enter as a product in Eq. (2), and thus this change makes no essential difference, with only a modification of the noise rescaling compared to other models. We further note that in order to employ the input–output sigmoid curve in the NMM we used the average firing rate as an output. Therefore, we have assumed stationary behaviour that ignores effects related to temporal fluctuations of the firing patterns. Possible effects of the fluctuations around the mean firing rate in the higher order NMM goes beyond the scope of this study.

## **2.5 Conclusion**

Single neuron firing can result in fast recruitment of interconnected cells by gap junctions, resulting in HFO-like action potential firing of a population of neurons and a change in the average firing rate of a single neuron. When these changes in the firing rate curve are embedded into the collective population firing rate in the higher order NMM, it resulted in phase space deformations with emergent bistability leading to epileptic type of behaviour. In this cascade of models, gap junctions are a common cause for both HFO-like oscillatory behaviour and epileptic seizures. We have further demonstrated that ad hoc HFO detectors used in previous studies are applicable to our simulated data.

## References

1. Bal, T. & McCormick, D. A. What stops synchronized thalamocortical oscillations? *Neuron* 17, 297–308 (1996).
2. Destexhe, A., Babloyantz, A. & Sejnowski, T. J. Ionic mechanisms for intrinsic slow oscillations in thalamic relay neurons. *Biophys. J.* 65, 1538–1552 (1993).
3. McCormick, D. A. et al. Persistent Cortical Activity: Mechanisms of Generation and Effects on Neuronal Excitability. *Cereb. Cortex* 13, 1219–1231 (2003).
4. Buzsáki, G., Horváth, Z., Urioste, R., Hetke, J. & Wise, K. High-frequency network oscillation in the hippocampus. *Science* (80-. ). 256, 1025–1027 (1992).
5. Csicsvari, J., Hirase, H., Czurkó, A., Mamiya, A. & Buzsáki, G. Fast network oscillations in the hippocampal CA1 region of the behaving rat. *J. Neurosci.* 19, RC20 (1999).
6. Axmacher, N., Elger, C. E. & Fell, J. Ripples in the medial temporal lobe are relevant for human memory consolidation. *Brain* 131, 1806–1817 (2008).
7. Draguhn, A., Traub, R. D., Bibbig, A. & Schmitz, D. Ripple (~200-HZ) oscillations in temporal structures. *J. Clin. Neurophysiol.* 17, 361–376 (2000).
8. Zijlmans, M. et al. High-frequency oscillations as a new biomarker in epilepsy. *Ann. Neurol.* 71, 169–178 (2012).
9. Allen, P. J., Fish, D. R. & Smith, S. J. M. Very high-frequency rhythmic activity during SEEG suppression in frontal lobe epilepsy. *Electroencephalogr. Clin. Neurophysiol.* 82, 155–159 (1992).
10. Fisher, R. S., Webber, W. R. S., Lesser, R. P., Arroyo, S. & Uematsu, S. High-frequency EEG activity at the start of seizures. *J. Clin. Neurophysiol.* 9, 441–448 (1992).
11. Huang, C. ming & White, L. E. High-frequency components in epileptiform EEG. *J. Neurosci. Methods* 30, 197–201 (1989).
12. Draguhn, A., Traub, R. D., Schmitz, D. & Jefferys, J. G. R. Electrical coupling underlies high-frequency oscillations in the hippocampus in vitro. *Nature* 394, 189–192 (1998).
13. Perez Velazquez, J. L. & Carlen, P. L. Gap junctions, synchrony and seizures. *Trends in Neurosciences* vol. 23 68–74 (2000).
14. Traub, R. D. et al. A possible role for gap junctions in generation of very fast EEG oscillations preceding the onset of, and perhaps initiating, seizures. *Epilepsia* 42, 153–170 (2001).

15. Traub, R. D. et al. Axonal gap junctions between principal neurons: A novel source of network oscillations, and perhaps epileptogenesis. *Rev. Neurosci.* 13, 1–30 (2002).
16. Dudek, F. E., Snow, R. W. & Taylor, C. P. Role of electrical interactions in synchronization of epileptiform bursts. *Adv. Neurol.* 44, 593–617 (1986).
17. Jefferys, J. G. R. Nonsynaptic modulation of neuronal activity in the brain: Electric currents and extracellular ions. *Physiol. Rev.* 75, 689–723 (1995).
18. Dzhala, V. I. & Staley, K. J. Mechanisms of fast ripples in the hippocampus. *J. Neurosci.* 24, 8896–8906 (2004).
19. Jacobs, J. et al. High-frequency electroencephalographic oscillations correlate with outcome of epilepsy surgery. *Ann. Neurol.* 67, 209–220 (2010).
20. Wendling, F. Computational models of epileptic activity: A bridge between observation and pathophysiological interpretation. *Expert Rev. Neurother.* 8, 889–896 (2008).
21. Suffczynski, P., Kalitzin, S. & Lopes Da Silva, F. H. Dynamics of non-convulsive epileptic phenomena modeled by a bistable neuronal network. *Neuroscience* 126, 467–484 (2004).
22. Koppert, M. M. J., Kalitzin, S., Lopes Da Silva, F. H. & Viergever, M. A. Plasticity-modulated seizure dynamics for seizure termination in realistic neuronal models. *J. Neural Eng.* 8, 046027 (2011).
23. Kandel, E. R., Schwartz, J. H. & Jessell, T. M. *Principles of Neural Science*, fourth addition. McGraw-Hill Co. (2000).
24. Huxley, A. F. Hodgkin and the action potential 1935-1952. *J. Physiol.* 538, 2 (2002).
25. Kalitzin, S., Koppert, M., Petkov, G., Velis, D. & da Silva, F. L. Computational model prospective on the observation of proictal states in epileptic neuronal systems. *Epilepsy Behav.* 22, (2011).
26. Kalitzin, S. et al. Quantification of spontaneous and evoked HFO's in SEEG recording and prospective for pre-surgical diagnostics. Case study. in *Proceedings of the Annual International Conference of the IEEE Engineering in Medicine and Biology Society, EMBS* vol. 6 1024–1027 (2012).
27. Geertsema, E. E. et al. Automated Seizure Onset Zone Approximation Based on Nonharmonic High-Frequency Oscillations in Human Interictal Intracranial EEGs. *Int. J. Neural Syst.* 25, 1550015 (2015).
28. Van'T Klooster, M. A. et al. Time-frequency analysis of single pulse electrical stimulation to assist delineation of epileptogenic cortex. *Brain* 134, 2855–2866 (2011).
29. Koppert, M., Kalitzin, S., Velis, D., Da Silva, F. L. & Viergever, M. A. Reactive control

- of epileptiform discharges in realistic computational neuronal models with bistability. *Int. J. Neural Syst.* 23, 121102031948003 (2013).
30. Kalitzin, S., Koppert, M., Petkov, G. & Da Silva, F. L. Multiple oscillatory states in models of collective neuronal dynamics. *Int. J. Neural Syst.* 24, 1450020 (2014).
  31. Kerber, K. et al. Differentiation of specific ripple patterns helps to identify epileptogenic areas for surgical procedures. *Clin. Neurophysiol.* 125, 1339–1345 (2014).
  32. Engel, J., Bragin, A., Staba, R. & Mody, I. High-frequency oscillations: What is normal and what is not? *Epilepsia* vol. 50 598–604 (2009).
  33. Kobayashi, K. et al. Scalp-recorded high-frequency oscillations in childhood sleep-induced electrical status epilepticus. *Epilepsia* 51, 2190–2194 (2010).
  34. RamachandranNair, R. et al. Epileptic spasms in older pediatric patients: MEG and ictal high-frequency oscillations suggest focal-onset seizures in a subset of epileptic spasms. *Epilepsy Res.* 78, 216–224 (2008).
  35. Guggisberg, A. G., Kirsch, H. E., Mantle, M. M., Barbaro, N. M. & Nagarajan, S. S. Fast oscillations associated with interictal spikes localize the epileptogenic zone in patients with partial epilepsy. *Neuroimage* 39, 661–668 (2008).
  36. Kimiskidis, V. K., Kugiumtzis, D., Papagiannopoulos, S. & Vlaikidis, N. Transcranial magnetic stimulation (TMS) modulates epileptiform discharges in patients with frontal lobe epilepsy: A preliminary EEG-TMS study. *Int. J. Neural Syst.* 23, 121102031948003 (2013).
  37. Carlen, P. L. et al. The role of gap junctions in seizures. *Brain Research Reviews* vol. 32 235–241 (2000).
  38. Volman, V., Perc, M. & Bazhenov, M. Gap junctions and epileptic seizures - two sides of the same coin? *PLoS One* 6, e20572 (2011).

## Chapter 3

Expert system for pharmacological epilepsy treatment prognosis and optimal medication dose prescription

Based on:

**Helling RM**, Petkov GH, Kalitzin SN. Expert system for pharmacological epilepsy treatment prognosis and optimal medication dose prescription. In *Proceedings of the 2nd International Conference on Applications of Intelligent Systems*. 2019. 1-6.

DOI: 10.1145/3309772.3309775

## **Abstract**

Epilepsy is a debilitating neurological condition that affect approximately 1% of the population. In most cases, it is treatable by anti-seizure medication (ASM) but still about 30% of the patients do not respond sufficiently to medication and continue suffering from seizures. Even for those who respond to ASM, determining the optimal dose requires lengthy periods of trial, error and adjustments. To address these challenges, the main objective of the present study is to find a biomarker for quantification of the level of responsiveness of people with epilepsy to anti-epileptic drugs on a personal level. We use a computational model of connected bistable units to generate and validate 'in silico' a robust biomarker hypothesis. Next, we applied the biomarker to EEG from a cohort of patients with known reaction to medication. The model showed that the aggregated functional connectivity is a critically important observable that reflects the state of epilepsy. Applied to the clinical data we were able to derive a criterion for pharmacological responsiveness as well as a paradigm for assessing the optimal medication dose.

### **3.1 Introduction**

Epilepsy is a serious neurological disorder characterized by the propensity of the brain to generate spontaneous and recurrent seizures. In most cases it is treatable by anti-seizure medication (ASM), but still about 30% of the patients do not respond sufficiently to medication and continue suffering from seizures. The transient nature of seizures makes epilepsy a dynamic disease where periods of normal brain function are intermittently interrupted by seizures that impair partial- or whole- brain function. The initiation, recruitment and spreading of seizures is facilitated by the network of synaptic connections between neurons and between regions of the brain. This is reflected in the recognition of the international league against epilepsy (ILAE) that many epilepsy syndromes are associated with disruptions to either global or local brain networks.<sup>1</sup>

One of the ongoing research topics is to predict or to measure the likelihood of seizures (ictogenicity) by studying structural brain networks. The underlying hypothesis here is that the structural connectivity of the brain may be responsible for its pathological dynamics. In clinical practice, the *in vivo* structural connectivity of the brain is largely unobservable and unknown. A large multitude of factors may influence the epileptic state, which can be of structural or functional nature, or are state-dependent properties of the system. A feasible approach therefore is to examine the statistical inter-relationship between electroencephalogram (EEG) time series recorded at different locations in the brain, thus defining a functional rather than a structural network. In contrast to the unobservable structural connectivity of the brain, the functional connectivity can be inferred from easily accessible resting state (RS) scalp EEG data through a variety of synchrony models.<sup>2</sup> The rationale behind the use of functional rather than structural networks to explain pathological brain dynamics is that functional networks are determined by the structural architecture of the brain but also carry information from the state-dependent dynamics of brain activity.<sup>3</sup>

The main objective of this study is to find an observable quantity, i.e. a biomarker, which reflects the likelihood of seizure transition. Our hypothesis in this work is that RS-EEG functional connectivity explains, at least partially, the ictogenicity of the brain. To test the hypothesis and the efficiency of the

suggested biomarker, we determine the level of association between the ictogenicity of the brain and the average connectivity of the reconstructed functional networks from RS-EEG. We assume that both the brain network properties and local tissue properties may influence the effective connectivity strength of the functional networks inferred from the resting state EEG measurements. First, we perform computational model simulations to validate the concept ‘in silico’. Afterwards, preliminary clinical testing is performed on EEG recordings from patients undergoing routine long-term monitoring diagnostics including drug dose changes.

## 3.2 Methods

An overview of the used methodological framework is presented in Fig. 1. In our model we first tested to what extent local and connectivity based parameter fluctuations impact mean functional connectivity (MFC) and the brain network ictogenicity (BNI)

### 3.2.1 Computational model

We model network brain structure as a random  $N=128$ -node's graph with a connectivity matrix  $\mathbf{G} = \{G_{ij}\}$ , i.e. computational model of the brain structure consists of 128 connected ‘single brain units’. The matrix  $\mathbf{G}$ 's values (corresponding to the pairwise connectivity strengths between the brain units) are drawn from a uniform distribution with mean 0.5 and unit variance. Single unit brain dynamics are modelled using a bistable mathematical model known as the  $Z^6$  model,<sup>4</sup> which is governed by the following equation:

$$\frac{d}{dt}Z = (a|Z|^4 + b|Z|^2 + c + i\omega)Z + \varepsilon(t) \quad (1)$$

Where  $Z$  is a complex variable as a function of time  $t$ ;  $a, b$  are real constants, and  $c + i\omega$  is a constant complex coefficient. The term  $\varepsilon(t)$  is the input to the system, which incorporates a white noise component to mimic the effects of exogenous fluctuations. A network model, with  $n$  nodes described in eq. (1) is constructed:

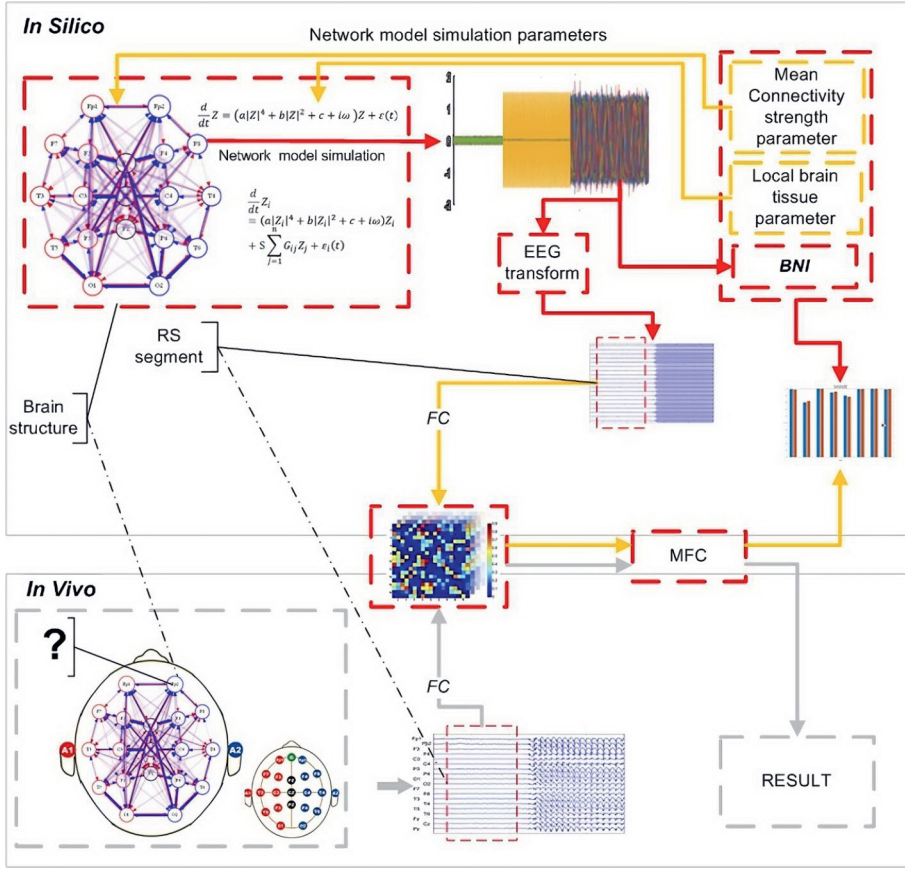


**Fig. 1.** Methodological framework. The figure contains two panels. The upper panel ‘in silico’ shows three computational flow using arrows in red and yellow. The middle (red arrows) flow corresponds to the modelling part: the left red rectangle shows the modelling settings, followed by the simulation resultant traces, BNI calculation, and the simulation of EEG measurements. The upper yellow flow shows the application of the hypotheses checking FC parameters based on modelling results and how they associate with the modelling settings. The lowest yellow flow shows the reconstruction of functional networks using RS segment only, the computation of MFC, and the obtained correlation levels with modelling parameters and BNI. The lower panel shows “in vivo” application of the modelling outcomes. From left to right (gray-arrows): the unknown brain structure; EEG RS segment selection; FC reconstruction and MFC calculation.

$$\frac{d}{dt} Z_i = (a|Z_i|^4 + b|Z_i|^2 + c + i\omega)Z_i + S \sum_{j=1}^n G_{ij} Z_j + \epsilon_i(t) \quad (2)$$

Here we consider the dynamics of  $n$  units, linearly interacting to each other through the connectivity matrix  $G_{ij}$ , rescaled with a coupling strength coefficient  $S$ . Using eq. (2) we perform simulations of 1000 time-points with step size of 10ms and initial conditions set to zero. We generated the white noise  $\epsilon_i(t)$  for

each node independently for the whole simulation duration with a small magnitude of 0.001 to prevent transitions driven only by noise. We choose the simulation parameters  $(a, b, \omega)$  allowing bistability for  $c \in (-1, 0)$ .<sup>5</sup> For every node, we choose the  $c$  parameter randomly distributed with a mean value of minus one, and unit variance so, that each node lies either in the bistability area to allow oscillations to occur or in the steady state region to allow for network driven oscillations. We investigated the influence of structural mean connectivity and the local brain tissue properties separately by using two different sets of multiplicative parameters for simulations. For local brain tissue testing, we multiply the  $c$  parameter with a multiplication parameter from a linear space between 0.5 and 1 in 16 steps. To investigate the influence of structural mean connectivity we multiplied  $G$  with a multiplication parameter from a linear space between 0.1 and 3 in 16 steps. To remove the influence of the initial network  $G$  we have repeated our calculations for ten different initial models of brain structure matrix  $G$ .

*EEG simulation.* To account for the fact that in in vivo measurements the number of EEG electrodes is much lower than the number of brain units or sources, we assumed that each electrode represents a linear combination of the simulated nodes. Accordingly, we prepared a random  $(8 \times 128)$  matrix  $T$ , which transfers the 128 “brain signals” into eight linear combinations, representing the signals obtained from the eight EEG channels. The values of  $T$  are drawn from a uniform distribution  $[-0.5, 0.5]$ . To study the influence of the EEG’s number of electrodes we repeated the above procedure with 64, 32, and 16 EEG channels. To consider RS, from each simulation we chose the longest segment without LC in any of the simulated channels.

*Brain Network Ictogenicity.* To quantify the ictogenicity of the simulated networks we used the Brain Network Ictogenicity (BNI) which was introduced in detail in our previous work.<sup>6</sup> In short: For each simulation, we calculated the time that each channel (node) spend in a limit cycle (LC), normalized to the total simulation time. Averaging over all the channels, we obtained the probability of any node to be in an LC, and we refer to this probability as BNI. The model LC state for any of the simulated channels is defined as a solution with local maxima or minima having magnitude with an absolute value bigger than 0.5.

*Functional connectivity (FC) reconstruction.* For each EEG RS segment the FC was reconstructed using the time-lagged  $h^2$  nonlinear association index as a synchrony model between each pair of signals.<sup>7</sup> The  $h^2$  has been applied to the absolute value of the reconstructed via Hilbert transform analytical signal (the so-called signal envelope or local magnitude) for each channel. Next the network's 'mean connectivity' (MFC) was calculated as the average of the association index over all pairs.

### 3.2.2 *In vivo RS-EEG*

To test the feasibility of the modelling outcomes we test on 2 datasets of empirical data. The first set is a prospective case study of 4 subjects with focal seizures who started treatment with an anti-epileptic drug. RS-EEG was measured before and after starting drug therapy with the Waveguard<sup>TM</sup> cap and ASALab<sup>TM</sup> software (ANT-neuro, Enschede, The Netherlands) recorded at 4000Hz sampling rate. Two patients responded well to therapy and had more than a 50% reduction in seizure frequency. The remaining two patients had an adverse reaction with an increase in their seizure frequency when compared to baseline. The second dataset was a prospective case study on 11 patients admitted to the epilepsy monitoring unit for long-term monitoring lasting several days during drug dose tapering. Each morning three-minute resting state EEG epoch was measured using the Micromed Experia EEG (32 electrodes), recorded with a 10-20 EEG system at the 2048 Hz sampling rate. The reference electrode is placed at the C1 position. We divided each epoch into twenty seconds time windows with sixteen seconds overlap and for each time window, the spectral norm of the signal's covariance matrix was calculated.

*Data Analysis.* From each resting state EEG three-minute epoch we chose a series of nine consecutive time-windows (52 seconds sub-epoch) for which the ratio of the standard deviation to the average value of the spectral norms is minimal. Further, for every time-window of the chosen sub-epoch, each EEG channel has been filtered using empirical decomposition (Huang transform) with stop criterion for the last level of having at least 1000 maxima. The functional connectivity for each time-window was reconstructed as explained above and MFC was calculated.

*Assessment of drug responsiveness and treatment prognosis.* For a given subject we average the measurements from the network connectivity  $G_k$  corresponding to each value from a set of strictly increasing levels of medication  $M_k, k = 1 \dots n, M_k < M_{k+1}$  and also take their standard deviations  $D_k$  as a measure of the connectivity fluctuations. The aim is to quantify the mutual relation between the two sets  $M$  and  $G$  and more specifically to assess to what extent  $G$  is a strictly monotonically decreasing function of  $M$  (drug dose positive effect). First we define the quantities:

$$Q_k \equiv \frac{G_{k+1} - G_k}{\max_k(G_k) - \min_k(G_k)};$$

$$S_k \equiv \frac{\sqrt{(D_k^2 + D_{k+1}^2)}/2}{\max_k(G_k) - \min_k(G_k)}; \quad k = 1 \dots n - 1, \quad (3)$$

This Equation introduces a measure of the relative fraction of connectivity change for each step of increase of the medication. The second equation accounts for possible variations in measured connectivity for the same medication doses, which would violate the strict monotonicity criteria. We can define the responsiveness at each consecutive increase of the medication dose as a percentage of the maximal effect:

$$R_k \equiv -100\% Q_k \frac{|Q_k|}{|Q_k + 2S_k|} \quad (4)$$

In eq. (4) the variation of response for the same medication level comes in the denominator as a “penalty” factor decreasing the effective shift in connectivity. The minus sign is to account for the fact that a positive drug effect is expected when global connectivity decreases. The overall responsiveness then can be conveniently defined as:

$$Res \equiv -100\% \frac{\sum_k Q_k}{\sum_k (|Q_k| + 2|S_k|)} \quad (5)$$

*Optimal dose assessment.* The optimal medication dose can be inferred by the relative amount of connectivity change caused by each increment of the medication dose:

$$M_{opt} \equiv M_v, v = \operatorname{argmax}(-Q_k) + 1 \quad (6)$$

In other words, the optimal dose is the one that gives the best shift in response when reached according to eq. (3).

### 3.3 Results

#### 3.3.1 Computational model

Changes in the local brain tissue parameter  $\mathbf{c}$  and connectivity matrix  $\mathbf{G}$  of the  $Z^6$ -model both resulted in changes in MFC. The association between the MFC and ictogenicity measure BNI for all connectivity matrices  $\mathbf{G}$  and transformation matrixes  $\mathbf{T}$  are shown in Fig 2. The modelling results indicated that MFC is highly associated with ictogenicity measure BNI, irrespective of whether fluctuations in MFC were driven by changes in connectivity matrix  $\mathbf{G}$  or local tissue parameter  $\mathbf{c}$ . We also found that MFC is associated above 90% on average to the local tissue & connectivity parameter fluctuations (not shown) for almost all network configurations and transformation matrixes.

#### 3.3.2 In vivo RS-EEG

The results of the dataset with two positive and negative responders and two negative responders are presented in Fig. 3. The positive responders show a reduction in MFC with the increase in medication dose. In contract, the negative responders showed an increase in MFC with the increase in dose. Almost all subjects in the second dataset showed small and most of the time insignificant decrease in MCF with the increase of the medication dose.

The overall assessment of the drug impact on the connectivity for all subjects is shown in Fig. 4.A. The two positive and negative responders shows that the connectivity can be controlled by the corresponding pharmacological agent. We note that one subject DT-10 of the EMU drug tapering dataset is considered a

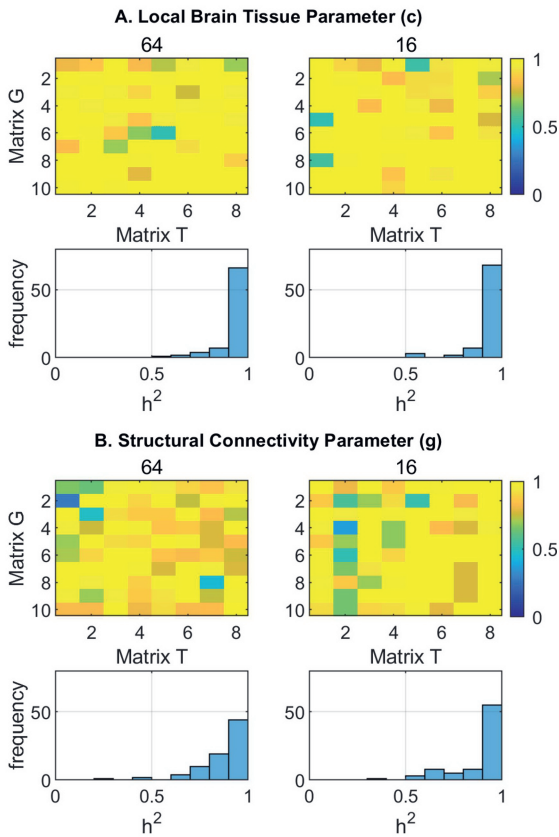


**Fig. 2.** In silico results for (a) local brain tissue parameter  $c$  and (b) structural connectivity parameter  $g$  variation. The top panels show the 64 and 16 channel EEG simulations, who each have ten rows for the ten connectivity matrices  $G$  and eight columns for the eight transformation matrices  $T$ . The colorcode shows the normalized value of the  $h^2$  between the MFC and the ictogenicity BNI measure. The bottom histograms show the frequency of each BNI-MFC  $h^2$  result for the corresponding 64 or 16 channel EEG simulations.

non-responder which scored relatively high responsiveness values. This subject's tonic-clonic seizures were in fact treated with medication, but this person still suffered from remaining focal seizures. They were thus responding only partially to medication. Their seizures under medication were less frequent and less severe although still present. Finally, Fig. 4.B illustrates a potential optimal medication dose prescription procedure. In the cases of a responder who was already seizure free after the first dose increase, we obtain at this dose  $>50\%$  biomarker decrease as fraction of the overall maximal decrease.

### 3.4 Discussion

The present study proposes a modelling-inspired methodology for assessment of ictogenicity of the brain from resting state EEG measurements. The results

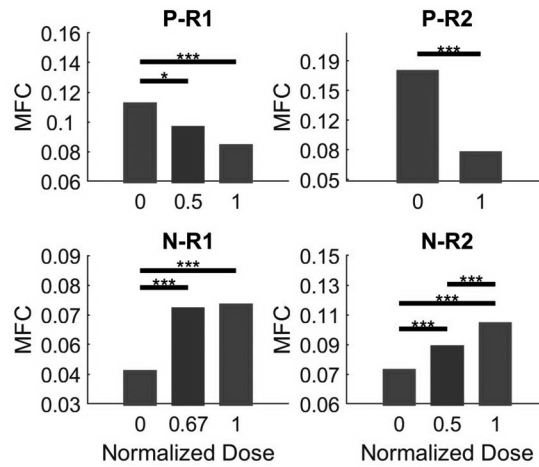


**Fig. 3.** The top row shows results of the positive and negative responders' dataset. The upper panels presents the MFC data for the positive responders, while the bottom panels present the data for the negative responders. Each panel shows the quantification of the level of significance of statistics of patient's MFC day values by performing a Mann-Whitney multiple comparative tests between the days based on the ANOVA test statistics, Bonferroni corrected for group comparison. Bars show the average value of MFC. The level of statistical significance of the differences between each couple of bars (within a panel) is presented through a black line over the bars couple, marked with one, two or three stars, corresponding to p-values accordingly of ( $p < 0.05$ ), ( $p < 0.01$ ), and ( $p < 0.001$ ).

showed that it is possible to assess the ictogenicity of the brain with high accuracy from the MFC measure inferred from RS-EEG segments. We used a general concept that the RS connectivity may explain the ictogenicity even when the functional-structural mapping is not present. A critical tool for this was the use of a nonlinear association measure reflecting the synchronization between the Hilbert envelopes of the signals. Using other correlation measures on the original EEG traces did not provide the desired results. This is conform with our core hypothesis that the epileptogenicity of brain tissue is reflected in the aggregated, large scale connectivity between brain area's expressed in amplitude correlations rather than in acute neuronal synchronization.

In our earlier work, using the same computational model, we have explored the option of analysing the properties of evoked responses to stimulations.<sup>8</sup> While this active paradigm may provide certain methodological advantages, the current

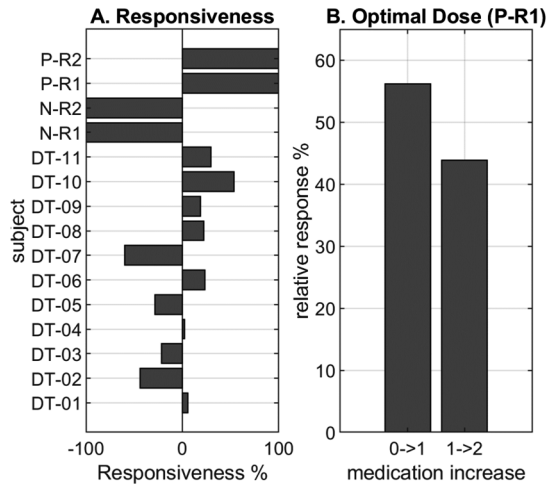


**Fig. 4.** (a) Analysis of drug responsiveness for all 15 subjects. The two drug responders and negative responders are indicated with P-R 1-2 and N-R 1-2 respectively. The 11 patients admitted to the EMU for drug tapering are indicated by DT1-11. Responsiveness shows, according to (6), the amount of total network connectivity change affected by the drug administration. The positive responders show maximal responsiveness of 100%, while both negative responders show -100% responsiveness. The DT patients all show relatively moderate responsiveness to their medication. (b) Relative fraction of epileptic biomarker decrease (vertical axis in %) of the global connectivity computed according to eq. (5) for subject (P-R1). The horizontal axis represents the two consecutive steps of dose increase.

approach allows to use retrospective data collected in monitoring facilities avoiding time consuming experimental protocols.

One critical issue associated with the use of RS-EEG data is the dependence of the results on selection of the data segments and especially on the subject condition. We can speculate that the dependency of functional/structural network's results on RS segment selection for the linear models of EEG synchronization provides a possible explanation for the relatively low reproducibility of some results in the field. Future studies using network-based methodology may at least consider the stability of the obtained results with regards to the RS epoch selection.

One application of the proposed methodology is to assess the effect of anti-epileptic drugs for particular patients. The *in vivo* RS-EEG results show that in case of positive responders (seizure free under medication) there is a significant

association between the medication dose and the proposed ictogenicity assessment through the MFC. In contrast, in non-responders the association between dose and MFC was erratic without clear monotonic shape or even indicating opposite trend of increased connectivity with the medication. The positive and negative responders were correctly identified by means of an appropriate quantifier of the above associations. These findings however need further validation with various types of epilepsy as well as larger variety of anti-epileptic drugs. Especially challenging in this effort is collecting data from clear responders. Those cases are not candidates for epilepsy surgery and accordingly long-term monitoring under changing medication levels in specialized clinical facilities is seldom performed. This last limitation is also affecting the second clinical objective in this work, the derivation of an objective scheme for determining the optimal medication dose.

The simulations using networks of different size show that the degree of explanation of BNI with structural and functional network measures is invariant with respect to network size. The result indicates that one may use networks with a small number of nodes to generate hypothesis for the larger network's dynamics. We also note that the MFC measure does not reflect the structural connectivity only, as our results show it can also account for a larger variety of underlying parameters that can be associated with the epileptic state (in our model exemplified by the local self-coupling parameter  $c$ ). We hypothesize that our result might be valid not only for the explored  $Z^6$ -model, but it might represent a common feature of all the multi-stable models.

From a pure modelling perspective, the importance of the results in this study is also in the establishment of the correspondence between the proposed functional connectivity measure, based on RS-EEG segment choice, and the underlying overall structural connectivity that is model specific. We have shown that this correspondence is largely independent on the specific topology of the connections and on the mixing model describing the EEG signal formation from the underlying neuronal dynamics. To our best knowledge, neither of those issues has been addressed earlier. While it is unclear to what extent we can generalize the above finding, using broader range of models of epilepsy may be

advantageous to further explore the limits of application of MFC as an ictogenicity biomarker.

### **3.5 Conclusion**

This present study proposes a model derived methodology for assessment of the effect of anti-epileptic drugs on the ictogenicity of the brain through biomarkers reconstructed from RS-EEG measurements. The method is based on hypotheses generated by computational model of epileptic state and transitions. The technique can be used within the routine long term monitoring diagnostic protocol and requires no additional hardware. If further successfully validated in larger cohort of patients, it can be used for early forecast of the effectiveness and optimal dose of ASM.

## References

1. Berg, A. T. *et al.* Revised terminology and concepts for organization of seizures and epilepsies: Report of the ILAE Commission on Classification and Terminology, 2005-2009. *Epilepsia* **51**, 676–685 (2010).
2. Kim, M., Kim, S., Mashour, G. A. & Lee, U. Relationship of topology, multiscale phase synchronization, and state transitions in human brain networks. *Front. Comput. Neurosci.* **11**, (2017).
3. Honey, C. J. *et al.* Predicting human resting-state functional connectivity from structural connectivity. *Proc. Natl. Acad. Sci. U. S. A.* **106**, 2035–2040 (2009).
4. Kalitzin, S. N., Velis, D. N. & Lopes da Silva, F. H. Stimulation-based anticipation and control of state transitions in the epileptic brain. *Epilepsy Behav.* **17**, 310–323 (2010).
5. Kalitzin, S., Koppert, M., Petkov, G. & Da Silva, F. L. Multiple oscillatory states in models of collective neuronal dynamics. *Int. J. Neural Syst.* **24**, 1450020 (2014).
6. Petkov, G., Goodfellow, M., Richardson, M. P. & Terry, J. R. A critical role for network structure in seizure onset: A computational modeling approach. *Front. Neurol.* **5**, (2014).
7. Kalitzin, S. N., Parra, J., Velis, D. N. & Da Silva, F. H. L. Quantification of unidirectional nonlinear associations between multidimensional signals. *IEEE Trans. Biomed. Eng.* **54**, 454–461 (2007).
8. Petkov, G. *et al.* Computational model exploration of stimulation based paradigm for detection of epileptic systems. in *Frontiers in Artificial Intelligence and Applications* vol. 310 324–335 (2018).



# Chapter 4

TMS-evoked EEG potentials demonstrate altered cortical excitability in migraine with aura

Based on:

**Helling RM**, Perenboom MJL, Bauer PR, Carpey J.A., Sander JW, Ferrari MD, Visser GH, Tolner EA. TMS-evoked EEG potentials demonstrate altered cortical excitability in migraine with aura. *Brain Topography*. 2023;36(2):269-81.

DOI: 10.1007/s10548-023-00943-2

## Abstract

Migraine is associated with altered sensory processing, that may be evident as changes in cortical responsivity due to altered excitability, especially in migraine with aura. Cortical excitability can be studied directly by combining transcranial magnetic stimulation with electroencephalography (TMS-EEG). We measured TMS evoked potential (TEP) amplitude and response consistency as these measures have been linked to cortical excitability but were not yet reported in migraine.

We recorded 64-channel EEG during single-pulse TMS on the vertex interictally in 10 subjects with migraine with aura and 10 controls matched for age, sex and resting motor threshold. On average 160 pulses around resting motor threshold were delivered through a circular coil in clockwise and counterclockwise direction. Trial-averaged TEP responses, frequency spectra and phase clustering (over the entire scalp as well as in frontal, central and occipital midline electrode clusters) were compared between groups, including comparison to sham-stimulation evoked responses.

Migraine and control groups had a similar distribution of TEP waveforms over the scalp. In migraine with aura, TEP responses showed reduced amplitude around the frontal and occipital N100 peaks. For both migraine and control groups, responses over the scalp were affected by current direction for the primary motor cortex, somatosensory cortex and sensory association areas, but not for frontal, central or occipital midline clusters.

This study provides evidence of altered TEP responses in-between attacks in migraine with aura. Decreased TEP responses around the N100 peak may be indicative of reduced cortical GABA-mediated inhibition and expand observations on enhanced cortical excitability from earlier migraine studies using more indirect measurements.

## 4.1 Introduction

Migraine is a brain disease characterized by recurring attacks of severe headaches, accompanied by other neurological symptoms like nausea, vomiting and sensitivity to light and sound.<sup>1</sup> Visual aura before the headache phase, experienced by about one third of people with migraine, is a transient focal symptom likely due to cortical spreading depolarization in the visual cortex.<sup>2</sup> People with migraine report increased visual sensitivity between and during attacks compared to healthy controls,<sup>3,4</sup> which appears most prominent in those with visual aura symptoms.<sup>5</sup> Altered visual cortex responsivity,<sup>6</sup> that could be caused by changes in cortical network excitability may explain these symptoms. However, both hyperexcitability<sup>7,8</sup> and hypoexcitability<sup>6</sup> have been suggested as underlying mechanism, largely based on indirect measures of cortical excitability.

Transcranial magnetic stimulation (TMS) has been one of the methods used to study cortical excitability in migraine, using subjective or indirect readouts.<sup>9</sup> Magnetophosphenes induction, by applying TMS over the occipital cortex while registering the reported threshold of perceived visual responses, is a direct but subjective measure of visual cortex excitability.<sup>10</sup> A meta-analysis suggested decreased phosphene thresholds in migraine with and without aura compared to controls when a large circular coil was used. More localized stimulation using a figure-of-eight coil resulted in increased phosphene prevalence in subjects with aura, and not in those without aura or controls.<sup>11</sup> Studies on motor cortex excitability have used the muscle response to single pulse TMS as indirect readout by determining a resting motor threshold (rMT). This threshold does not reflect cortical excitability exclusively, as subcortical pathway excitability will also affect muscle responses.<sup>12</sup> Using this method, no changes were demonstrated between migraine with or without aura in-between attacks and controls.<sup>9</sup> Stimulus response curves of the motor response recorded by varying stimulation intensity showed contradictory patterns in migraine as well, with indications of motor cortex hyperexcitability at high stimulus intensities.<sup>13,14</sup> Motor responses to short-burst repetitive TMS differed over the migraine cycle for migraine with and without aura, which relates TMS-induced measures to cyclic changes in cortical excitability.<sup>15</sup>

Advances in electroencephalography (EEG) amplifier technology allow direct recordings of the cortical network response to TMS.<sup>16</sup> Using TMS-EEG, magnetically evoked cortical responses can be evaluated as direct and objective markers of cortical responsivity, and provide information on changes in network excitation or inhibition.<sup>17</sup> Single pulse stimulation at one location generates responses measurable over the entire scalp, enabling comparison of cortical excitability across cerebral regions.<sup>18</sup> The TMS-evoked potential (TEP) follows a specific pattern, of which peak amplitudes are altered by neuroactive drugs that modulate excitatory or inhibitory neurotransmission.<sup>19,20</sup> TEP amplitudes are also affected in conditions such as epilepsy and schizophrenia in which altered cortical excitability is implicated.<sup>21,22</sup> TEPs, however, have not yet been assessed in the context of migraine. In addition to amplitude characteristics, the phase of frequency components in evoked potentials<sup>23</sup> and ongoing EEG<sup>24</sup> also contains relevant information on cortical excitability. Occipital phase clustering of visually evoked responses between repetitions is predictive of a photoparoxysmal response in photosensitive epilepsy,<sup>25</sup> suggesting a relation between consistency of phase responses across stimulation trials and excitability levels.

We aimed to study possible alterations in cortical excitability directly using TMS-EEG in subjects with migraine with aura (in-between migraine attacks) and controls. Using a circular TMS coil, we induced broad, scalp-wide activation thus not limiting the study to a predefined local stimulation site. The combination with EEG allowed us to explore local alterations in cortical excitability over the whole scalp based on local changes in TEP responses as direct measure of cortical excitability. We compared TEPs over the entire scalp to study the distribution, amplitude and phase characteristics of response patterns at frontal, central and occipital electrode clusters along the midline. These readouts could provide objective parameters on cortical excitability and allow identification of migraine-specific changes in excitability across cerebral regions including the visual cortex.

## 4.2 Methods

### 4.2.1 Participants

Participants (aged 18 or over) were recruited locally through digital and paper adverts and through the LUMINA study population of the Leiden University Medical Centre.<sup>26</sup> Matching controls were selected from a cohort of 38 healthy controls that have been described elsewhere.<sup>27</sup> Migraine diagnosis was based on the International Classification of Headache Disorders (ICHD-3-beta) criteria.<sup>28</sup> Subjects with migraine headache preceded by visual aura in at least 30% of the attacks were included. Participants had to have at least 1 migraine attack per year, at least one in the year preceding the study and no more than eight attacks or 15 headache days per month (thus excluding chronic migraine). People using prophylactic migraine medication were not included. Experimental sessions were performed at least 72 hours after a migraine attack. Sessions that were followed by a migraine attack within 72 hours, verified by follow-up, were excluded.

Participants with migraine were matched with controls based on age, gender and rMT. Matching on rMT was performed to correct for effects of stimulation intensity and thereby prevent possible differences in threshold between groups to confound TEP readouts. Only controls without a history of epilepsy or migraine were included. Participants (with migraine and controls) with contraindication to TMS, pregnant women and people with diabetes mellitus, psychiatric conditions and people using medication that could affect cortical excitability (such as psychoactive drugs and beta-blockers) were excluded. We established that participants did not smoke, used drugs or drank alcohol or coffee in the 12 hours preceding the measurement and to maintain a normal sleep pattern the night prior to the measurement. Written informed consent was obtained from all individual participants included in the study. The study was approved by Ethical Committee of Erasmus University Medical Centre, Rotterdam, the Netherlands, and conducted according to the Declaration of Helsinki.

### 4.2.2 Recording setup

*Transcranial Magnetic Stimulation.* TMS was performed with a MagPro X100 magnetic stimulator (Magventure, Denmark), a 14 cm diameter parabolic circular coil (type MMC-140) using biphasic pulses with a width of 280  $\mu$ s, to activate a

large region of the cortex, including the motor cortex,<sup>29</sup> or a sham coil (type MCF-P-B65). Measurements were conducted between 09.00 AM and 04.00 PM and distributed evenly between AM and PM in both participant groups. Soft foam earplugs were used to dampen the TMS-induced coil click.

*Electromyography.* Motor evoked potentials were recorded bilaterally from the Abductor Pollicis Brevis muscles with a Nicolet Viking EDX electromyograph (Natus, Madison, WI, USA). Muscle activity was monitored using real-time visual feedback. Data were recorded with a sampling frequency of 4 kHz and stored for offline analysis.

*Electroencephalography.* EEG was recorded during the TMS sessions with a 64-channel TMS-compatible EEG system (Waveguard™ cap and ASAlab™ software, ANT Neuro, Enschede, The Netherlands), a sampling frequency of 4 kHz and a common average reference. Electrode impedance was kept below 5 kOhm during the experiment. Participants were seated in a comfortable chair with their eyes open and arms in supine position. Prior to stimulation, baseline EEG was recorded for 10 minutes with eyes open (5 min) and closed (5 min).

#### 4.2.3 *Single pulse TMS protocol*

To be suitable for clinical settings, the stimulation protocol we employed was designed to be short while yielding maximum information at once.<sup>27</sup> The stimulation procedure was performed using counterclockwise (right hemisphere) and clockwise (left hemisphere) stimulation. With the centre of the circular coil on electrode position Cz (vertex) the rMT, defined as lowest stimulation intensity evoking motor evoked potentials larger than 50  $\mu$ V in 50% of the trials,<sup>30</sup> was determined. Then, a semi-automated, in-house designed stimulation protocol (created in Matlab® (release 2007b, The MathWorks, Natick, MA)) was used to deliver stimuli with a frequency of 0.5 Hz.<sup>31</sup> Stimulation started at a stimulator output value of rMT minus 10% and increased in 2% steps until a reproducible motor evoked potential ( $>200 \mu$ V) was seen after every stimulus ( $\pm 110$ -120% rMT). At each intensity 20 stimuli were given and aggregated for TEP analyses to limit the participant's exposure to TMS stimuli. This stimulation procedure was repeated for the sham protocol using the sham coil, including the stepwise increments in stimulation intensity with matching intensities to the active coil.

#### 4.2.4 Data analysis

*Data pre-processing* Off-line analyses were performed in Matlab® (release 2015a) using custom-written scripts and the FieldTrip Matlab toolbox.<sup>32</sup> A TMS-EEG artefact removal pipeline was used to eliminate ringing, decay, muscle and eye movement artefacts.<sup>31</sup> Only trials performed at stimulation intensities between +0% and +6% stimulator output relative to the averaged rMT of two hemispheres were pooled and used for further analyses. All the datasets, both active and sham stimulation, were split in trial epochs starting 1 s before and ending 1 s after the TMS pulse. Ringing artefacts were segmented out from 0 to 6 ms relative to the time of stimulation and baseline corrected using the window from -200 ms to -1 ms relative to the start of the stimulus. Electrodes showing contaminated activity (e.g. excessive line noise) over the averaged trials were removed for each participant (average: 1 channel per participant, range: 0-4 channels). EEG data were then re-referenced to the common grand average of all non-interpolated EEG channels.

Next, independent component analysis (ICA) was used to remove exponential decay artefacts, recharge artefacts, eye blinks, eye movements and line noise for both the active coil and sham datasets. A maximum of 63 components were extracted from the data (number of components equal to the number of non-interpolated EEG channels minus 1), on average 8 components were removed in the first round of ICA (range: 3-18 components). The ICA decomposition was back-projected to the channel level after removal of the independent components containing the artefacts. Trial epochs were shortened to windows starting 200 ms before and ending 600 ms after the TMS pulse, followed by a second round of ICA to remove muscle related artefacts and remaining line noise artefacts (average of 8 components, range: 4-15). After reconstruction of the channel level data the split trials were re-combined. To completely remove residual time-locked muscle artefacts not captured by ICA, cubic interpolation was used from -1 ms to 15 ms around the stimulus. Next, some additional pre-processing steps were performed, dependent on the type of analysis (time-amplitude or time-frequency), as specified below.

*Time-amplitude processing.* Individual trials were baseline corrected and band-pass filtered between 1 and 80 Hz using a 3th order Butterworth filter. Removed electrodes were spherically interpolated. Trials were visually inspected and those

which still showed contaminated activity were discarded. The resulting dataset consisted of 80 trials per current direction per participant (excluding removed trials). The TEP waveform was averaged over all trials and per current direction for each electrode. In addition, the global mean field power (GMFP), was calculated over both current directions and for each current direction separately.<sup>33</sup>

*Time-frequency processing.* Frequency spectra and phase clustering index<sup>34</sup> were calculated at all electrodes using Morlet wavelets. Three cycles/frequency were used for high temporal resolution, in 1 Hz frequency steps between 5 and 80 Hz and 5 ms time steps. To limit the number of comparisons (time-frequency versus time-frequency-electrode points) and to study in particular occipital responses in migraine with aura, the frequency spectra and phase clustering index were compared for the three a priori defined frontal, central and occipital electrode clusters. Phase clustering index values vary between 0 (random phase clustering between trials) and 1 (all trials have equal phase clustering) per time-frequency point.

#### 4.2.5 Statistical analysis

Magnetic or sham stimulation responses were compared between migraine and control groups for the window from 20 to 200 ms after stimulation (720 samples per channel at 4000 Hz sampling rate with a total of 62 channels). Within this time window the commonly reported TEP peaks are present across all channels (Suppl. Fig. 2), allowing time-electrode cluster analysis of evoked activity. Statistical analysis was performed over all channels within the specified window for the combined dataset (with pooling of both current directions). To investigate consistency of the results, we also repeated the statistical analysis for each current direction separately.

TEPs were compared between groups using dependent *t*-tests (using the matched case-control design) at all samples within the pre-defined time window for the electrodes. In addition, we identified three regions of interest a priori: frontal (electrodes F1, F2, Fz, FCz, AF4, AF3), central (Cz, C1, C2, CPz, CP1, CP2) and occipital (Oz, O1, O2, POz, PO3, PO4), to limit the number of comparisons and to especially study occipital responses in migraine with aura. Exact *p*-values were calculated by enumeration using cluster-based permutation testing to correct for multiple comparisons and the small sample size<sup>35</sup> using the

FieldTrip Matlab toolbox.<sup>32</sup> Clusters based on adjacency in time and electrode space were formed using samples with a cluster-alpha of 0.10 (independent  $t$ -test). This threshold allows for detection of larger clusters in the time-electrode space, without selection of separate clusters of single time-electrode points detected at  $p < 0.05$  as a cut-off.<sup>35</sup> Within each cluster,  $t$ -values (for both time samples and electrodes) were summed and compared to a dataset of all possible combinations of the original data (1024 combinations using the matched pair design). Clusters were considered significantly different between groups when their summed  $t$ -values were lower or higher than 2.5% ( $p < 0.025$ ) of all permuted clusters.

### 4.3 Results

Ten individuals with migraine were assessed (9 females, 1 male; mean age 41 years, range 21-62; 3 left-handed), who were also included in previous research.<sup>27</sup> The migraine attack frequency was between 0.3 and 2 per month (average of 0.9 attacks). Ten controls were included. Characteristics of participants, including sex, age, attack frequency and duration, are summarised in Table 1. Data from the individual participants with migraine are summarized in Supplementary Table S1. All participants tolerated the experimental sessions. No migraine attacks were reported in the 72 hours following the experiment.

**Table 1.** Demographic, clinical and experimental data for healthy controls and migraine patients with aura reported as mean ( $\pm$  SD) or number.

	Control	Migraine with aura
No. (female / male)	10 (9/1)	10 (9/1)
Age [years]	39.8 ( $\pm 11.1$ )	41.0 ( $\pm 12.6$ )
Age at onset [years]	-	17.8 ( $\pm 4.5$ )
Attack frequency [/month]	-	0.9 ( $\pm 0.6$ )
Mean headache duration [hrs]	-	25 ( $\pm 19$ )
Aura frequency [% of attacks]	-	86 ( $\pm 28$ )
rMT [%]	41.1 ( $\pm 6.6$ )	41.3 ( $\pm 4.4$ )
Number of pulses	298 ( $\pm 29$ )	293 ( $\pm 35$ )
Removed ICA components	8.1 ( $\pm 2.7$ )	7.4 ( $\pm 1.9$ )

*rMT: resting motor threshold; ICA: independent component analyses*

### 4.3.1 Effect of TMS current direction

First, possible differences between clockwise and counterclockwise stimulation trials were analysed within all subjects (60-80 trials per participant), combining migraine and control groups. The GMFP for both current directions and the combined dataset was computed (Fig. 1). Averaged TEP waveforms did not differ between polarities over time and electrodes for frontal ( $p=0.28$ ), central ( $p=0.20$ ), and occipital waveforms ( $p=0.30$ ), but differed when analysed over the entire scalp ( $p=0.004$ ; Suppl. Fig. 1A). The difference clusters were present over primary motor and somatosensory cortices (Suppl. Fig. 1B), likely due to the relationship between current direction and preferential activation.<sup>36</sup> Clockwise and counterclockwise trials were grouped for further analyses, and, as secondary outcome, also analysed per current direction. The GMFP and the corresponding topographical distributions are visualized in Fig. 2. Although the averaged TEP waveforms differed between current direction over the scalp in response to stimulation at Cz, they were of similar shape at the same electrode locations for migraine and control groups (Suppl. Fig. 2).

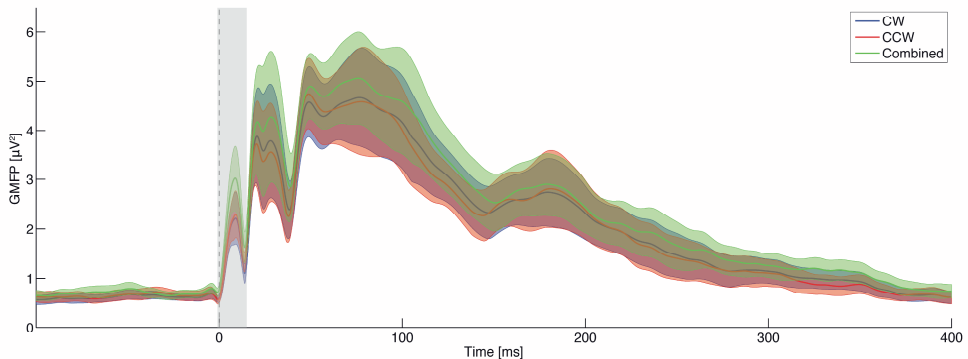


**Fig. 1.** In controls and people with migraine the global mean field power (GMFP) of the average TEP responses show no waveform differences (i.e. direction and delay of the various peaks) with comparable peak distributions between clockwise (blue line) and counterclockwise (red line) current direction and when both current directions are combined (green line) Plot shows mean and patched standard error, the grey bar indicate the spherically interpolated parts of the EEG traces (-1 to 15 ms). *CW*: clockwise; *CCW*: counterclockwise.

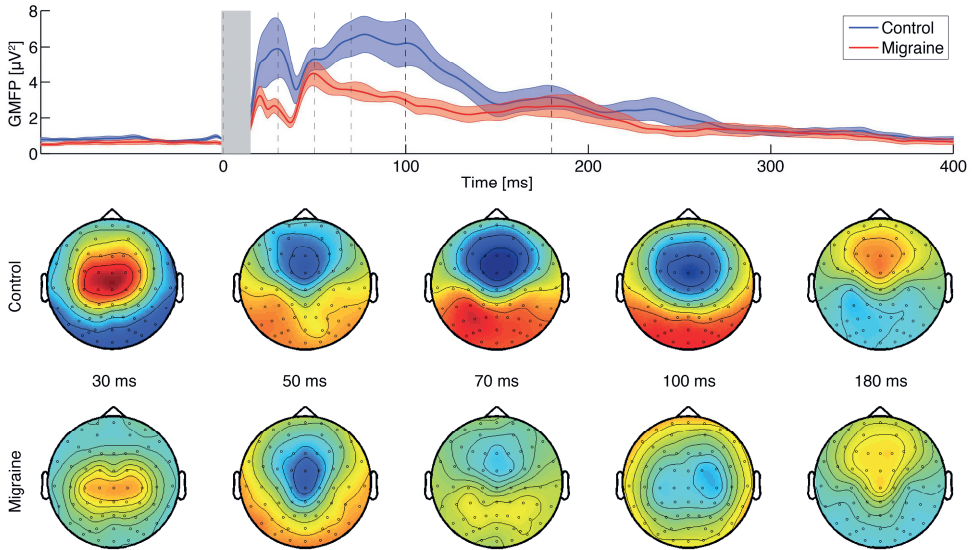


**Fig. 2.** Comparison of the global mean field power (GMFP) of the TMS-evoked potentials of the combined clockwise and counterclockwise trials between control (blue) and migraine groups (red). Top plot shows mean and patched standard error, the grey bar indicate the spherically interpolated parts of the EEG traces (-1 to 15 ms) and dashed black lines the time corresponding to the topoplots. Bottom: the corresponding topographical plots for the P30, P50, P70, N100, and P180 peaks.

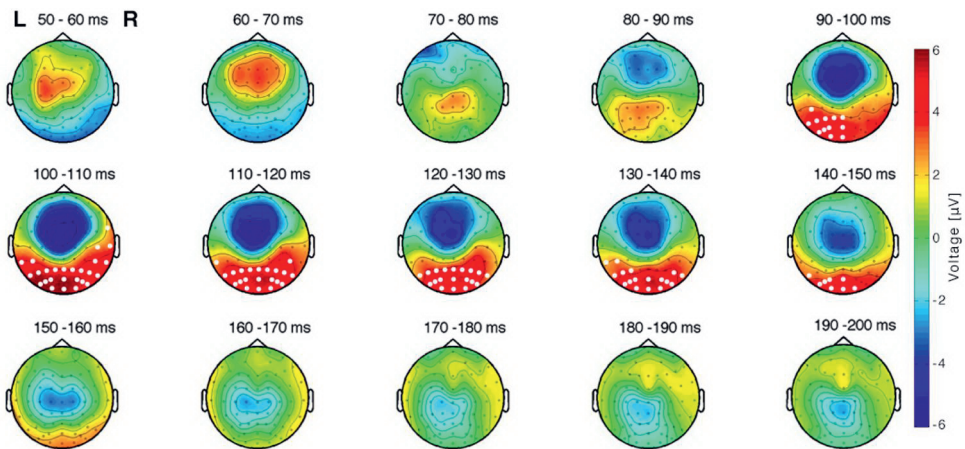


**Fig. 3.** Topographical plots of difference in TEP amplitude between controls and migraine subjects show one distinct difference component. Plots display the averaged difference (control minus migraine) in 10-ms windows between 50 and 200 ms. Note that statistical analyses were carried out per ms; results were pooled in 10-ms bins for visualization purposes only. The significant cluster is highlighted over time with white dots at the significantly differing electrode positions, mainly located over the occipital cortex between 90 and 150 ms.

### 4.3.2 Sham stimulation evoked potentials

Evoked responses induced by sham stimulation (averaged over 80 trials) showed a clear N100-P180 auditory complex<sup>37</sup> (Suppl. Fig. 3 and 4) in both healthy controls and participants with migraine. Averaged waveforms after sham stimulation did not differ between migraine and controls over time and all electrodes ( $p=0.59$ ) nor over the predefined electrode groups (all  $p>0.28$ ).

### 4.3.3 TMS evoked responses

No significant differences were observed for the peak-to-peak amplitude analysis of the motor evoked potentials for people with migraine compared to their matched controls (Suppl. Table S2).

Cluster-based permutation analysis of TEP amplitudes over time and electrodes showed a significant difference in the a priori selected time interval between 20 and 200 ms after stimulation ( $p=0.012$  for combined polarities,  $p=0.013$  for CW stimulation and  $p=0.018$  for CCW stimulation) for people with migraine compared to controls. The revealed cluster was grouped around the N100 peak, between 60 and 120 ms after stimulation, and located mainly at the occipital cortex (Fig. 3). When analysed in the predefined electrode groups (frontal, central and occipital), no statistically significant difference was present at the central electrodes ( $p=0.050$  for combined polarities,  $p=0.060$  for CW stimulation and  $p=0.025$  for CCW stimulation). The N100 peak, however, was smaller in the migraine group at the frontal electrodes ( $p=0.009$  for combined polarities,  $p=0.019$  for CW stimulation and  $p=0.009$  for CCW stimulation). The largest difference in the frontal cluster ( $4.9\pm 0.9$   $\mu\text{V}$ ) was present at 77 ms after stimulation (Fig. 4A). Also at the occipital cortex, the N100 peak was decreased in people with migraine compared to controls ( $p=0.008$  for combined polarities,  $p=0.009$  for CW stimulation and  $p=0.005$  for CCW stimulation). Here, the largest difference ( $5.9\pm 0.9$   $\mu\text{V}$ ) was found at 78 ms after stimulation, similar to the frontal cluster (Fig. 4B). The TEP P180 peak between 120 and 180 ms was not different for any of the electrode locations in people with migraine compared to controls, as no significantly different clusters were found.

*Post hoc* analysis of the TEP responses with sham responses subtracted revealed similar results (Suppl. Fig. 5), albeit with slight differences in cluster sizes and their  $p$ -values. For the comparison over time and all electrodes we observed a

significant difference in the a priori selected time interval between 20 and 200 ms after stimulation ( $p=0.008$  for a positive and  $p=0.0167$  for a negative cluster for combined polarities, a single positive cluster  $p=0.0156$  for CW and no significant cluster for CCW stimulation) for people with migraine compared to controls. The observed cluster was grouped around the N100 peak between 60-120 ms after stimulation and located mainly at the occipital cortex. When analysed in the predefined electrode groups (frontal, central and occipital), the N100 peak was smaller in the migraine group at the frontal cortex ( $p < 0.001$  for combined polarities,  $p=0.005$  for CW stimulation and  $p=0.041$  for CCW stimulation) and occipital cortex ( $p=0.009$  for combined polarities,  $p=0.012$  for CW stimulation and  $p=0.0016$  for CCW stimulation) electrodes when compared to controls. For the central electrode cluster a significant difference was present only for the CCW stimulation ( $p=0.035$  for combined polarities,  $p=0.038$  for CW stimulation and  $p=0.008$  for CCW stimulation).

Time-frequency analyses between 20-200 ms and for the 5-80 Hz frequency bands, of spectral power and phase clustering over trials within the time-frequency domain, resulted in no significant clusters for any of the comparisons made. The statistics are reported in the Supplementary Results.

#### **4.4 Discussion**

Our data show altered cortical EEG responses to transcranial magnetic stimulation in-between attacks in migraine with aura compared to controls. We demonstrated that TEP amplitude waveforms in migraine with aura are distinct from those in healthy controls, by displaying a reduced amplitude around the frontal and occipital N100 peak. No difference was observed between people with migraine and controls in the distribution of waveforms over the entire scalp. We cannot rule out, however, that the N100 amplitude reduction observed for migraine may (in part) reflect differences in sensory activation between groups that were not adequately compensated for by the utilized sham protocol without a sound masking procedure or electrical stimulation component. Our findings nevertheless suggest that TEP features could be suitable markers of cortical excitability changes in migraine. Alterations in cortical excitability over the

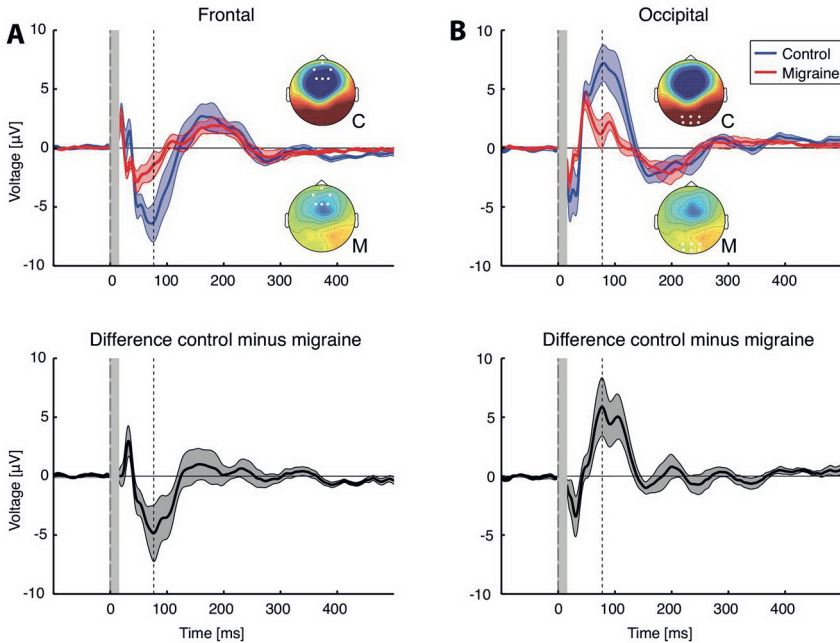


**Fig. 4.** Grand-averaged TEP responses and difference waveform (control minus migraine) at frontal (F1, F2, Fz, Fpz, AF4, AF3) and occipital (Oz, O1, O2, POz, PO3 and PO4) electrodes show differences in TEP peaks between controls and migraine subjects. Two separate components of a negative waveform cluster were found using exact cluster-based permutation testing (enumeration). (a) Migraine group (red line) shows decreased frontal activity around the TEP N100 peak compared to control group (blue line), with largest difference of  $-4.9 \mu\text{V}$  at 77 ms after stimulation (dashed line). Bottom plot shows the difference between migraine and control groups (standard error of the mean calculated using 10,000 bootstraps over both groups). (b) Occipitally, the TEP N100 peak decreased as well in migraine, with largest difference of  $-5.9 \mu\text{V}$  at 78 ms after stimulation (dashed line). Bottom plot shows the difference between migraine and control groups. Insets show topographical distribution in control (C) and migraine (M) at the time point of maximal difference with electrodes highlighted in white dots. Traces show grand-averaged mean with patched standard error. The grey bars indicate the spherically interpolated parts of the EEG traces (-1 to 15 ms).

migraine cycle, as indicated by indirect studies of brain excitability,<sup>15</sup> could possibly be studied by longitudinal application of TMS-EEG.

Analyses of TEP waveforms showed two distinct regions in which the N100 amplitude responses were decreased in migraine with aura: i) at the level of the frontal cortex, and ii) at the level of the occipital cortex. Our finding of a *decreased* N100 peak may reflect decreased cortical inhibition at the level of the frontal

and occipital cortex, since *increased* N100 peak amplitude has been indicated to reflect increased inhibitory GABA<sub>B</sub> mediated receptor activation.<sup>19,38</sup> A larger N100 peak in epilepsy was attributed to increased activation of inhibitory circuits as a possible result of the use of anti-epileptic drugs, which could have enhanced GABA-ergic activity.<sup>22</sup> The physiological underpinnings of various TEP peaks are, however, not straightforward.<sup>39,40</sup> While some studies report a linear dependency of the GABA<sub>B</sub>-ergic effect on N100 and P180 TEP peak amplitudes,<sup>19,41</sup> other studies only report a direct effect of GABA<sub>B</sub> on the N100 peak, but not the P180 peak amplitude.<sup>19,42</sup>

The frontal cortex was suggested to play a role in controlling pain processing in migraine. Reduced EEG-based activation of the anterior-medial prefrontal cortices during contact-heat stimuli in migraine with aura was interpreted as a heightened state of readiness to anticipated pain, compared to controls.<sup>43</sup> Also, the dorsolateral pre-frontal cortex (DLPFC) inhibits cortical as well as subcortical pain pathways.<sup>44</sup> If decreased DLPFC cortical inhibition represents reduced DLPFC inhibitory output, it could contribute to enhanced pain perception in migraine. Alternatively, if decreased DLPFC cortical inhibition represents reduced intracortical inhibition within the DLPFC, this would be expected to result in an enhanced inhibitory output from the DLPFC on cortical and subcortical pain processing. This could be hypothesized to represent a protective mechanism against recurrent headaches in episodic migraine. Indeed, modulating DLPFC activity using high-frequency repetitive TMS decreased the number of monthly attacks in chronic migraine.<sup>45</sup> This suggests a role for the frontal cortex in migraine susceptibility, although the precise contribution of GABAergic inhibition remains unclear.

The observed decreased occipital TEP waveform around the N100 peak in migraine patients may also be explained by a decrease in cortical GABAergic inhibition, as indicated by TEP studies in healthy subjects.<sup>19</sup> With repeated visual stimulation in migraine, a decrease in habituation was attributed to lateral inhibitory processes in the thalamocortical network that was suggested to be mediated by GABAergic neurons in the occipital cortex.<sup>46</sup> Preclinically, single pulse TMS applied to the occipital cortex in rodents increased the threshold for inducing cortical spreading depolarization, the neurobiological correlate of the migraine aura, in the visual cortex.<sup>47</sup> GABA<sub>A/B</sub> antagonists reversed this effect,

which indicates that TMS can suppress cortical neuronal activity by influencing GABAergic circuits.<sup>47</sup> Paired pulse TMS to study short-interval intracortical inhibition could be used to further investigate the role of GABAergic networks in altered cortical responsivity in migraine.<sup>48</sup>

A decreased N100 peak was related to disrupted phase coherence in patients with Huntington's Disease.<sup>41</sup> We found no altered phase clustering in people with migraine while the TEP N100 amplitude was decreased compared to controls. However, our approach of full TEP waveform analyses instead of peak amplitude extraction limits the possibility of a direct comparison. In future studies, the electrode clusters and time windows of interest as revealed by our exploratory approach could be used to further explore the relationship between TEP amplitude and phase coherence in migraine.

A critical limitation of our study is the concern that the EEG response to TMS-related sound and sensory activation may differ between migraine patients and controls. TEP N100 and P180 peaks have been associated with auditory evoked responses<sup>37</sup> and somatosensory activation.<sup>39</sup> With realistic sham stimulation at different locations on the scalp, activation patterns similar to TEPs have been measured with prominent N100 and P180 peaks.<sup>39,49,50</sup> However, especially the N100 peak has been related to cortical excitability using direct intervention with benzodiazepines,<sup>51</sup> in line with our finding that the P180 peak was not changed in people with migraine. As sensory processing of different modalities, including differences in the processing of auditory stimuli, appears altered in migraine,<sup>52</sup> the sound of the coil click during stimulation could partially explain observed differences in the TEP N100 response. However, we controlled for auditory as well as vibration-related effects of TMS by using sham stimulation, which produces a coil click and mechanical vibrations matched to those of the active coil. Furthermore, all participants wore soft foam earplugs during real and sham stimulation. In our *post hoc* analyses we subtracted sham waveforms from the TEP, assuming a linear interaction between active and sham responses. Similar results were obtained as with the TEP based analyses, indicating that differences between migraine and control groups in our study may reflect alterations in cortical excitability, but could also be due to differences in sensory activation not adequately compensated for by the used sham protocol. A linear subtraction, however, is limited in its application as the brain is a complex dynamical system

with many nonlinear interactions, also between different types of somatosensory stimulation.<sup>49,53</sup> Modern sham stimulation, including an electric stimulation component to evoke somatosensory evoked potentials, shows activation patterns highly similar to TEPs with prominent N100 and P180 peaks,<sup>49,50</sup> indicating that those peaks are at least partially generated by somatosensory and/or auditory potentials. Those studies used below rMT stimulation intensities to limit the impact of sensory re-afferents, which as a trade-off may have limited the amplitude and phase locking of any late evoked cortical potentials. This contrasts with our work where we utilized stimulation intensities around and above rMT (i.e. ranging from +0% to +6% stimulator output relative to rMT) without active noise masking (i.e. only foam ear-plugs) and observed N100 peaks with much higher amplitudes when compared to the sham evoked potentials. Considering that we observed no differences in evoked motor responses (Suppl. Table S1) and that the location of the observed N100 cluster differed from those of the CW versus CCW comparison, we consider it unlikely, but cannot rule out, that the observed results are attributable to differences in processing of the motor responses by sensory re-afferents of peripheral muscles. Another group explored the input-output curves of TEPs, ranging from 20% rMT to 120% rMT, using modern sham with an electrical stimulation component.<sup>40</sup> They observed TEP waveforms with region-specific profiles depending on stimulation location, including differences in the waveforms of the late components at higher stimulation intensities. The interpretation of TMS evoked potentials and the origin of peaks is thus anything but straightforward and remains difficult and ambiguous. Future studies can address the contribution of auditory and sensory components to the TMS-evoked response features in migraine by using a realistic sham stimulation, such as synchronous sound masking and an electrical stimulation component for masking skin sensation.<sup>49,54</sup>

Besides the used sham procedure, there are additional methodological limitations and considerations. Firstly, to improve artefact removal using independent component analysis, we combined trials at suprathreshold stimulation intensities and both current directions. The signal-to-noise ratio of our waveforms, frequency spectra and phase clustering readouts also benefitted from the larger number of trials. The pooling of trials at multiple stimulation intensities shortens the stimulation protocol and is supported by the relatively

similar TEP waveforms in the small range of stimulation intensities, between 100-110% of rMT.<sup>18,27</sup> The within-subject comparison of the effect of current direction over all electrodes revealed significant clusters located over the centroparietal electrodes corresponding to the primary and somatosensory motor cortex, probably due to the preferential activation of a hemisphere with clockwise and counterclockwise current direction.<sup>36</sup> Comparison of the frontal, central and occipital electrode clusters, however, revealed no significant difference between current directions. We therefore used the combined trials for the primary endpoints in the group comparisons. The independence of our results from the used current direction was demonstrated by the separate analyses per current direction, which showed no differences to the results for the combined trials.

Secondly, we used non-focal stimulation over the vertex using a circular coil to achieve diffuse activation of the cortex. This approach has been utilized to investigate the widely distributed epileptogenic networks of genetic generalized epilepsy by using high intensity stimuli to provoke epileptiform discharges.<sup>29</sup> In the context of our explorative study we considered the use of a circular coil most appropriate to induce broad cortical activations, without limiting the measurement to a pre-defined stimulation region of interest with a focal figure-of-eight coil. This allowed comparison of responses in various cortical regions, despite limiting the physiological interpretation of our findings. TEP waveforms induced by circular coil stimulation have been shown to be similar to focally induced waveforms in research with figure-of-eight coils.<sup>19,39</sup> Localization of responses was limited to their scalp distribution, as we have not implemented source localization. In future studies, probing the here identified regions, i.e. the frontal and occipital cortices, with focal stimulation with similar readouts would be a way to verify the present findings.

Thirdly, we cannot exclude a possible neuromodulatory effect of the repeated stimulation procedure. Stimuli were not jittered in this study because the stimulation protocol was specifically adapted to allow phase clustering analysis.<sup>27</sup> Using a non-jittered stimulation protocol we hypothesized to see differences in entrainment around the occipital cortex,<sup>31</sup> however, no significant clusters across electrodes or between groups, were observed. The number of stimuli (at maximum 160 per direction) and stimulation frequency (0.5 Hz), was based on

TMS-EEG literature where no neuromodulatory effects were reported.<sup>21,31,37</sup> A much more elaborate stimulation of 1200 stimuli presented at 1 Hz over the motor cortex in healthy controls revealed a regional inhibitory effect of prolonged stimulation, limited to the motor cortex and not affecting the visual cortex.<sup>55</sup> The differences between migraine and control groups reported here are therefore unlikely to result from neuromodulatory effects due to prolonged single pulse TMS. Attention to auditory stimuli may be altered in migraine patients and attending to upcoming stimuli in a sequence can alter the response to a mixture of cortical and sensory stimulation.<sup>56</sup> We did not observe significant clusters in the analysis of the sham measurements, indicating that an auditory-driven attention effect likely was minimal within our study population.

Lastly, our exploratory study is limited by a small sample size. To increase comparability between groups, we matched the subjects with migraine to healthy controls based on age, sex, and rMT. Matching cases and controls on rMT is not a standard approach, but we believe that this reduces the possibility of bias. The stimulation intensity was based on the rMT and matching on rMT ensures that the stimulation intensity was comparable for both groups and diminishes the effect of high rMT inter-individual variance on our readouts.<sup>57,58</sup> Although matching based on rMT resulted in similar variance in both groups, we cannot exclude a possible effect of the migraine or menstrual cycle on rMT variance.<sup>59</sup> We did not collect data about the menstrual cycle in our study. The limited number of studies assessing TMS-based cortical excitability measures in relation to the menstrual cycle indicate that cortical excitability might be unrelated from the menstrual hormone status in migraine,<sup>60</sup> as well as in epilepsy.<sup>61</sup> We used exact permutation-based tests by enumeration, an approach known to remain robust with relatively small sample sizes.<sup>35</sup> To increase the robustness of our statistical results, we compared the exact enumeration statistics with Monte Carlo permutation tests, which yielded similar results. Instead of performing peak-only analyses, our analyses were strengthened by analyzing the data for differences over time-electrode clusters (for TEPs). The finding of statistically significant differences in frontal and occipital TEP N100 amplitudes, despite the small number of study participants, indicates robust results with a large effect and only little inter-individual variation. Still, generalizability of our findings to the general migraine population may be limited due to the sample size and by the inclusion of only participants with migraine with aura. Future studies

including larger numbers of participants with migraine with and without aura should therefore determine the reproducibility and generalizability of our observations.

### **6.3 Concluding statements and future perspective**

In conclusion, people with migraine with aura show distinct cortical EEG responses to magnetic stimulation compared to controls in the periods in-between attacks. The observed peak amplitude differences suggest a possible reduction in cortical inhibition in migraine, but alternatively they could also reflect changes in sensory activation between groups, or involve both mechanisms. Our findings are in line with reports of altered interictal cortical excitability in migraine that were based on indirect measures, using e.g. visual or somatosensory inputs, or magnetic stimulation with peripheral readouts. In our study, all participants tolerated the TMS-EEG experimental procedure well and no induced migraine attacks were reported. This opens up possibilities for follow-up TMS studies in subjects without aura or with exclusive aura, studies exploring the correlation between clinical parameters (such as attack frequency or duration) and TEP peak amplitudes, and for longitudinal TMS-EEG studies during the migraine cycle. Such studies could strengthen the specificity of our findings for migraine with aura, and provide insight in changes of cortical excitability related to the onset of a migraine attack.

## References

1. Goadsby, P. J. *et al.* Pathophysiology of migraine: A disorder of sensory processing. *Physiol. Rev.* **97**, 553–622 (2017).
2. Ferrari, M. D., Klever, R. R., Terwindt, G. M., Ayata, C. & van den Maagdenberg, A. M. J. M. Migraine pathophysiology: Lessons from mouse models and human genetics. *Lancet Neurol.* **14**, 65–80 (2015).
3. Bigal, M. E., Liberman, J. N. & Lipton, R. B. Age-dependent prevalence and clinical features of migraine. *Neurology* **67**, 246–251 (2006).
4. Perenboom, M. J. L., Najafabadi, A. H. Z., Zielman, R., Carpay, J. A. & Ferrari, M. D. Quantifying visual allodynia across migraine subtypes: The Leiden Visual Sensitivity Scale. *Pain* **159**, 2375–2382 (2018).
5. Cucchiara, B., Datta, R., Aguirre, G. K., Idoko, K. E. & Detre, J. Measurement of visual sensitivity in migraine: Validation of two scales and correlation with visual cortex activation. *Cephalalgia* **35**, 585–592 (2015).
6. Coppola, G., Pierelli, F. & Schoenen, J. Is the cerebral cortex hyperexcitable or hyperresponsive in migraine? *Cephalalgia* **27**, 1427–1439 (2007).
7. Aurora, S. K. & Wilkinson, F. The brain is hyperexcitable in migraine. *Cephalalgia* **27**, 1442–1453 (2007).
8. Datta, R., Aguirre, G. K., Hu, S., Detre, J. A. & Cucchiara, B. Interictal cortical hyperresponsiveness in migraine is directly related to the presence of aura. *Cephalalgia* **33**, 365–374 (2013).
9. Magis, D. *et al.* Pearls and pitfalls: Electrophysiology for primary headaches. *Cephalalgia* **33**, 526–539 (2013).
10. Salminen-Vaparanta, N. *et al.* Subjective characteristics of TMS-induced phosphenes originating in human V1 and V2. *Cereb. Cortex* **24**, 2751–2760 (2014).
11. Brigo, F., Storti, M., Tezzon, F., Manganotti, P. & Nardone, R. Primary visual cortex excitability in migraine: A systematic review with meta-analysis. *Neurol. Sci.* **34**, 819–830 (2013).
12. Bestmann, S. & Krakauer, J. W. The uses and interpretations of the motor-evoked potential for understanding behaviour. *Exp. Brain Res.* **233**, 679–689 (2015).
13. Khedr, E. M., Ahmed, M. A. & Mohamed, K. A. Motor and visual cortical excitability in migraineurs patients with or without aura: Transcranial magnetic stimulation. *Neurophysiol. Clin.* **36**, 13–18 (2006).
14. Cosentino, G. *et al.* Impaired glutamatergic neurotransmission in migraine with aura? evidence by an input-output curves transcranial magnetic stimulation study. *Headache*

- 51, 726–733 (2011).
15. Cosentino, G. *et al.* Cyclical changes of cortical excitability and metaplasticity in migraine: Evidence from a repetitive transcranial magnetic stimulation study. *Pain* **155**, 1070–1078 (2014).
  16. Ilmoniemi, R. J. & Kičić, D. Methodology for combined TMS and EEG. *Brain Topogr.* **22**, 233–248 (2010).
  17. Chung, S. W., Rogasch, N. C., Hoy, K. E. & Fitzgerald, P. B. Measuring brain stimulation induced changes in cortical properties using TMS-EEG. *Brain Stimul.* **8**, 1010–1020 (2015).
  18. Komssi, S., Kähkönen, S. & Ilmoniemi, R. J. The Effect of Stimulus Intensity on Brain Responses Evoked by Transcranial Magnetic Stimulation. *Hum. Brain Mapp.* **21**, 154–164 (2004).
  19. Premoli, I. *et al.* TMS-EEG signatures of GABAergic neurotransmission in the human cortex. *J. Neurosci.* **34**, 5603–5612 (2014).
  20. Ziemann, U. *et al.* TMS and drugs revisited 2014. *Clin. Neurophysiol.* **126**, 1847–1868 (2015).
  21. Farzan, F. *et al.* Evidence for gamma inhibition deficits in the dorsolateral prefrontal cortex of patients with schizophrenia. *Brain* **133**, 1505–1514 (2010).
  22. ter Braack, E. M., Koopman, A. W. E. & van Putten, M. J. A. M. Early TMS evoked potentials in epilepsy: A pilot study. *Clin. Neurophysiol.* **127**, 3025–3032 (2016).
  23. Suffczynski, P. *et al.* Dynamics of epileptic phenomena determined from statistics of ictal transitions. *IEEE Trans. Biomed. Eng.* **53**, 524–532 (2006).
  24. Meisel, C. *et al.* Intrinsic excitability measures track antiepileptic drug action and uncover increasing/decreasing excitability over the wake/sleep cycle. *Proc. Natl. Acad. Sci. U. S. A.* **112**, 14694–14699 (2015).
  25. Parra, J. *et al.* Gamma-band phase clustering and photosensitivity: Is there an underlying mechanism common to photosensitive epilepsy and visual perception? *Brain* **126**, 1164–1172 (2003).
  26. Van Oosterhout, W. P. J. *et al.* Validation of the web-based LUMINA questionnaire for recruiting large cohorts of migraineurs. *Cephalalgia* **31**, 1359–1367 (2011).
  27. Bauer, P. R. *et al.* Phase clustering in transcranial magnetic stimulation-evoked EEG responses in genetic generalized epilepsy and migraine. *Epilepsy Behav.* **93**, 102–112 (2019).
  28. Olesen, J. *et al.* The International Classification of Headache Disorders, 3rd edition (beta version). *Cephalalgia* **33**, 629–808 (2013).
  29. Kimiskidis, V. K. *et al.* TMS combined with EEG in genetic generalized epilepsy: A

- phase II diagnostic accuracy study. *Clin. Neurophysiol.* **128**, 367–381 (2017).
30. Groppa, S. *et al.* A practical guide to diagnostic transcranial magnetic stimulation: Report of an IFCN committee. *Clin. Neurophysiol.* **123**, 858–882 (2012).
  31. Herring, J. D., Thut, G., Jensen, O. & Bergmann, T. O. Attention modulates TMS-locked alpha oscillations in the visual cortex. *J. Neurosci.* **35**, 14435–14447 (2015).
  32. Oostenveld, R., Fries, P., Maris, E. & Schoffelen, J. M. FieldTrip: Open source software for advanced analysis of MEG, EEG, and invasive electrophysiological data. *Comput. Intell. Neurosci.* **2011**, (2011).
  33. Esser, S. K. *et al.* A direct demonstration of cortical LTP in humans: A combined TMS/EEG study. *Brain Res. Bull.* **69**, 86–94 (2006).
  34. Kalitzin, S., Parra, J., Velis, D. N. & Lopes Da Silva, F. H. Enhancement of phase clustering in the EEG/MEG gamma frequency band anticipates transitions to paroxysmal epileptiform activity in epileptic patients with known visual sensitivity. *IEEE Trans. Biomed. Eng.* **49**, 1279–1286 (2002).
  35. Maris, E. & Oostenveld, R. Nonparametric statistical testing of EEG- and MEG-data. *J. Neurosci. Methods* **164**, 177–190 (2007).
  36. Rösler, K. M., Hess, C. W., Heckmann, R. & Ludin, H. P. Significance of shape and size of the stimulating coil in magnetic stimulation of the human motor cortex. *Neurosci. Lett.* **100**, 347–352 (1989).
  37. ter Braack, E. M., de Vos, C. C. & van Putten, M. J. A. M. Masking the Auditory Evoked Potential in TMS–EEG: A Comparison of Various Methods. *Brain Topogr.* **28**, 520–528 (2015).
  38. Rogasch, N. C., Daskalakis, Z. J. & Fitzgerald, P. B. Mechanisms underlying long-interval cortical inhibition in the human motor cortex: A TMS-EEG study. *J. Neurophysiol.* **109**, 89–98 (2013).
  39. Conde, V. *et al.* The non-transcranial TMS-evoked potential is an inherent source of ambiguity in TMS-EEG studies. *Neuroimage* **185**, 300–312 (2019).
  40. Raffin, E. *et al.* Probing regional cortical excitability via input–output properties using transcranial magnetic stimulation and electroencephalography coupling. *Hum. Brain Mapp.* **41**, 2741–2761 (2020).
  41. Casula, E. P. *et al.* Motor cortex synchronization influences the rhythm of motor performance in premanifest huntington’s disease. *Mov. Disord.* **33**, 440–448 (2018).
  42. Rogasch, N. C. & Fitzgerald, P. B. Assessing cortical network properties using TMS-EEG. *Hum. Brain Mapp.* **34**, 1652–1669 (2013).
  43. Lev, R., Granovsky, Y. & Yarnitsky, D. Enhanced pain expectation in migraine: EEG-based evidence for impaired prefrontal function. *Headache* **53**, 1054–1070 (2013).

44. Lorenz, J., Minoshima, S. & Casey, K. L. Keeping pain out of mind: The role of the dorsolateral prefrontal cortex in pain modulation. *Brain* **126**, 1079–1091 (2003).
45. Brighina, F. *et al.* rTMS of the prefrontal cortex in the treatment of chronic migraine: A pilot study. *J. Neurol. Sci.* **227**, 67–71 (2004).
46. Coppola, G. *et al.* Lateral inhibition in visual cortex of migraine patients between attacks. *J. Headache Pain* **14**, (2013).
47. Lloyd, J. O. *et al.* Cortical Mechanisms of Single-Pulse Transcranial Magnetic Stimulation in Migraine. *Neurotherapeutics* **17**, 1973–1987 (2020).
48. Cash, R. F. H. *et al.* Characterization of Glutamatergic and GABA A-Mediated Neurotransmission in Motor and Dorsolateral Prefrontal Cortex Using Paired-Pulse TMS-EEG. *Neuropsychopharmacology* **42**, 502–511 (2017).
49. Gordon, P. C. *et al.* Recording brain responses to TMS of primary motor cortex by EEG – utility of an optimized sham procedure. *Neuroimage* **245**, (2021).
50. Rocchi, L. *et al.* Disentangling EEG responses to TMS due to cortical and peripheral activations. *Brain Stimul.* **14**, 4–18 (2021).
51. Premoli, I. *et al.* Characterization of GABAB-receptor mediated neurotransmission in the human cortex by paired-pulse TMS-EEG. *Neuroimage* **103**, 152–162 (2014).
52. De Tommaso, M. *et al.* Altered processing of sensory stimuli in patients with migraine. *Nat. Rev. Neurol.* **10**, 144–155 (2014).
53. Chowdhury, N. S. *et al.* The influence of sensory potentials on transcranial magnetic stimulation – Electroencephalography recordings. *Clin. Neurophysiol.* **140**, 98–109 (2022).
54. Grasin, E., Loginov, I., Masliukova, A. & Smirnov, N. Realistic sham TMS. *Brain Stimul.* **12**, 418 (2019).
55. Casula, E. P. *et al.* Low-frequency rTMS inhibitory effects in the primary motor cortex: Insights from TMS-evoked potentials. *Neuroimage* **98**, 225–232 (2014).
56. Masson, R. *et al.* Auditory attention alterations in migraine: A behavioral and MEG/EEG study. *Clin. Neurophysiol.* **131**, 1933–1946 (2020).
57. Kimiskidis, V. K. *et al.* The repeatability of corticomotor threshold measurements. *Neurophysiol. Clin.* **34**, 259–266 (2004).
58. Koski, L., Schrader, L. M., Wu, A. D. & Stern, J. M. Normative data on changes in transcranial magnetic stimulation measures over a ten hour period. *Clin. Neurophysiol.* **116**, 2099–2109 (2005).
59. Cortese, F. *et al.* Excitability of the motor cortex in patients with migraine changes with the time elapsed from the last attack. *J. Headache Pain* **18**, 16–21 (2017).

60. Boros, K., Poreisz, C., Paulus, W. & Antal, A. Does the menstrual cycle influence the motor and phosphene thresholds in migraine? *Eur. J. Neurol.* **16**, 367–374 (2009).
61. Badawy, R. A. B., Jackson, G. D., Berkovic, S. F. & MacDonell, R. A. L. Cortical excitability and refractory epilepsy: A three-year longitudinal transcranial magnetic stimulation study. *Int. J. Neural Syst.* **23**, (2013).

## Supplementary information

*Time-frequency spectra.* To assess differences in time-frequency power of TEPs between migraine and controls, cluster-based permutation analyses were conducted for the time-frequency spectra of the averaged responses (using wavelet analysis between 20-200 ms, and 5-80 Hz) for frontal, central, and occipital regions. No differences in time-frequency spectra were found in any of the predefined electrode clusters: (frontal  $p=0.09$  (combined polarities),  $p=0.29$  (CCW),  $p=0.04$  (CCW)), central ( $p=0.12$ ,  $p=0.34$ ,  $p=0.08$ ) nor occipital ( $p=0.29$ ,  $p=0.35$ ,  $p=0.11$ ).

*Phase clustering over trials.* Consistency of TEP responses over trials was compared between groups using phase clustering analyses in the time-frequency domain. Statistical cluster-based permutation analyses were conducted for phase clustering over trials within the time-frequency domain over frontal, central and occipital electrode groups. There were no differences in phase clustering in migraine compared to controls, for none of the electrode groups and irrespective of current direction (frontal electrodes  $p=0.17$  (combined polarities),  $p=0.33$  (CCW),  $p=0.13$  (CCW); central electrodes  $p=0.23$ ,  $p=0.11$ ,  $p=0.47$ ; occipital electrodes  $p=0.17$ ,  $p=0.089$ ,  $p=0.18$ ).

*Time-frequency analyses of sham results.* Analysing the sham dataset, again frequency spectra were not different between groups for the electrode clusters (all  $p>0.13$ ). Phase clustering over trials did not include significantly different time-frequency clusters for the three electrode groups (all  $p>0.23$ ).

**Table S1.** Individual patients' data

<b>Subject</b>	<b>M/F</b>	<b>Age at inclusion</b>	<b>Disease duration (years)</b>	<b>Attack frequency (events/month)</b>	<b>% attacks with aura</b>	<b>Mean attack duration (hours)</b>
M01	M	50	35	1	100	12
M02	F	27	12	0.3	90	34
M03	F	48	12	0.5	100	10
M04	F	21	2	0.3	100	24
M05	F	45	32	1	100	34
M06	F	35	13	0.5	30	6
M07	F	40	15	2	100	24
M08	F	62	45	0.5	100	34
M09	F	51	33	1	100	72
M10	F	31	20	1.5	35	13.5

**Table S2.** Motor evoked potential (MEP) peak-to-peak amplitude (between 15-50 ms after stimulation) statistics for both groups, for the clockwise (CW), counterclockwise (CCW), combined current directions, and the comparison of the lowest rMT hemisphere and the corresponding contralateral hand motor responses only.

Comparison	MEP peak-to-peak amplitude		<i>p</i> -value
	Controls Mean (std)	Migraine Mean (std)	
CW	108 (94) $\mu$ V	118 (127) $\mu$ V	0.86
CCW	117 (63) $\mu$ V	92 (106) $\mu$ V	0.51
Combined	112 (78) $\mu$ V	105 (115) $\mu$ V	0.84
Lowest rMT	156 (86) $\mu$ V	145 (126) $\mu$ V	0.83

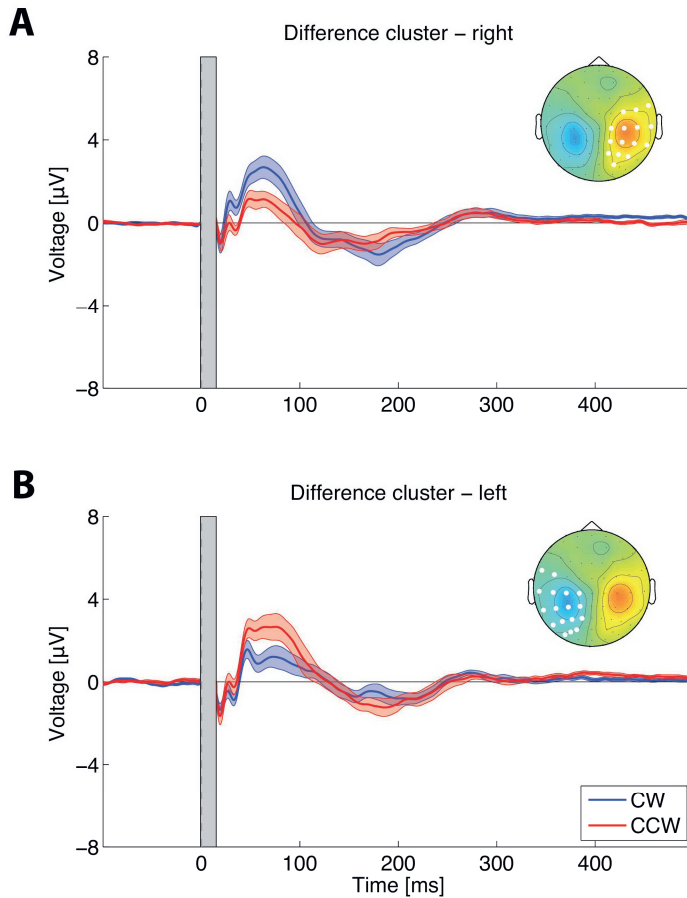


**Fig. S1.** Waveforms differ between CW and CCW stimulation over the primary and somatosensory motor cortices (per plot, the average waveform over the indicated electrodes is shown). The side of the difference depends on the current direction, i.e., CW stimulation evoking strongest response in the right hemisphere (**a**), and CCW stimulation evoking strongest response in the left hemisphere (**b**). Inserts show topoplots of the TEP difference waveform (CW minus CCW) distribution averaged between 70-80 ms after stimulation, where the mirrored activation between hemispheres is clearly visible. White dots display electrodes within the significantly different clusters, which are also mirrored between hemispheres depending on current direction.

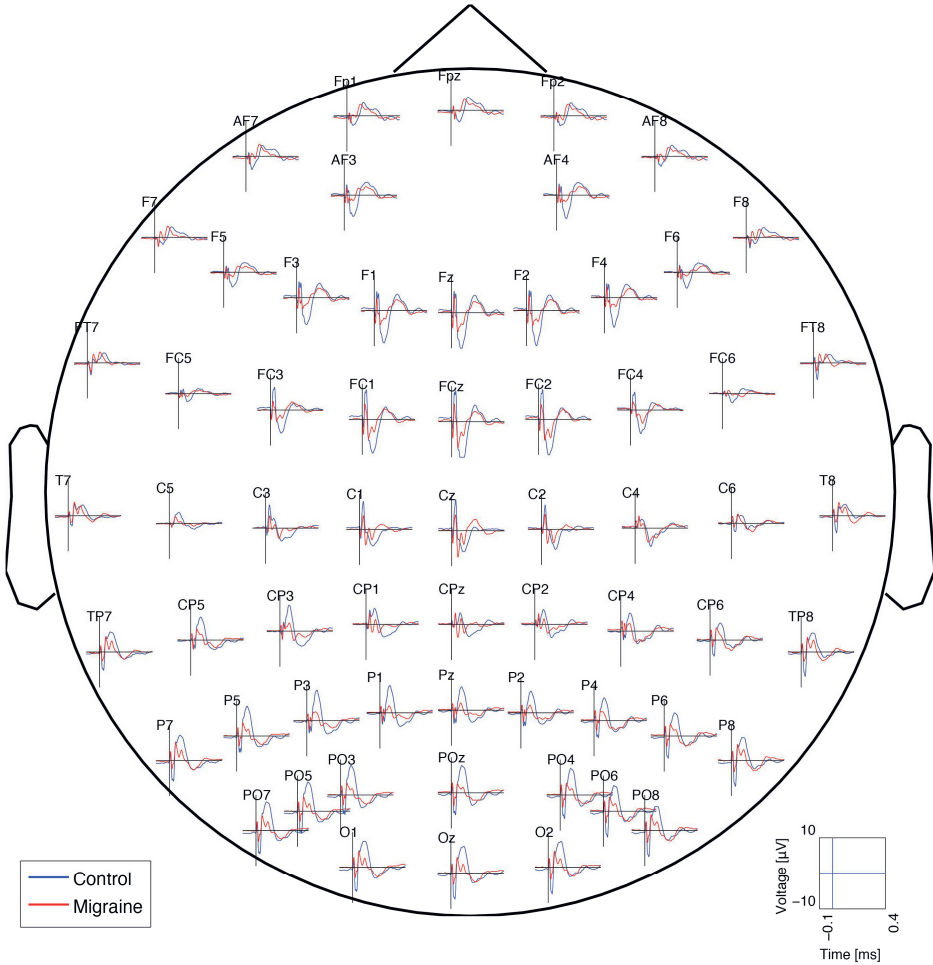


**Fig. S2.** Distribution of average TEP waveforms over the scalp for control (blue) and migraine groups (red). Note the similarities in waveform between groups (e.g. direction and delay of the N100 and P180 peaks).

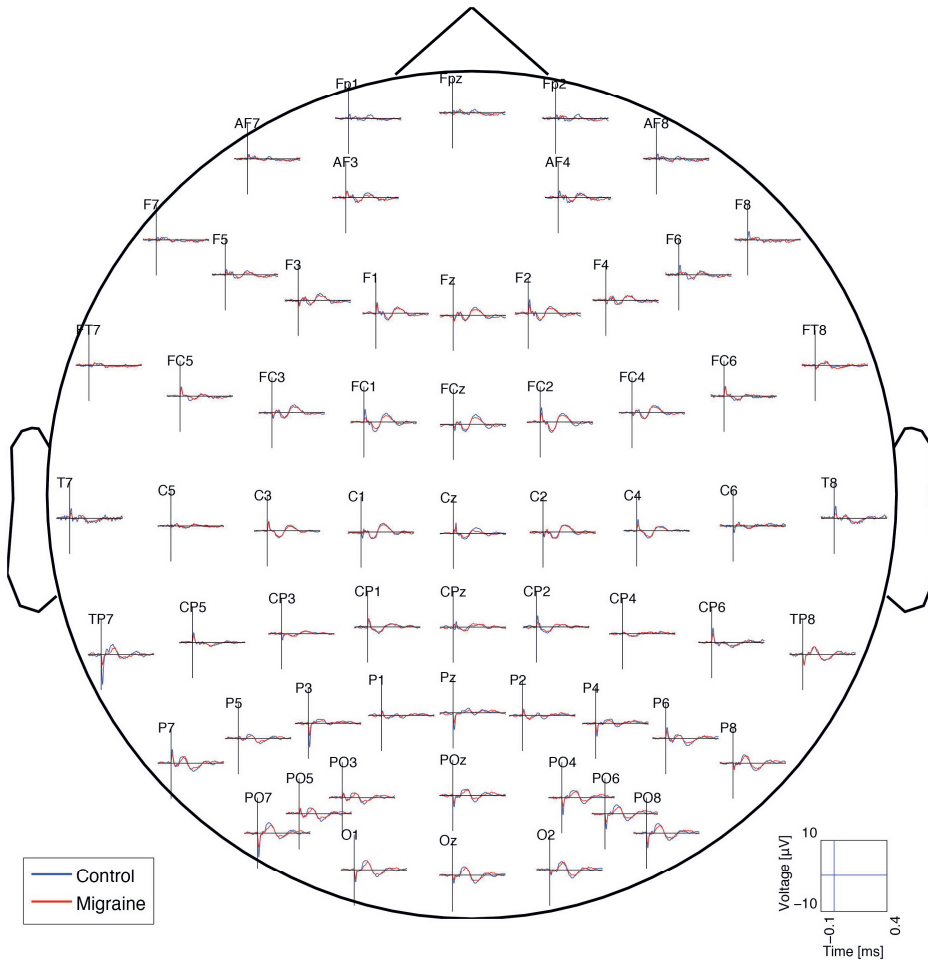


**Fig. S3.** Distribution of sham waveforms over the scalp for control (blue) and migraine (red) groups. Amplitude of the sham waveforms is much smaller compared to TEP waveforms (same y-axis limits are used as in Figure S2). Note the similarities in waveform between groups, like direction and delay of the sham-coil induced peaks around 100 and 180 ms.

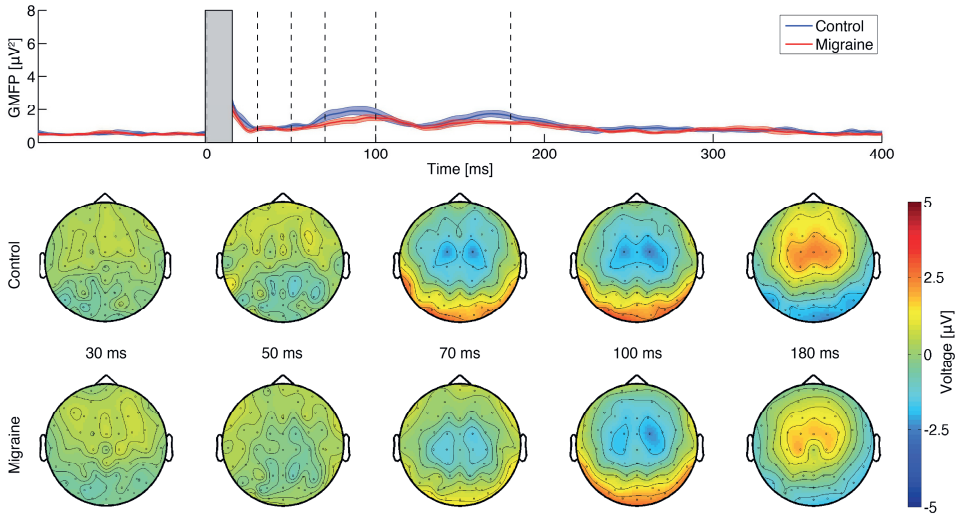


**Fig. S4.** Comparison of the global mean field power (GMFP) of the sham measurements between control (blue) and migraine groups (red). Top plot shows mean and patched standard error, the grey bar indicates the spherically interpolated parts of the EEG traces (-1 to 15 ms) and dashed black lines the time corresponding to the topoplots. Bottom: the corresponding topographical plots for the P30, P50, P70, N100, and P180 peaks.

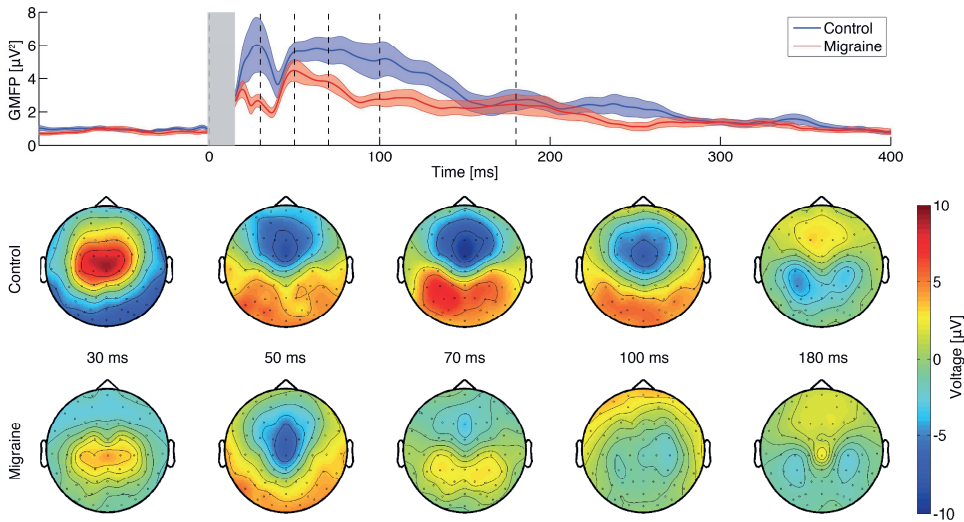


**Fig. S5.** Comparison between control (blue) and migraine groups (red) of the global mean field power (GMFP) of the TMS-evoked potentials (combined clockwise and counterclockwise trials) with the sham-evoked potentials linearly subtracted. Top plot shows mean and patched standard error, the grey bar indicates the spherically interpolated parts of the EEG traces (-1 to 15 ms) and dashed black lines the time corresponding to the topoplots. Bottom: the corresponding topographical plots for the P30, P50, P70, N100, and P180 peaks.

# Chapter 5

Phase clustering in transcranial magnetic stimulation-evoked EEG responses in genetic generalized epilepsy and migraine

Based on:

Bauer PR, **Helling RM**, Perenboom MJL, Lopes da Silva FH, Tolner EA, Ferrari MD, Sander JW, Visser GH, Kalitzin SN. Phase clustering in transcranial magnetic stimulation-evoked EEG responses in genetic generalized epilepsy and migraine. *Epilepsy & Behaviour*. 2019;93:102–12.

DOI: [10.1016/j.yebeh.2019.01.029](https://doi.org/10.1016/j.yebeh.2019.01.029)

## Abstract

Epilepsy and migraine are paroxysmal neurological conditions associated with disturbances of cortical excitability. No useful biomarkers to monitor disease activity in these conditions are available. Phase clustering was previously described in electroencephalographic (EEG) responses to photic stimulation and may be a potential epilepsy biomarker. The objective of this study was to investigate EEG phase clustering in response to transcranial magnetic stimulation (TMS), compare it with photic stimulation in controls, and explore its potential as a biomarker of genetic generalized epilepsy or migraine with aura.

People with (possible) juvenile myoclonic epilepsy (JME), migraine with aura, and healthy controls underwent single-pulse TMS with concomitant EEG recording during the interictal period. We compared phase clustering after TMS with photic stimulation across the groups using permutation-based testing.

We included eight people with (possible) JME (five off medication, three on), 10 with migraine with aura, and 37 controls. The TMS and photic phase clustering spectra showed significant differences between those with epilepsy without medication and controls. Two phase clustering-based indices successfully captured these differences between groups. One participant was tested multiple times. In this case, the phase clustering-based indices were inversely correlated with the dose of antiepileptic medication. Phase clustering did not differ between people with migraine and controls.

We present methods to quantify phase clustering using TMS–EEG and show its potential value as a measure of brain network activity in genetic generalized epilepsy. Our results suggest that the higher propensity to phase clustering is not shared between genetic generalized epilepsy and migraine.

## 5.1 Introduction

Epilepsy and migraine are paroxysmal conditions characterized by a temporary disruption of normal neurological function. Recurrent epileptic seizures are linked to hypersynchronous neuronal activity.<sup>1</sup> Migraine attacks are characterized by headache and sensory hyper-sensitivity without excessive synchronous neuronal activity.<sup>2,3</sup>

Epilepsy and migraine were suggested to share pathophysiological mechanisms based on epidemiological and genetic evidence.<sup>4,5</sup> The diagnosis of both conditions is made on clinical grounds and is, for epilepsy, often supported by electroencephalographical (EEG) findings. There are no reliable markers to assess the likelihood of a paroxysmal event occurring. In migraine and epilepsy, it is thought that altered neuronal excitation–inhibition dynamics, resulting in cerebral hyperexcitability, underlie attack susceptibility.<sup>5–8</sup> Cortical excitability, measured using transcranial magnetic stimulation (TMS), was shown to be elevated in those with epilepsy compared with controls on group level.<sup>9</sup> This was also the case in several studies of juvenile myoclonic epilepsy (JME), one of the most common forms of genetic generalized epilepsy,<sup>9,10</sup> which is characterized by myoclonus and generalized tonic–clonic seizures shortly after awakening. In children, JME is more often associated with migraine than other types of epilepsy, such as absence epilepsy.<sup>11</sup> People with JME are more than four times as likely to have migraine than people without JME.<sup>12</sup>

Findings of TMS studies in people with migraine are more complex, with several studies showing increased excitability of the visual cortex, reflected by a lower phosphene threshold, especially in migraine with aura (see for review<sup>13</sup>). Several studies show no difference in resting motor threshold (rMT) between people with migraine and controls.<sup>14–18</sup> Combining TMS with EEG offers new options to assess cortical excitability, bypassing sensory and motor areas.<sup>19,20</sup> Previous TMS–EEG studies in epilepsy investigating TMS-evoked potential and the epileptiform EEG discharges triggered by TMS have identified aberrant excitability and connectivity.<sup>21–27</sup> The only TMS–EEG study in JME to date found increased amplitude potentials in those with JME compared with controls and increased amplitude of late peaks when participants with JME were sleep-

deprived, demonstrating cortical hyperexcitability.<sup>21</sup> Such TMS–EEG studies were thus far not conducted in people with migraine.

One novel way of assessing cortical excitability using TMS–EEG is by determining the uniformity of phase angles across trials in EEG responses.<sup>20</sup> On a single electrode, the phase of TMS-evoked responses aligns between trials shortly after the TMS pulse. A recent study suggests that phase clustering 20–60 ms poststimulus in the 8–70-Hz frequency band may be a good candidate for measuring cortical excitability.<sup>20</sup> One measure of phase clustering, the relative phase clustering index (rPCI), was successfully used in magnetoencephalography to quantify the neural response to periodic photic stimulation and to identify dynamic states leading to photoparoxysmal responses in epilepsy.<sup>28</sup> In temporal lobe epilepsy, it was shown that high values of rPCI were correlated with the probability of occurrence of epileptic seizures.<sup>29</sup> Recently, it was demonstrated that an index derived from the PCI, computed from local field potentials recorded *in vitro* or *in vivo* using intracranial recordings during very weak periodic pulse stimulation, can be used to quantify the state of excitability of neuronal networks in epileptogenic brain tissue.<sup>30</sup>

Increased phase synchronization in the gamma frequency range in the ongoing EEG was linked to increased neuronal excitability in epilepsy.<sup>31</sup> Phase synchrony in response to photic stimulation was also elevated in those with migraine with and without aura compared with controls, especially in the alpha frequency range.<sup>32–35</sup> One study showed beta frequency desynchronization in migraine with aura,<sup>36</sup> potentially linked to hyperresponsivity of the sensory cortices.<sup>37</sup>

We assessed whether phase clustering in the TMS–EEG response differs in people with JME compared with controls or people with migraine with aura.

## 5.2 Methods

### 5.2.1 Participants

*Controls.* Healthy volunteers aged 12 years or over were recruited locally through digital and paper adverts. Those with a history of epilepsy or migraine were

excluded. Hand dominance was assessed with a clinically validated questionnaire.<sup>38</sup>

*JME.* Participants, diagnosed with JME or possible JME by their treating neurologist, were recruited from outpatient clinics. The diagnosis was based on the clinical history and a clinical interictal EEG recording performed at least one week prior to the TMS–EEG session. Participants aged 12 years and over, with a history of myoclonic seizures and/or at least one generalized tonic–clonic seizure, who were either not taking antiepileptic drugs (active epilepsy off drugs) or considering tapering antiepileptic drugs (in remission) in conjunction with the attending neurologist, could be included. Subjects with comorbid migraine were excluded. In the Netherlands, where this study was conducted, the presence of myoclonus is not considered compulsory for the diagnosis of JME.<sup>39</sup>

*Migraine with Aura.* Participants with migraine with visual aura were recruited locally through digital and paper adverts at a clinic. The diagnosis was based on the International Classification of Headache Disorders criteria.<sup>40</sup> People aged 18 years and over with migraine headache preceded by visual aura in at least 30% of the attacks were included. Subjects needed to have at least one migraine attack per year, at least one in the preceding year, and less than eight attacks or 15 headache days per month. We excluded people using prophylactic medication and those with a history of epilepsy, and those without aura and with “aura sans migraine”.

*Exclusion criteria for all groups.* These were the exclusion criteria: contraindications to TMS, pregnancy, any neurological condition other than epilepsy or migraine, any psychiatric condition, the use of medication affecting cortical excitability other than antiepileptic drugs (such as psychoactive drugs and beta blockers), and diabetes mellitus, as this can affect peripheral nerves which were investigated for a separate study (not reported here). Experimental sessions were performed more than 24 h after a convulsive seizure and more than 72 h after a migraine attack; sessions followed by a convulsive seizure within 24 h and a migraine attack within 72 h, identified at follow-up, were also excluded. Participants were asked not to smoke, take drugs, or drink alcohol or coffee 12 h preceding the measurement and to maintain a normal sleep pattern the night prior to the measurement.

### 5.2.2 *Material*

*TMS.* Magnetic stimulation was performed with a MagPro X100 stimulator (Magventure, Denmark), a 14-cm diameter parabolic circular coil (type MMC-140), and a sham coil (type MCF-P-B65). Measurements were conducted at 09.00 AM or 02.00 PM and spread evenly between AM and PM. No significant differences in TMS measures were reported between these times of the day,<sup>41</sup> except a larger TMS-evoked potential 100 ms after the stimulus.<sup>42</sup> Soft earplugs were used to reduce the coil click.

*Electromyography.* Motor-evoked potentials were recorded bilaterally from the abductor pollicis brevis muscles with a Nicolet Viking EDX electromyograph (Natus, Madison, WI, USA). The coil size and design activated these muscles in N 90% of participants. Muscle activity was monitored using real-time visual feedback. Data were recorded with a sampling frequency of 4 kHz and stored for offline analysis.

*EEG.* Electroencephalography was recorded during the TMS sessions with a 64-channel TMS-compatible EEG system (Waveguard™ cap and ASAlab™ software, ANT-neuro, Enschede, The Netherlands), a sampling frequency of 4 kHz, and a ground electrode located on the AFz electrode position. Participants were seated in a comfortable chair with their eyes open and arms in supine position.

### 5.2.3 *Stimulation Protocols*

*Photic Stimulation.* After a 10-minute baseline EEG recording, photic stimulation (Sigma, Is FSA 10-2D-I, SIGMA Medizin-Technik GmbH, Gelsenau, Germany) was performed according to a standard clinical protocol: stimulation started at 2 Hz; followed by 10-s runs of increasing frequency at 6, 12, 20, 30, 40, 50, and 60 Hz with eyes closed and open ( $\pm 5$  s each). If an epileptiform discharge was elicited, stimulation was stopped and resumed at 60 Hz. Stimulation was thereafter performed at decreasing frequencies until another discharge occurred, to determine the range of frequencies to which an individual was sensitive. Photic stimulation was performed in controls and people with epilepsy but not in people with migraine, as several people in our sample indicated that this could trigger a migraine attack. The aim of this study was to assess TMS–EEG parameters of cortical excitability outside migraine attacks, and thus, we

avoided to trigger attacks. We used the photic stimulation in controls and people with epilepsy to validate the results obtained with TMS–EEG.

*Single-Pulse TMS stimulus response curve.* The rMT, defined as the lowest stimulation intensity that evokes a peak-to-peak electromyographic amplitude larger than 50  $\mu\text{V}$  in 50% of the trials,<sup>43</sup> was measured with the coil on the vertex (electrode position Cz) and a scanning procedure described hereafter. For a first approximation of the motor threshold, stimulation was started at 20% stimulator output and increased with 5% steps until a consistent twitch in the hand contralateral to the stimulated hemisphere was seen in 50% of the trials. Then, a semi-automated, in-house designed scanning protocol (created in Matlab® (version 7.5.0 R2007b The MathWorks Inc., Natick, MA, USA)) was used to determine the rMT as follows: scanning started at a stimulator output value of 10–12% below the visually determined motor threshold and increased in 2% steps until a reproducible motor-evoked potential (N 200  $\mu\text{V}$ ) was seen after every stimulus ( $\pm 110$ –120% rMT). Stimuli were given with interstimulus intervals of 2 s. This frequency was not shown to alter motor-evoked potentials.<sup>44,45</sup> The scanning procedure was performed using counterclockwise (right hemisphere) and clockwise (left hemisphere) stimulation as part of the artifact reduction strategy (see Section 2.4.4) and repeated with the sham coil. To be useful in clinical settings, the stimulation protocol was designed to be a short protocol yielding maximum information at once.

To assess long-term reproducibility of the TMS–EEG parameters, controls were re-measured after 10–12 months at the same time of the day. We also explored whether the measure of EEG phase clustering (see below) is affected by the number of stimuli per intensity. The control group was measured twice with different numbers of stimuli per intensity: during the first measurement, we used eight stimuli per stimulus, and in the second measurement, we used 20 stimuli per stimulus intensity. People with epilepsy were measured following each medication change. To reduce the theoretical risk of eliciting a seizure in participants with epilepsy off medication, we used eight stimuli per stimulus intensity minimizing the number of pulses.<sup>46</sup> In the group with epilepsy on medication, we used 20 stimuli per stimulus intensity, as the theoretical risk of a seizure is lower in these groups. People with migraine were measured only once using 20 stimuli per stimulus intensity.

### 5.2.4 Data Analysis

Offline analyses were performed in Matlab® (8.5.0 R2015a). The phase clustering analysis described below was applied on data acquired with the two TMS polarities, sham stimulation, and photic stimulation.

*Removal of Artifactual Channels.* For each subject, artifactual channels were automatically detected: for each channel, the norm covariance matrix was computed for the window  $-0.1$  to  $0$  s relative to the TMS stimulus. Then, the Z-score was computed from the norm covariance of each channel relative to the other channels. Channels with a Z-score  $\geq 3$  were excluded from the reference montage and subsequent analyses. On average, 4 channels were removed for each subject (range: 2–7 channels). The M1, M2, T7, and T8 electrodes were most often detected as ‘outlier’ channels.

*Phase clustering and neuronal network excitability indices.* Electroencephalography phase clustering analysis was previously described.<sup>28,47</sup> The phase clustering index (PCI) describes the phase consistency of the complex Fourier components across the stimulation trials, with zero representing completely scattered phases and one maximal phase grouping. To obtain the PCI, we used epochs of 100 ms (corresponding to a base frequency of  $1 \text{ s} / 100 \text{ ms} = 10 \text{ Hz}$ ) starting 15 ms after TMS or sham stimulation (see also below regarding TMS artifact reduction) and without delay (0 ms) for photic stimulation. After linear detrending, the complex Fourier components of the signal were computed using the fast Fourier transform after application of a Hamming taper, yielding complete frequency and phase representation of the responses. The length of the window defines the base frequency of the representation with the harmonic component representing an integer multiple of the base frequency. For photic stimulation, only responses to 6 Hz stimulation when subjects had their eyes closed were analyzed to ensure enough stimulation trials (30 trials for each subject).

The PCI was computed for each complex number  $F$  obtained from the Fourier transform using Eq. (1).

$$PCI_c^f = \frac{|\langle F_{c,i}^f \rangle_i|}{\langle |F_{c,i}^f| \rangle_i} \quad (1)$$

where  $f$  is frequency band,  $i$  is stimulus number (from  $N_i$  in total),  $c$  is the EEG channel, the symbol  $|z|$  represents the magnitude (the absolute value) of a complex number  $z$ , and  $\langle \cdot \rangle_i$  indicates averaging over all stimuli. For more information regarding the pathophysiological interpretation of the PCI in terms of system dynamics, see Supplementary information S1.

The rPCI, i.e., the maximal PCI at a given frequency relative to the PCI at the base frequency ( $PCI^1$  reflects the clustering at 10 Hz), was then computed by:

$$rPCI = \langle \max_f (PCI_c^f - PCI_c^1) \rangle_c \quad (2)$$

The neural network excitability index (NNEI) introduced in the previous work<sup>30</sup> is determined by the PCI at the base frequency:

$$NNEI = \langle 1 - PCI_c^1 \rangle_c \quad (3)$$

While both measures were initially computed using the whole epoch in-between successive stimuli, TMS has restrictions because of the ringing and muscle artifacts present in the window shortly after the stimulus (see below), so we calculated the PCI for a fixed window length of 100 ms starting 15 ms after a TMS stimulus. In theory, the window length can influence the general spectral resolution of the PCI. In our sample, windows of 50 ms to 500 ms (base frequencies from 20 Hz to 2 Hz) showed a similar PCI spectrum with comparable rPCI values.

*Time-Frequency Analysis.* For TMS time–frequency analyses, we used epochs of 1 s (4000 samples), starting 0.5 s before the magnetic stimulus to avoid convolution edge effects in the window of interest from 15 ms to 115 ms. The part of the signal containing TMS ringing artifacts (0–6 ms after the stimulus) was cut. Cubic interpolation was used from 0 to 15 ms around the stimulus to reduce muscle artifact contamination. The trials were baseline-corrected using a baseline window from –50 ms to 0 ms relative to the TMS stimulus. The time–frequency wavelet components for frequencies between 8 and 50 Hz were computed using Morlet wavelets with a width of 5 for the window of 15 ms to 115 ms in steps of 5 ms in order to gain sufficient temporal resolution for the low frequency content with adequate frequency resolution in the higher

frequencies. Because of our window selection of  $[-0.5:0.5]$  s, we can compute the Time-frequency (TF) with the chosen cycle width for the window [15 ms:115 ms] without any border distortions.

Next, the time-phase clustering response was computed using a modified version of Eq. (1):

$$PCI_{t,c}^f = \frac{\langle |F_{t,c,i}^f| \rangle_i}{\langle |F_{t,c,i}^f| \rangle_i} \quad (1a)$$

where  $t$  is time. For the photic stimulation time–frequency analysis of the PCI, the interval of interest was an epoch of 167 ms, with a mirror buffer of 500 ms on each side to avoid convolution edge effects in the time–frequency analysis. Detrending was applied before computing the time–frequency Fourier components for frequencies between 5 and 50 Hz using Morlet wavelets with a width of 5 cycles for the whole window of interest in steps of 5 ms. The PCI was again computed using Eq. (1A), and the results were averaged over all channels.

*TMS and muscle artifact reduction.* We included several strategies to reduce stimulation and muscle artifacts related to magnetic stimulation. Firstly, Eq. (2) allows to cancel out broadband artifacts, such as sharp spikes induced by, and time-locked to, the magnetic stimulus as they will result in a high PCI for all frequencies. Secondly, we performed the phase clustering analysis using a window that started 15 ms after the magnetic stimulation. The largest TMS and muscle artifacts are expected within the first 15 ms after the stimulus. To ensure that our results are not due to muscle artifact contamination, the analysis was repeated for epochs starting at 20 ms, 25 ms, and 30 ms relative to the TMS stimulus, with similar results. Only data from the final analysis with a window length of 100 ms starting 15 ms after the TMS stimulus were included. Thirdly, to reduce linear volume conduction effects caused by the magnetic stimulus, we added the clockwise and counterclockwise stimulation responses offline in a pairwise fashion to compensate the linear component, containing the artifact, in the response to each polarity (Eq. (4))<sup>48</sup>:

$$F_{c,i}^{(c)f} \equiv F_{c,i}^{(+f)} + F_{c,i}^{(-f)} \quad (4)$$

$F_c^{(+)}$  and  $F_c^{(-)}$  are the response amplitudes to the clockwise and counterclockwise current stimulations from a series of equal number of stimuli. We will refer to this as polarity compensation and to  $F_{c,i}^{(c)f}$  as polarity-compensated amplitudes, which were used in Eqs. (1) and (2). All analyses were done on polarity-compensated signal as theoretically, it is less affected by artifacts (see Eq. (4)). Unless stated otherwise, “rPCI” refers to polarity-compensated rPCI. Sham stimulation was done in the three groups to evaluate the effect of the audible coil, as the earplugs did not mask the click completely.

In controls, we compare the compensated stimulation with the individual stimulation polarities, and in addition, we compare TMS to sham stimulation and photic stimulation in the group with epilepsy and the control group. In the group with migraine, we compare TMS with sham stimulation.

### 5.2.5 Statistical Analysis

We took the small sample size of the group with epilepsy (on and off medication) and the group with migraine into account by using nonparametric, Monte Carlo-based statistics, which were shown to be robust in such small sample sizes.<sup>49</sup> For all statistical analyses, the group with epilepsy off medication was compared with the first measurement of the controls (8 stimuli per intensity) while the group with epilepsy on medication and the group with migraine were compared with the second measurement of the controls (20 stimuli per intensity).

The rMT was compared across groups using an independent sample permutation test using 10,000 permutations and a significance level of 0.05. The TMS-evoked potentials and time–frequency PCI spectra were compared across groups using the cluster-based Monte Carlo permutation testing<sup>50</sup> using 2500 permutations, a cluster-alpha of 0.01, and a significance level of 0.025.

To assess possible biomarkers of epileptogenicity, we quantified the rPCI (Eq. (2)) and NNEI (Eq. (3)) averaged over all EEG channels after magnetic, sham, and photic stimulations in controls, people with epilepsy on and off medication, and participants with migraine. These rPCI and NNEI values averaged over all channels were compared across groups using an independent sample permutation test using 10,000 permutations with a significance level of 0.05.

To assess the robustness of TMS-evoked rPCI, we compared the rPCI obtained after clockwise, counterclockwise, sham, polarity-compensated, and photic stimulations in the control group using the independent sample permutation test. Still in the control group, for polarity-compensated stimulation and sham stimulation, we compared the rPCI after 8 pulses per intensity (the first measurement) and after 20 stimuli per intensity (the second measurement) using the paired sample permutation test. For polarity-compensated stimulation, sham stimulation, and photic stimulation, we also compared the rPCIs measured during the morning with those measured in the afternoon, and the rPCIs measured in men and women using the independent sample permutation test. We used a permutation test based on Spearman's rho correlation coefficient to estimate the effect of age on the polarity-compensated rPCI, and rPCI as estimated by sham and photic stimulations in the control groups.

## 5.3 Results

### 5.3.1 Participants

We included 38 controls (25 women, mean age: 38.1 years, range: 15–62 years) between May 2014 and October 2014. Five were left-handed. Of those 38 controls, thirty were measured a second time after an average of 350 days (range: 296–378 days). One participant was excluded from the analyses because of nonspecific EEG abnormalities. From another control, we excluded the first measurement as it contained a large artifact due to incorrect settings of the magnetic stimulator. Thus, the analysis of the first measurement was based on 36 controls, and the analysis of the second measurement on 29 controls. Eight participants with JME were included (4 women, mean age: 31.5 years, range: 14–59) between May 2014 and October 2015. All were right-handed (Table 1). Five were not taking antiepileptic drugs at inclusion (E1–E5). Two were photosensitive (E3 and E4). Three were treated with antiepileptic drugs for two years or more and were contemplating drug withdrawal (EM1, EM2, EM3). To ensure adherence, drug levels were monitored. None of the participants had a seizure during the time that they were included in the study (7–12 months).

Twelve people with migraine were recruited (10 women, mean age: 38 years; range: 21–62, 4 left-handed, Table 2). One female was excluded because of beta

blocker use; one male was excluded, as he did not have an attack in the preceding year. The attack frequency for the remaining ten participants was between 0.3 and 2 per month. Apart from one participant who habitually drank seven cups of coffee per day, daily coffee consumption in this group was limited. Three female participants were first-degree relatives. We analyzed the results with and without two of these family members. Given the small differences between the two analyses, we report here the results including the three family members.

All participants tolerated the experimental sessions. None had a seizure or migraine attack following stimulation.

**Table 1.** Clinical features of participants with juvenile myoclonic epilepsy.

Nr	M/F	Age	Age at onset	Handedness	PS	Last seizure	Clinical features	EEG features at diagnosis	TMS rPCI	TMS NNEI	Photic rPCI	Photic NNEI
E1	F	14	14	9	N	28 days	TC, 1 febrile seizure	Normal background activity, spikes and spike-and-wave complexes with anterior maximum	0.22	0.40	0.30	0.84
E2	M	29	22	8	N	158 days	Nocturnal TCs triggered by alcohol	Normal background activity, (poly) spike-and-wave complexes with anterior maximum, increased abnormalities under hyperventilation	0.23	0.44	0.29	0.87
E3	M	20	20	9	Y	6 days	Nocturnal TCs triggered by alcohol, myoclonic jerks upon photic stimulation	Normal background activity without spontaneous epileptic abnormalities. Very clear photosensitivity (Waltz 3 between 6 and 40 Hz) accompanied by myoclonic jerks	0.24	0.49	0.29	0.79
E4	F	34	16	7	Y	8 years	Myoclonic jerks + TCs	Normal background activity with spontaneous 3–4 Hz (poly) spike-and-wave complexes with alternating maximum, sometimes accompanied by myoclonic jerks	0.20	0.45	0.19	0.62
E5	M	17	15	9	N	3 months	Myoclonic jerks + TCs	Normal background activity with 3 Hz (poly) spike-and-wave complexes with frontal maximum	0.22	0.33	0.28	0.68
EM1 <sup>1</sup>	F	59	16	9	N	24 months	Myoclonic jerks + TCs + absences	Normal background activity without epileptiform discharges	0.14	0.29	0.14	0.72
EM2 <sup>2</sup>	M	24	15	8	N	42 months	Myoclonic jerks + TCs + absences	Normal background activity with subtle generalized epileptiform discharges	0.29	0.58	0.26	0.77
EM3 <sup>3</sup>	F	55	8	8	N	18 years	Myoclonic jerks + TCs	Not available	0.19	0.41	0.02	0.54

*M: male, F: female, PS: photic sensitivity, N: no, Y: yes, Handedness: according to the Edinburgh handedness questionnaire, TC: tonic-clonic seizures. Medication at time of measurement: 1depakine chrono 2000 mg 1/day, 2depakine 750 mg 2/day, 3depakine 500 mg 2/day.*

**Table 2.** Characteristics of participants with Migraine with aura.

nr	M/F	age at inclusion n	age at onset	Handed ness	attacks per month	% of attacks with aura	TMS rPCI	TMS NNEI
<b>M1</b>	F*	29	11	-5	1	40	0.0445	0.1998
<b>M2</b>	M	50	15	-7	1	100	0.1355	0.3676
<b>M3</b>	F	27	15	9	0.3	90	0.0109	0.1822
<b>M4</b>	F	21	19	9	0.3	100	0.2231	0.3822
<b>M5</b>	F	45	13	8	1	100	0.1220	0.4509
<b>M6</b>	F	35	22	8	0.5	30	0.0190	0.1136
<b>M7</b>	F	40	25	9	2	100	0.1294	0.4386
<b>M8</b>	F*	62	17	-8	0.5	100	0.1487	0.5183
<b>M9</b>	F	51	18	9	1	100	0.1442	0.4363
<b>M10</b>	F*	31	11	7	1.5	35	0.1775	0.4615

*\*first degree family members Handedness according to the Edinburgh handedness questionnaire (scores <-5 indicate left-hand dominance)*

### 5.3.2 rMT

The median rMT data and number of stimuli during each TMS procedure and photic stimulation are shown in Table 3. There was no significant difference in rMT between the groups.

### 5.3.3 Time and frequency characteristics of the PCI of magnetic and photic stimulation

We first explored the polarity-compensated TMS-evoked potential for each group (see Fig. 1A). Permutation testing revealed no significant clusters in the group comparisons of the averaged time–amplitude results. Post hoc analysis of the stimulated area (central electrode cluster consisting of electrode Cz and neighboring electrodes) where the evoked response should be most prominent showed a difference between the first measurement of the controls and the group with epilepsy off medication ( $p = 0.016$ , see Fig. 1A for the cluster). The visual-evoked potential shown in Fig. 2A did not differ between the control and the groups with epilepsy. Photic stimulation was not done in the group with migraine.

Next, we explored the time–frequency characteristics of the TMS and photic stimulation PCI spectra (Eq. (1A), Figs. 1B and 2B). The TMS spectrum differed between the group with epilepsy off medication and the first measurement of the controls (Fig. 3A,  $p = 0.024$ ). This cluster showed increased PCI in the group with epilepsy off medication in the gamma frequency band (30–40 Hz) around 50 to 80 ms. The PCI spectrum, in contrast, showed decreased PCI in the group with epilepsy off medication in the 10–14-Hz frequency band over the whole epoch (Fig. 3B,  $p = 0.004$ ). There were no differences in the other group comparisons. The analysis of Fig. 3A suggests that the feature that best distinguishes TMS-evoked responses in epilepsy from controls is the rPCI defined in Eq. (2), as the high-frequency phase information is taken into account. For photic-evoked responses, in contrast, Fig. 3B suggests that the rPCI and the NNEI (Eq. (3)) may be suitable markers as they reflect phase clustering in the lower frequencies. As shown in Eq. (2), the rPCI can increase either due to an increase of PCI or to a decrease of PCI. The NNEI is useful to discriminate between these two alternatives. This is further tested in the next section.

#### 5.3.4 rPCI and NNEI for TMS and photic stimulation

To quantify the difference in PCI between the different groups, we used the rPCI (Eq. (2)) and the NNEI (Eq. (3)). The median rPCI and NNEI elicited by the different stimulation modalities (polarity- compensated, sham, photic) in the different groups and the corresponding 5–95 percentiles are shown in Table 4.

**Table 3.** Median (range) number of TMS and photic stimuli and resting motor threshold (rMT) values.

	# TMS stimuli	# Photic stimuli	rMT right hemisphere	rMT left hemisphere
<b>controls 1</b>	112 (96-208)	30	42% (31-68%)	40% (31-59%)
<b>controls 2</b>	400 (280-480)	30	39% (29-57%)	43% (25-59 %)
<b>epilepsy no med</b>	176 (112-290)	30	51% (41-53%)	46% (39-53%)
<b>epilepsy + med</b>	280 (160-320)	30	61.5% (45-78%)	47% (43-74%)
<b>migraine</b>	340 (280-440)		43% (33-57%)	45% (31-47%)

*TMS: transcranial magnetic stimulation, rMT: resting motor threshold.*

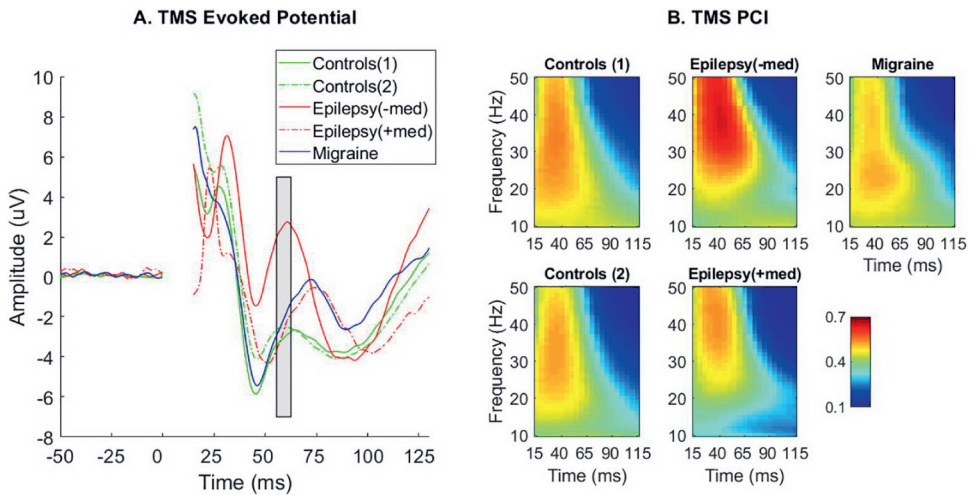


**Fig. 1.** (a). TMS-evoked potential over the central electrode cluster for control, group with epilepsy, and group with migraine. Evoked responses averaged over a central electrode cluster, consisting of electrode Cz (the TMS target) and the neighboring electrodes surrounding electrode Cz. The gray area highlights the significantly different time samples between epilepsy (–med) and controls(1) ( $p = 0.016$ ). (b). Time–frequency representation of polarity-compensated PCI averaged over all channels. For Controls 1st, Controls 2nd, Migraine, Epilepsy without medication, and Epilepsy with medication. TMS frequency was 0.5 Hz. Wavelet analysis was performed using Morlet wavelets with 5 cycles.

The polarity-compensated rPCI was significantly higher in the group with epilepsy off medication than in controls ( $p = 0.023$ ) while the NNEI showed a weak trend for being higher ( $p = 0.147$ ). The group with epilepsy off medication also had significantly higher rPCI values than controls ( $p = 0.021$ ). Photic stimulation showed higher rPCI ( $p = 0.009$ ) and NNEI ( $p = 0.025$ ) values in the group with epilepsy off medication compared with controls. The rPCI and NNEI elicited by sham stimulation did not differ between controls and the groups with epilepsy. The rPCI and NNEI in the group with migraine did not significantly differ from controls (Fig. 4). In controls, the polarity-compensated rPCI, photic rPCI, and sham rPCI did not differ between the first and second measurement, between men and women, nor between the times of the day the measurement took place (AM or PM). Age correlated with photic rPCI ( $r = 0.399$ ,  $p = 0.012$ ) and photic NNEI ( $r = 0.411$ ,  $p = 0.010$ ) in the control group but not with TMS rPCI and NNEI. An example of the rPCI and NNEI following changes in the dose of levetiracetam in one participant with epilepsy is shown in Fig. 5. The decrease of the rPCI and NNEI is inversely proportional

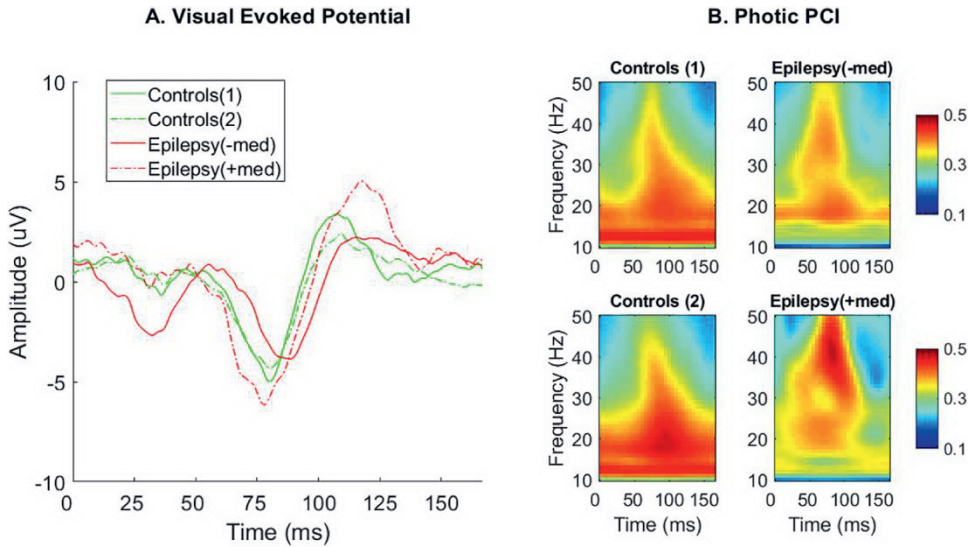


**Fig. 2.** (a). Visual-evoked potential averaged over the occipital electrode cluster. Evoked photic response for the occipital electrode cluster consisting of Oz and the neighboring electrodes. (b). Time–frequency profile of 6 Hz photic PCI from controls and groups with epilepsy, averaged over all channels. For Controls 1st, Controls 2nd, Epilepsy without medication, and Epilepsy with medication. The group with migraine was not visually stimulated. Wavelet analysis was performed using Morlet wavelets with 5 cycles.

to the dose. A similar trend was seen for the photic rPCI but not for the photic NNEI (figure not shown).

## 5.4 Discussion

We confirmed the feasibility of assessing EEG phase clustering using a TMS single-pulse paradigm and validate the results with photic stimulation. We found that rPCI elicited by TMS was increased in those with JME on and off medication compared with controls but not in those with migraine with aura. The rPCI elicited by photic stimulation was also increased in those with JME off medication compared with controls. In line with a recent study, we show that phase clustering of evoked responses may be a candidate biomarker to monitor cortical excitability,<sup>20</sup> and we show its potential for diagnostic value in epilepsy. An interesting additional finding, although preliminary, is that in one participant,

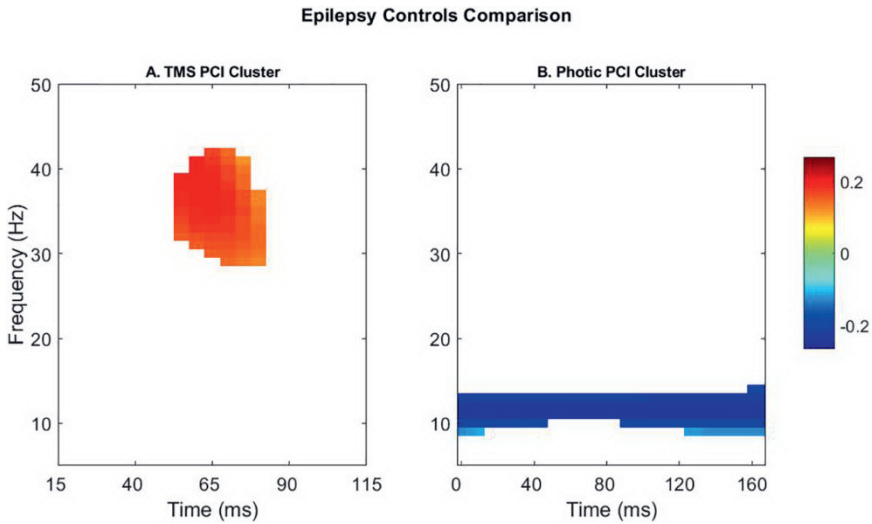


**Fig. 3.** Monte Carlo permutation testing revealed significant differences in TMS (a) and photic stimulation (b) for the epilepsy(-med) versus controls(1) group comparison. Monte Carlo permutation testing with 2500 permutations, a cluster-alpha of 0.01 and significance of 0.025 revealed a significant difference between epilepsy without medication and controls(1). The TMS PCI cluster is located from 50 ms to 80 ms in the gamma frequency range, with increased PCI in the group with epilepsy when compared with the control group. The photic PCI cluster is located over the whole time window in the 10–14 Hz frequency band, with decreased PCI in the group with epilepsy when compared with the control group.

the decrease of the rPCI and NNEI was linked to increased doses of levetiracetam. Replication of this finding is needed to evaluate the value of rPCI as cortical excitability marker. These findings are in line with a previous study using magnetoencephalography and photic stimulation that reported an elevated rPCI in photosensitive absence epilepsy; it increased gradually in the period preceding the occurrence of a paroxysmal response.<sup>28</sup>

The rPCI is a relative measure. Reduced phase clustering at lower frequencies and increased phase clustering at higher frequencies can theoretically result in high rPCI values. We previously introduced the NNEI to quantify excitability determined at the neuronal level.<sup>30</sup> The NNEI specifically reflects the low frequency spectral components. We previously showed that NNEI is small at low excitability levels but is high at high excitability levels.<sup>30</sup> Thus, given Eq. (3), a low PCI value at the base frequency corresponds to a high NNEI, i.e., a high neural network excitability. We confirmed this after photic stimulation. We

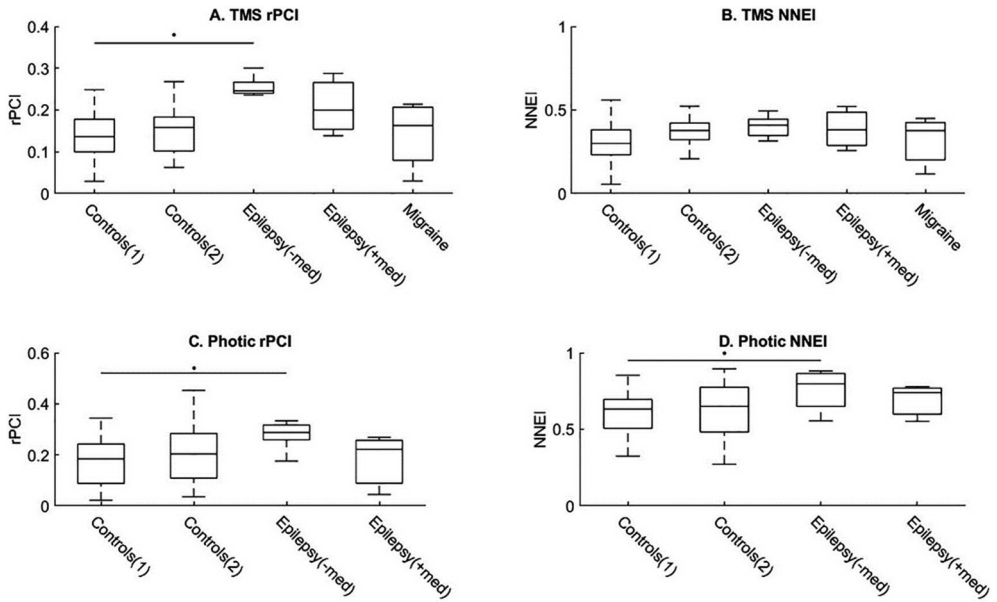


**Fig. 4.** Excitability biomarker boxplots for all groups. Median TMS polarity-compensated relative phase clustering index (rPCI) and neural network excitability index (NNEI) for all groups and stimulation modalities. The boxes show the 25–75th percentiles, the line in the box is the sample median. The polarity-compensated transcranial magnetic stimulation (0.5 Hz) results are shown in panels A. and B. 6 Hz photic stimulation results are shown in panels C. and D. Photic stimulation was not done in the group with migraine. \*indicates significant difference between the indicated groups.

found lower phase clustering in lower frequency ranges (alpha and beta bands) and a higher NNEI in the group with epilepsy off medication compared with controls. Conversely, after TMS, we found increased phase clustering in gamma range frequencies in the group with epilepsy without medication compared with controls. The net result was a higher relative PCI in the group with epilepsy off medication for both stimulation modalities. This suggests that different mechanisms are at play following TMS and photic stimulation. In our sample, the NNEI only differentiates the group with epilepsy from controls after photic stimulation. Alpha desynchronization was previously shown to be linked to an increase in oscillations at higher frequencies while an increase of activity in the alpha band is as a sign of cortical hypoexcitability.<sup>51–53</sup> It was recently shown that diazepam, a gamma aminobutyric acid-A (GABA-A) receptor agonist, increased TMS-induced alpha band synchronization in healthy subjects.<sup>54</sup> Interestingly,

**Table 4.** Median relative Phase Clustering Index and 5-95 percentile for all groups.

		<b>Controls(1)</b>	<b>Controls(2)</b>	<b>Epilepsy (-med)</b>	<b>Epilepsy (+med)</b>	<b>Migraine</b>
	N	36	30	5	3	10
<b>TMS</b>	rPCI	0.113 (0.033-0.232)	0.114 (0.046-0.215)*	0.224 (0.182-0.244)*	0.185 (0.141-0.293)*	0.132 (0.0109-0.223)
	NNEI	0.327 (0.128-0.583)	0.4 (0.192-0.556)	0.437 (0.335-0.488)	0.414 (0.29-0.576)	0.409 (0.114-0.518)
	N	35	29	5	3	-
<b>Photic</b>	rPCI	0.143 (0.0392-0.324)	0.172 (0.0442-0.351)	0.291 (0.193-0.301)*	0.143 (0.0236-0.256)	-
	NNEI	0.631 (0.398-0.802)	0.624 (0.317-0.872)	0.785 (0.617-0.866)*	0.72 (0.544-0.768)	-
	N	35	29	4	3	10
<b>Sham</b>	rPCI	0.089 (0.0274-0.175)	0.0473 (0.0239-0.124)	0.113 (0.026-0.128)	0.0558 (0.026-0.106)	0.0466 (0.019-0.0786)
	NNEI	0.756 (0.53-0.853)	0.82 (0.688-0.881)	0.801 (0.513-0.868)	0.864 (0.513-0.923)	0.809 (0.718-0.893)

*N: number of participants in whom data were collected. PC: Polarity-compensated (age adjusted in the epilepsy groups only). Photic stimulation at 6Hz was not performed in the migraine group. \* indicates significant difference with the respective control population*

diazepam is used to terminate seizures. The decreased phase clustering in the alpha range after photic stimulation in epilepsy off drugs may thus indicate decreased GABAergic inhibition<sup>55,56</sup> and may facilitate phase clustering in the gamma range. In migraine, phase synchronization in the alpha band following visual stimulation was increased.<sup>35</sup> As we did not visually stimulate participants with migraine, we cannot confirm this finding. In controls, age positively correlated with NNEI and rPCI, in line with previous observations of decreasing alpha band phase locking with increasing age, especially in occipital regions.<sup>57</sup>

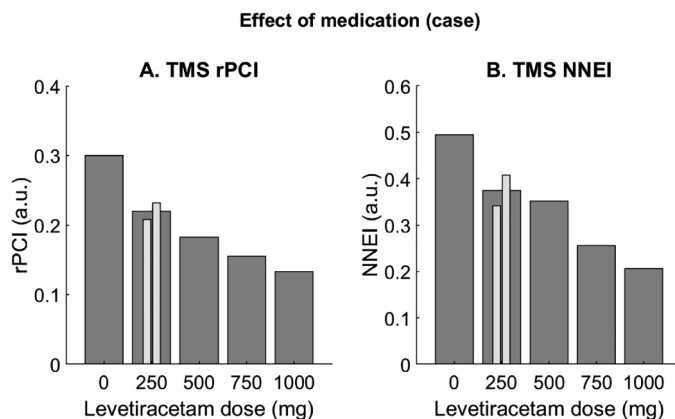


**Fig. 5.** Effect of medication (levetiracetam) on rPCI and NNEI for one participant with juvenile myoclonic epilepsy. For case E3 of Table 1, the evolution of the polarity-compensated rPCI & NNEI against the levetiracetam dose is depicted. This is the only participant in whom several measurements were done with different medication doses. The polarity-compensated rPCI and NNEI are shown on the y-axis and each dose of levetiracetam on the x-axis. The plots are not shown in chronological order, as the participant started with 1000 mg levetiracetam. The dose was gradually lowered to 250 mg because of side effects. Two measurements were done while the participant was taking 250 mg levetiracetam; the average is shown in gray. The participant remained seizure-free for the duration of the study. During the last measurement (250 mg), no photoparoxysmal reaction was seen whereas this had been present during the other measurements.

Our finding of high NNEI and reduced photic stimulation phase clustering in the alpha band in the group with epilepsy may be age related. High NNEI, reflecting low phase clustering in the alpha band (corresponding to a low value of PCI1), suggests a state of high excitability which may contribute to this form of epilepsy affecting mainly young adults between 12 and 20 years old.

The increased phase clustering in the gamma range in epilepsy off medication after TMS and photic stimulation may indicate increased propensity to synchronization and entrainment of neural populations due to recurrent connectivity.<sup>28</sup> Recurrent connectivity and reduced GABAergic inhibition may set migraine and epilepsy apart, as the rPCI and PCI frequency spectrum of migraine did not differ from controls. Migraine and epilepsy showed increased cortical excitability in previous studies.<sup>13,21,58–60</sup> Further studies are needed to understand the mechanisms underlying the reported cortical hyperexcitability in migraine.

In all groups, the highest PCI following magnetic and photic stimulations was found in the gamma range (30–40 Hz), consistent with previous findings.<sup>20</sup> Artifacts elicited by TMS (muscle and stimulation artifacts) can also occur in the gamma frequency range.<sup>61</sup> Transcranial magnetic stimulation-induced muscle artifacts usually peak around 7 ms and return to baseline around 15 ms.<sup>60</sup> We therefore analyzed the rPCI in epochs that theoretically start after or at the tail end of the muscle artifact and repeated the analysis for windows starting at 20, 25, and 30 ms without changing the results. We introduced several novel strategies to reduce artifacts. Firstly, the rPCI analysis (Eq. (2)) corrects large stimulus-locked artifacts. The NNEI is, however, still affected by these artifacts. Secondly, we compensated the magnetic charge of the stimulation (Eq. (3)), cancelling volume conductance and polarity-dependent TMS decay artifacts. Lastly, the rPCI obtained with TMS is consistent with the rPCI obtained with photic stimulation. Both stimulation modalities, however, differ in terms of PCI. We therefore conclude that the rPCI and its elevation in the group with epilepsy compared to controls represent a neuronal process rather than a measurement artifact.

Our comparison of the rPCI elicited by magnetic and photic stimulation modalities shows that magnetic stimulation elicits a larger rPCI difference between people with epilepsy and controls and may have greater potential for clinical application. The rPCI analysis yields one mean value per individual, making statistical analysis relatively straightforward. Similar to TMS-evoked potential analysis, rPCI analysis can also be done on each EEG channel. Our experimental set-up with a circular coil was not directed towards localization, but in a design with image-guided focal magnetic stimulation in focal epilepsy, the rPCI may potentially help localize cortical areas with aberrant inhibition. Image-guided focal magnetic stimulation was previously successful in localizing cortical areas connected to subcortical heterotopic gray matter in periventricular nodular heterotopia using the TMS-evoked potential.<sup>25</sup>

The phase clustering measures reported here are obtained from the TMS-triggered responses per channel over stimulation trials. We did not address phase synchronization between EEG channels (see for review<sup>62</sup>). A recent TMS–EEG study showed that TMS-induced activity persists up to 800 ms poststimulus.<sup>63</sup> We have studied the TMS intertrial phase clustering response up to 750 ms after

the stimulus. In our data, phase clustering decays shortly after the TMS stimulus, with clustering at higher frequencies decaying faster than at low frequencies. There was no apparent clustering of phases of the higher frequencies (>20 Hz) after ~ 120 ms while there is no clustering of lower frequencies (<20 Hz) after 400 ms. More than 400 ms after the TMS stimulus, phase clustering was only present in the low frequency bands (<8 Hz).

The limitations of our study include the small sample size in the groups with epilepsy and with migraine, which we dealt with by using permutation-based statistics that are robust even when small and groups of varying sample size are considered,<sup>64</sup> and the need to optimize the stimulation protocol for the analysis of phase clustering. Repetitive magnetic stimulation can alter cortical excitability, and 5 Hz, but not 0.5 Hz stimulation, significantly increased the motor-evoked potential.<sup>45</sup> A subsequent study did show a small inhibitory effect of 0.5 Hz stimulation, especially during the first 20 stimuli.<sup>65</sup> Others showed that the motor evoked potential (MEP) amplitude increased after 200 TMS pulses given every 4 s.<sup>66</sup> Only one study investigated the effect of 15-minute trains of 0.6 Hz stimulation on the EEG and found a significant increase of the N45 amplitude.<sup>67</sup> Our choice for a ramped stimulus–response curve with an interstimulus interval of 0.5 Hz was based on the fact that stimulus–response curves were shown to be invariant to interstimulus intervals from 1.4 to 4 s,<sup>68</sup> and that there was no difference between stimulus–response curves acquired with a ramped (increasing) or random stimulation intensity order.<sup>69</sup> Several studies have shown the effect of stimulation intensity on the EEG response, such that a cortical excitability threshold could be measured.<sup>20,70</sup> As a first approach, we chose to pool different stimulus intensities to calculate the rPCI, further research will include the identification of stimulus intensity effects on this parameter. Cortical excitability is dynamic and changes throughout the day.<sup>71</sup> Our measurements were conducted at 9 AM or 2 PM. No significant differences in TMS measures were reported between these times of the day,<sup>41</sup> except a larger TMS-evoked potential 100 ms after the stimulus.<sup>42</sup> We did not find a difference in rPCI between the people measured at 9 AM and those measured at 2 PM. Cortical excitability was also shown to change between, before, and after epileptic seizures<sup>72–74</sup> and migraine attacks.<sup>14</sup> We took care to conduct our measurements in the interictal period. Previously, the rPCI was shown to increase when photic stimulation was followed by an epileptic discharge.<sup>28</sup> To improve the

understanding of the clinical significance of the rPCI and NNEI as biomarkers for a brain state with increased cortical excitability and seizure propensity, further studies will need to assess its change just before, after, and between seizures. Another important clinical question is whether the rPCI could help differentiate responders to antiepileptic therapy from non-responders.

## **5.5 Conclusion**

We showed that EEG phase clustering elicited by TMS and photic stimulation is a potential marker of epileptogenicity in people with JME. The systematic application of rPCI may contribute to a better understanding of pathophysiological mechanisms in epilepsy and may have a direct clinical application.

## References

1. Jefferys, J. G. R. Advances in understanding basic mechanisms of epilepsy and seizures. *Seizure* **19**, 638–646 (2010).
2. Pietrobon, D. & Moskowitz, M. A. Pathophysiology of migraine. *Annu. Rev. Physiol.* **75**, 365–391 (2013).
3. Tolner, E. A. *et al.* From migraine genes to mechanisms. *Pain* **156**, S64–S74 (2015).
4. Bauer, P. R. *et al.* Headache and epilepsy topical collection on secondary headache. *Curr. Pain Headache Rep.* **17**, 351–60 (2013).
5. Mantegazza, M. & Cestè, S. Pathophysiological mechanisms of migraine and epilepsy: Similarities and differences. *Neuroscience Letters* vol. 667 92–102 (2018).
6. Haut, S. R., Bigal, M. E. & Lipton, R. B. Chronic disorders with episodic manifestations: Focus on epilepsy and migraine. *Lancet Neurol.* **5**, 148–157 (2006).
7. Rogawski, M. A. Common pathophysiological mechanisms in migraine and epilepsy. *Arch. Neurol.* **65**, 709–714 (2008).
8. Vecchia, D. & Pietrobon, D. Migraine: A disorder of brain excitatory-inhibitory balance? *Trends Neurosci.* **35**, 507–520 (2012).
9. de Goede, A. A., ter Braack, E. M. & van Putten, M. J. A. M. Single and paired pulse transcranial magnetic stimulation in drug naïve epilepsy. *Clin. Neurophysiol.* **127**, 3140–3155 (2016).
10. Brigo, F. *et al.* Resting motor threshold in idiopathic generalized epilepsies: A systematic review with meta-analysis. *Epilepsy Res.* **101**, 3–13 (2012).
11. Kelley, S. A., Hartman, A. L. & Kossoff, E. H. Comorbidity of migraine in children presenting with epilepsy to a tertiary care center. *Neurology* **79**, 468–473 (2012).
12. Schankin, C. J. *et al.* Headache in juvenile myoclonic epilepsy. *J. Headache Pain* **12**, 227–233 (2011).
13. Brigo, F. *et al.* Transcranial magnetic stimulation of visual cortex in migraine patients: A systematic review with meta-analysis. *J. Headache Pain* **13**, 339–349 (2012).
14. Cortese, F. *et al.* Excitability of the motor cortex in patients with migraine changes with the time elapsed from the last attack. *J. Headache Pain* **18**, 16–21 (2017).
15. Aurora, S. K., Al-Sayeed, F. & Welch, K. M. A. The cortical silent period is shortened in migraine with aura. *Cephalalgia* **19**, 708–712 (1999).
16. Werhahn, K. J. *et al.* Motor cortex excitability in patients with migraine with aura and hemiplegic migraine. *Cephalalgia* **20**, 45–50 (2000).

17. Siniatchkin, M. *et al.* Peri-ictal changes of cortical excitability in children suffering from migraine without aura. *Pain* **147**, 132–140 (2009).
18. Neverdahl, J. P., Omland, P. M., Uglem, M., Engstrøm, M. & Sand, T. Reduced motor cortical inhibition in migraine: A blinded transcranial magnetic stimulation study. *Clin. Neurophysiol.* **128**, 2411–2418 (2017).
19. Miniussi, C. & Thut, G. Combining TMS and EEG offers new prospects in cognitive neuroscience. *Brain Topogr.* **22**, 249–256 (2010).
20. Saari, J., Kallioniemi, E., Tarvainen, M. & Julkunen, P. Oscillatory TMS-EEG-Responses as a Measure of the Cortical Excitability Threshold. *IEEE Trans. Neural Syst. Rehabil. Eng.* **26**, 383–391 (2018).
21. Del Felice, A., Fiaschi, A., Bongiovanni, G. L., Savazzi, S. & Manganotti, P. The sleep-deprived brain in normals and patients with juvenile myoclonic epilepsy: A perturbational approach to measuring cortical reactivity. *Epilepsy Res.* **96**, 123–131 (2011).
22. Julkunen, P. *et al.* TMS-EEG reveals impaired intracortical interactions and coherence in Unverricht-Lundborg type progressive myoclonus epilepsy (EPM1). *Epilepsy Res.* **106**, 103–112 (2013).
23. Valentin, A. *et al.* Late EEG responses triggered by transcranial magnetic stimulation (TMS) in the evaluation of focal epilepsy. *Epilepsia* **49**, 470–480 (2008).
24. Kimiskidis, V. K., Kugiumtzis, D., Papagiannopoulos, S. & Vlaikidis, N. Transcranial magnetic stimulation (TMS) modulates epileptiform discharges in patients with frontal lobe epilepsy: A preliminary EEG-TMS study. *Int. J. Neural Syst.* **23**, 121102031948003 (2013).
25. Shafi, M. M. *et al.* Physiological consequences of abnormal connectivity in a developmental epilepsy. *Ann. Neurol.* **77**, 487–503 (2015).
26. Kimiskidis, V. K. *et al.* TMS combined with EEG in genetic generalized epilepsy: A phase II diagnostic accuracy study. *Clin. Neurophysiol.* **128**, 367–381 (2017).
27. ter Braack, E. M., Koopman, A. W. E. & van Putten, M. J. A. M. Early TMS evoked potentials in epilepsy: A pilot study. *Clin. Neurophysiol.* **127**, 3025–3032 (2016).
28. Parra, J. *et al.* Gamma-band phase clustering and photosensitivity: Is there an underlying mechanism common to photosensitive epilepsy and visual perception? *Brain* **126**, 1164–1172 (2003).
29. Kalitzin, S., Velis, D., Suffczynski, P., Parra, J. & Lopes Da Silva, F. Electrical brain-stimulation paradigm for estimating the seizure onset site and the time to ictal transition in temporal lobe epilepsy. *Clin. Neurophysiol.* **116**, 718–728 (2005).
30. Wendling, F. *et al.* Brain (Hyper)Excitability Revealed by Optimal Electrical Stimulation of GABAergic Interneurons. *Brain Stimul.* **9**, 919–932 (2016).

31. Meisel, C. *et al.* Intrinsic excitability measures track antiepileptic drug action and uncover increasing/decreasing excitability over the wake/sleep cycle. *Proc. Natl. Acad. Sci. U. S. A.* **112**, 14694–14699 (2015).
32. Yum, M. K. *et al.* Timely event-related synchronization fading and phase de-locking and their defects in migraine. *Clin. Neurophysiol.* **125**, 1400–1406 (2014).
33. Angelini, L. *et al.* Steady-state visual evoked potentials and phase synchronization in migraine patients. *Phys. Rev. Lett.* **93**, 038103–1 (2004).
34. Gantenbein, A. R. *et al.* Sensory information processing may be neuroenergetically more demanding in migraine patients. *Neuroreport* **24**, 202–205 (2013).
35. De Tommaso, M. *et al.* Visually evoked phase synchronization changes of alpha rhythm in migraine: Correlations with clinical features. *Int. J. Psychophysiol.* **57**, 203–210 (2005).
36. de Tommaso, M. *et al.* Functional connectivity of EEG signals under laser stimulation in migraine. *Front. Hum. Neurosci.* **9**, 1–10 (2015).
37. De Tommaso, M. *et al.* Altered processing of sensory stimuli in patients with migraine. *Nat. Rev. Neurol.* **10**, 144–155 (2014).
38. Oldfield, R. C. The assessment and analysis of handedness: The Edinburgh inventory. *Neuropsychologia* **9**, 97–113 (1971).
39. Kasteleijn-Nolst Trenité, D. G. A. *et al.* Consensus on diagnosis and management of JME: From founder's observations to current trends. *Epilepsy Behav.* **28**, (2013).
40. Olesen, J. *et al.* The International Classification of Headache Disorders, 3rd edition (beta version). *Cephalalgia* **33**, 629–808 (2013).
41. Koski, L., Schrader, L. M., Wu, A. D. & Stern, J. M. Normative data on changes in transcranial magnetic stimulation measures over a ten hour period. *Clin. Neurophysiol.* **116**, 2099–2109 (2005).
42. ter Braack, E. M., de Goede, A. A. & van Putten, M. J. A. M. Resting Motor Threshold, MEP and TEP Variability During Daytime. *Brain Topogr.* **32**, 17–27 (2019).
43. Groppa, S. *et al.* A practical guide to diagnostic transcranial magnetic stimulation: Report of an IFCN committee. *Clin. Neurophysiol.* **123**, 858–882 (2012).
44. Pascual-leone, A., Valls-solé, J., Wassermann, E. M. & Hallett, M. Responses to rapid-rate transcranial magnetic stimulation of the human motor cortex. *Brain* **117**, 847–858 (1994).
45. Gorsler, A., Bäumer, T., Weiller, C., Münchau, A. & Liepert, J. Interhemispheric effects of high and low frequency rTMS in healthy humans. *Clin. Neurophysiol.* **114**, 1800–1807 (2003).
46. Rossi, S. *et al.* Safety, ethical considerations, and application guidelines for the use of

- transcranial magnetic stimulation in clinical practice and research. *Clin. Neurophysiol.* **120**, 2008–2039 (2009).
47. Kalitzin, S., Parra, J., Velis, D. N. & Lopes Da Silva, F. H. Enhancement of phase clustering in the EEG/MEG gamma frequency band anticipates transitions to paroxysmal epileptiform activity in epileptic patients with known visual sensitivity. *IEEE Trans. Biomed. Eng.* **49**, 1279–1286 (2002).
  48. Kalitzin, S. *et al.* Quantification of spontaneous and evoked HFO's in SEEG recording and prospective for pre-surgical diagnostics. Case study. in *Proceedings of the Annual International Conference of the IEEE Engineering in Medicine and Biology Society, EMBS* vol. 6 1024–1027 (2012).
  49. Groppe, D. M., Urbach, T. P. & Kutas, M. Mass univariate analysis of event-related brain potentials/fields I: A critical tutorial review. *Psychophysiology* **48**, 1711–1725 (2011).
  50. Maris, E. & Oostenveld, R. Nonparametric statistical testing of EEG- and MEG-data. *J. Neurosci. Methods* **164**, 177–190 (2007).
  51. Toro, C. *et al.* Event-related desynchronization and movement-related cortical potentials on the ECoG and EEG. *Electroencephalogr. Clin. Neurophysiol. Evoked Potentials* **93**, 380–389 (1994).
  52. Lopes da Silva, F. Neural mechanisms underlying brain waves: from neural membranes to networks. *Electroencephalogr. Clin. Neurophysiol.* **79**, 81–93 (1991).
  53. Thut, G. *et al.* Differential effects of low-frequency rTMS at the occipital pole on visual-induced alpha desynchronization and visual-evoked potentials. *Neuroimage* **18**, 334–347 (2003).
  54. Premoli, I. *et al.* The impact of GABAergic drugs on TMS-induced brain oscillations in human motor cortex. *Neuroimage* **163**, 1–12 (2017).
  55. Wendling, F., Bartolomei, F., Bellanger, J. J. & Chauvel, P. Epileptic fast activity can be explained by a model of impaired GABAergic dendritic inhibition. *Eur. J. Neurosci.* **15**, 1499–1508 (2002).
  56. Avoli, M. & de Curtis, M. GABAergic synchronization in the limbic system and its role in the generation of epileptiform activity. *Progress in Neurobiology* vol. 95 104–132 (2011).
  57. Kolev, V., Yordanova, J., Basar-Eroglu, C. & Basar, E. Age effects on visual EEG responses reveal distinct frontal alpha networks. *Clin. Neurophysiol.* **113**, 901–910 (2002).
  58. Reutens, D. C., Berkovic, S. F., Macdonell, R. A. L. & Bladin, P. F. Magnetic stimulation of the brain in generalized epilepsy: Reversal of cortical hyperexcitability by anticonvulsants. *Ann. Neurol.* **34**, 351–355 (1993).
  59. Akgun, Y. *et al.* Cortical excitability in juvenile myoclonic epileptic patients and their

- asymptomatic siblings: A transcranial magnetic stimulation study. *Seizure* **18**, 387–391 (2009).
60. Manganotti, P., Bongiovanni, L. G., Fuggetta, G., Zanette, G. & Fiaschi, A. Effects of sleep deprivation on cortical excitability in patients affected by juvenile myoclonic epilepsy: A combined transcranial magnetic stimulation and EEG study. *J. Neurol. Neurosurg. Psychiatry* **77**, 56–60 (2006).
  61. Rogasch, N. C. *et al.* Removing artefacts from TMS-EEG recordings using independent component analysis: Importance for assessing prefrontal and motor cortex network properties. *Neuroimage* **101**, 425–439 (2014).
  62. Varela, F., Lachaux, J. P., Rodriguez, E. & Martinerie, J. The brainweb: Phase synchronization and large-scale integration. *Nat. Rev. Neurosci.* **2**, 229–239 (2001).
  63. Gordon, P. C., Desideri, D., Belardinelli, P., Zrenner, C. & Ziemann, U. Comparison of cortical EEG responses to realistic sham versus real TMS of human motor cortex. *Brain Stimul.* **11**, 1322–1330 (2018).
  64. Legendre, P. & Legendre, L. *Statistical testing by permutation. Numerical Ecology* vol. 2 (Elsevier Science BV, 1998).
  65. Julkunen, P., Säisänen, L., Hukkanen, T., Danner, N. & Könönen, M. Does second-scale intertrial interval affect motor evoked potentials induced by single-pulse transcranial magnetic stimulation? *Brain Stimul.* **5**, 526–532 (2012).
  66. Pellicciari, M. C., Miniussi, C., Ferrari, C., Koch, G. & Bortoletto, M. Ongoing cumulative effects of single TMS pulses on corticospinal excitability: An intra- and inter-block investigation. *Clin. Neurophysiol.* **127**, 621–628 (2016).
  67. Van Der Werf, Y. D. & Paus, T. The neural response to transcranial magnetic stimulation of the human motor cortex. I. Intracortical and cortico-cortical contributions. *Exp. Brain Res.* **175**, 231–245 (2006).
  68. Mathias, J. P., Barsi, G. I., Van De Ruit, M. & Grey, M. J. Rapid acquisition of the transcranial magnetic stimulation stimulus response curve. *Brain Stimul.* **7**, 59–65 (2014).
  69. Pearce, A. J., Clark, R. A. & Kidgell, D. J. A comparison of two methods in acquiring stimulus-response curves with transcranial magnetic stimulation. *Brain Stimul.* **6**, 306–309 (2013).
  70. Komssi, S., Kähkönen, S. & Ilmoniemi, R. J. The Effect of Stimulus Intensity on Brain Responses Evoked by Transcranial Magnetic Stimulation. *Hum. Brain Mapp.* **21**, 154–164 (2004).
  71. Chellappa, S. L. *et al.* Circadian dynamics in measures of cortical excitation and inhibition balance. *Sci. Rep.* **6**, 1–13 (2016).
  72. Cosentino, G. *et al.* Cyclical changes of cortical excitability and metaplasticity in

- migraine: Evidence from a repetitive transcranial magnetic stimulation study. *Pain* **155**, 1070–1078 (2014).
73. Delvaux, V. *et al.* Reduced excitability of the motor cortex in untreated patients with de novo idiopathic ‘grand mal’ seizures. *J. Neurol. Neurosurg. Psychiatry* **71**, 772–776 (2001).
74. Badawy, R., MacDonell, R., Jackson, G. & Berkovic, S. The peri-ictal state: Cortical excitability changes within 24 h of a seizure. *Brain* **132**, 1013–1021 (2009).

## Supplementary information

### *Interpretation of the Phase Clustering Index (PCI) in terms of system dynamics*

Definitions (1), (2) and (3) of the main text, give a formal signal-analytical algorithm but do not reveal the properties of the dynamic system that may generate those features of phase clustering. Here we present a simple, analytical model of the response of the neuronal system to external perturbation:

$$F_{ci}^{(\pm)f} = A_c^{(\pm)}V^f + R_c^{(\pm)f} + B_{ci}^f \quad (S1)$$

In the above equation  $F$  are the Fourier response amplitudes as introduced previously;  $V$  is volume conductance term including all linear artefacts related to the stimulus;  $R$  is the polarity dependent physiological response and  $B$  is the background activity, not locked in time to the stimulus. It follows that the stimulation amplitude  $A$   $A_\alpha^{(+)} = -A_\alpha^{(-)}$  if the stimulation current is matched exactly for both polarities. Inserting the response model (S1) into the combined, polarity-compensated amplitudes in eq (4) of the main text, the first term from (S1) cancels. Note that the norm in the denominator in (1) can also be written as follows:

$$PCI_c^f = \frac{\langle \sqrt{|F_{c,i}^f|^2} \rangle_i}{\sqrt{\langle |F_{c,i}^f|^2 \rangle_i}} \quad (S2)$$

This form is different from earlier publications [5,6]. While the results calculated in both ways are similar, this norm allows for a better pathophysiological interpretation of the underlying mechanism.

Substituting the result into the PCI definition eq (S2) and assuming that the background activity  $B$  and the physiological response to the stimulation  $R$  are not correlated, we obtain after simple calculus:

$$PCI_c^f = \frac{RBR_c^f}{\sqrt{1+|RBR_c^f|^2}}; RBR_c^f \equiv \frac{R_c^{(+f)}+R_c^{(-f)}}{\sqrt{2\langle |B_{ci}^f|^2 \rangle_i}} \quad (S2)$$

In the above equation, *RBR* is the ratio between the evoked physiological response and the magnitude of on-going background activity (the factor 2 under the root in the denominator reflects the summation of the two polarities). We can interpret this quantity as a measure of the sensitivity of the system to external perturbations. The PCI is then just the *RBR* but with its magnitude functionally mapped to the [0,1] interval.

The above response model (S1) and the assumptions related to it, are, although realistic, purely “ad hoc” at this stage. A more detailed response model of the neuronal dynamics underlying the PCI will be reported elsewhere.

# Chapter 6

Cortical excitability before and after long-term perampanel treatment for epilepsy

Submitted for journal publication.

## Abstract

Antiseizure medications (ASM), which may influence cortical excitability, are the mainstay of epilepsy treatment. Transcranial magnetic stimulation (TMS) is helpful to evaluate cortical excitability. We assessed changes in TMS responses using serial TMS measurements in people treated with an adjuvant non-competitive AMPA-receptor agonist.

We included adults with refractory, active epilepsy ( $\geq 1$  seizure/month), advised to start adjuvant treatment with non-competitive AMPA-receptor agonist perampanel as outpatients. After informed consent, we performed TMS measurement at three points: baseline before starting perampanel, at around two months after starting (4mg/day) and at a final/effective dose around six months. Dependent on seizure reduction ( $>50\%$ ), participants were dichotomized into responders (R) and non-responders (NR). We compared changes in motor cortex excitability through the rMT using a linear mixed-effects model. We evaluated TMS evoked potentials (TEPs) to single pulse and paired-pulse using within-subject Montecarlo based permutation analysis.

We included 18 adults, of whom seventeen (6R; 11NR; 1 lost to follow-up) had baseline and second-month measurements, and nine (4R; 5 NR) had all three. In responders, motor cortex excitability, quantified by rMT, significantly increased with increasing dose. Conversely, no significant changes were seen in the non-responder subgroup. TEPs for the single pulse and paired-pulse showed no significant clusters for any peaks between measurement and group comparisons.

The TEPs showed no significant changes between measurements and/or groups. Motor cortex excitability quantified by rMT is a potential biomarker to track or predict treatment outcomes in people starting adjuvant perampanel for epilepsy.

## 6.1 Introduction

The normal functioning of cortical networks critically depends on a finely tuned level of excitability, believed to be a product of excitation and inhibition within networks.<sup>1,2</sup> Monitoring cortical excitability in brain networks is advantageous for understanding normal and pathological brain function.<sup>3,4</sup> There are still gaps in understanding fluctuations in cortical excitability.<sup>5</sup> Epilepsy is a condition in which regular brain activity is interrupted by periods of abnormal hypersynchronous activity, i.e. seizures. Networks with a shifted or aberrant excitation:inhibition (E:I) balance are thought to facilitate seizures.<sup>1,6</sup> Treatment with antiseizure medication (ASM) may help restore the E:I balance.<sup>7</sup>

Glutamate is the primary excitatory neurotransmitter, acting on ionotropic and metabotropic receptors at the synapse. When glutamate binds to the ionotropic  $\alpha$ -amino-3-hydroxyl-5-methyl-4-isoxazole-propionate (AMPA) receptor, the receptor gate opens, enabling the transfer of cations and the generation of fast excitatory postsynaptic potentials.<sup>8</sup> The fast synaptic transmission mediated by AMPA-receptors allows for synchronization of the firing of pyramidal neurons and can play an essential role in seizure initiation and the spread of seizures.<sup>9</sup> Perampanel is the first ASM that targets the AMPA-receptor by blocking the receptor using allosteric regulation, exerting a broadband antiseizure effect.<sup>10-12</sup>

Transcranial magnetic stimulation (TMS) allows for direct non-invasive stimulation of cortical areas.<sup>13</sup> Motor cortex excitability is assessed by stimulating the motor system and recording the motor response in the target muscle. The resting motor threshold (rMT) is the stimulus strength needed to elicit a motor response of sufficient voltage recorded through the electromyogram (EMG). Previous studies using serial TMS measurements within-subjects have demonstrated that the rMT can be used to monitor changes in motor cortex excitability when starting a ketogenic diet or when tapering medication.<sup>14,15</sup> Measuring the cortical response through combined TMS-EEG is a relatively new modality of functional brain mapping.<sup>7</sup> The TMS-evoked EEG potential (TEP) is a time-varying signal with multiple peaks at different latencies and locations.<sup>16</sup> Multichannel EEG recordings of cortical responses to TMS have been increasingly used to assess drug effects.<sup>17-19</sup> A recent pharmaco-TMS-EEG study has shown that GABA-ergic and glutamatergic pharmaceutical agents modulate

the TEP shortly after using a single oral dose in healthy subjects.<sup>20</sup> It demonstrated modulation of the peak at 60ms by perampanel in the non-stimulated hemisphere, suggestive of a role of AMPA-receptors in the interhemispheric spread of activity. Previous single-dose TMS-EMG studies utilizing paired-pulse TMS (ppTMS) protocols demonstrated that NMDA antagonist dextromethorphan and AMPA-type glutamate receptor antagonist memantine decreased intracortical facilitation (ICF) while enhancing short-interval intracortical inhibition (SICI).<sup>21,22</sup> Thus, ICF is mainly associated with glutamate receptor-mediated excitatory functions in the motor cortex. Together, TMS combined with EMG and EEG allows for a multi-modal approach for quantifying cortical excitability.

We assessed the effect of long-term adjuvant perampanel treatment on cortical excitability in people with refractory epilepsy. We conducted a within-subject controlled longitudinal study to elucidate the effect of long-term perampanel treatment on cortical excitability measured by TMS-EEG for single-pulse TMS (spTMS) and the ppTMS ICF protocol. We compared pre-treatment evoked responses to responses at a fixed ASM dose in all subjects to evaluate the effect on motor cortex excitability as measured by the rMT and TEPs. We also compare these measures in responders and non-responders to assess if there are predictive markers and/or diagnostic markers for treatment effect.

## **6.2 Methods**

### *6.2.1 Population*

Adults with refractory localization-related epilepsy or generalized tonic-clonic seizures with a minimum of 1 seizure/month advised to start perampanel treatment at specialist epilepsy clinics in Stichting Epilepsie Instellingen Nederland (SEIN) and Academic Centre for Epileptology (ACE) Kempenhaeghe were candidates for the study. They were screened for contraindications to TMS other than seizures. Exclusion criteria included deep brain stimulators in-situ, pacemakers or other implanted devices other than nervus vagus stimulators, clinical or radiological evidence of major structural abnormalities of the motor cortex or pyramidal tract, pregnancy, evidence of a major neurological or psychiatric condition other than epilepsy, and/or change

in concomitant medication known to affect cortical excitability. All participants provided informed written consent. The ethics committee of Leiden University Medical Center approved the study (CME Leiden, NL53005.058.15).

### *6.2.2 Experimental design*

TMS measurements were performed before starting titration (T0), a second measurement at a fixed perampanel dose of 4mg/day dose (T1), and a final measurement after reaching the maximum tolerated or effective stable dose (T2). Participants kept a seizure diary prospectively for four weeks before T0. If the information on seizure frequency was already available, the baseline T0 measurement was scheduled as soon as possible. Perampanel titration followed standard clinical practice and was at the discretion of the treating neurologist. Participants were asked not to smoke, use alcohol or coffee in 12 hours preceding measurements and maintain a regular sleep pattern the night before the measurement, which was conducted either at 09.00 AM or 04.00 PM (fixed for each participant) and spread evenly between AM and PM.

### *6.2.3 Measurement setup*

We used a MagPro X100 magnetic stimulator (Magventure, Farum, Denmark) and a 14cm diameter parabolic circular coil (type MMC-140) or a sham TMS coil (type MCF-P-B65) in SEIN. In Kempenhaeghe the Magstim® BiStim stimulator (Magstim Co Ltd, Whitland, UK) was used in combination with a 9cm round coil. Sham stimulation in Kempenhaeghe was performed by rotating the coil 90 degrees along the vertical axis. The round coil was used because it diffusely activates the cortex compared to focal figure-of-eight coils and is less sensitive to small changes in coil position.<sup>23</sup> The current direction through the coil influences the direction of the induced magnetic field, resulting in preferential activation of either the left and/or right motor cortex. Muscle activity of the abductor pollicis brevis muscle (belly-tendon montage) was monitored using a Viking Nicolet EMG system recording at 16kHz. Electrode positioning was determined as the site that produced the highest MEPs with above threshold peripheral stimulation of the median nerve. Both centers recorded EEG using a 64-electrode EEG amplifier (SEIN: ANT-EEGO amplifier sampling at 4kHz, ANT Neuro b.V., Hengelo, the Netherlands; Kempenhaeghe: tMSI Refa amplifier sampling at 2048Hz, Twente Medical Systems International B.V, Oldenzaal, The Netherlands), in combination with a 64-channel TMS-

compatible EEG CAP (Waveguard™ cap, ANT Neuro b.V., Hengelo, the Netherlands). Participants were seated in a comfortable chair with their eyes open and arms in the supine position and instructed to blink 1 to 2 seconds after receiving a TMS stimulus. Earplugs were used to reduce the effect of the auditory evoked potential.

#### 6.2.4 Measurement TMS protocol

TMS stimulation sessions involved round coil and sham TMS centred above the vertex (Cz electrode position). The resting motor threshold (rMT) was first estimated starting at 30% maximum stimulator output (MSO) with 5% stepwise increments until a motor evoked response of  $>50\mu\text{V}$  in hand contralateral to the stimulated hemisphere was observed in  $>5$  out of 10 trials<sup>24</sup>. Next 1% adjustments were made until the lowest intensity was reached, where  $>5$  out of 10 trials were above  $50\mu\text{V}$ . This was repeated for both current directions, which depending on the current direction, either preferentially activates the right or left hemisphere. Then, a session of spTMS (50 pulses at 90% rMT), sham TMS (50 pulses at 90% rMT) and ppTMS ICF (50 pulses, 90% rMT conditioning, 110% rMT test stimulus with 10 ms interstimulus interval) were performed in normal and reversed current direction with 5 seconds in between stimuli with 20% jitter. Current direction through the round coil was shifted in a cyclical fashion. Between rounds of stimulation, five-minute breaks were scheduled as a slight pause to instruct and prepare the participant for the session.

#### 6.2.5 Data processing

The raw EEG data were processed using a combination of in-house scripts programmed in Matlab (The Math Works, Inc. MATLAB, version 2021a) and the Fieldtrip toolbox for EEG/MEG-analysis.<sup>25</sup> Firstly, data were visually inspected to remove artefactual channels and then re-referenced to the common reference of all remaining EEG channels. Epochs of 2 seconds were used for each TMS protocol, with 1000ms pre- and 1000ms post- stimulus. Trials that included blink artefacts -100ms pre- to 500ms post-stimulus were removed from the dataset ( $2.6\pm 1.3$  trials on average). The TMS pulse artefact was segmented out from -1 ms pre- to 10 ms post-stimulus. For each trial, the mean was subtracted based on a baseline window of -200 ms to -50 ms relative to the magnetic stimulus. Data were cleaned using two rounds of independent component analysis (FastICA). The first round was performed over the whole

epoch to capture and reject blink, saccade, line-noise and slow-decay components. The epoch was redefined to -500 ms pre to 750 ms post-stimulus for a subsequent second round of ICA decomposition focused on the TMS-related pre-and-post stimulus activation patterns where remaining line noise and time-locked and continuous muscle components were rejected. Then we applied a 4th order bandpass Butterworth zero-phase filter from 1-80Hz. A final step of automated quality control was the rejection of trials with a norm covariance of >2 standard deviations from the dataset (3 trials, on average, were removed).

### *6.2.6 Statistics*

For the responder/non-responder group comparison, participants were assigned to the responder (>50% reduction) or non-responder ( $\leq$ 50% reduction) group depending on seizure frequency at last follow-up compared to the seizure frequency at baseline).

Magnetic or sham stimulation responses were compared between measurement T0 and T1 for the individual peak time of interest (TOI) windows all located between 15 ms before to 262 ms after the magnetic pulse. For each peak, a predefined window was used to compare groups (P25: 16-34ms, N45: 38-55ms, P70: 56-82ms, N100: 89-133ms, P180: 173-262ms).<sup>18</sup> TEPs were compared for the whole epoch from 15-262ms and the predefined peaks, between measurements, using dependent sample t-tests, or between centers and between responders/non-responders using independent t-tests. Exact p-values were calculated by enumeration using cluster-based permutation testing to correct for multiple comparisons and the small sample size<sup>26</sup>. Clusters based on adjacency in time and electrode space (minimum of 2 electrodes) were formed using samples with a cluster-alpha of 0.05 (independent t-test). Each cluster's t-values (for time samples and electrodes) were summed and compared to a dataset of 2500 random permutations of the original data. Clusters were considered significantly different between groups when their summed t-values were lower or higher than 2.5% ( $p < 0.025$ ) of all permuted clusters.

The rMT was modelled using linear mixed-effect analysis of the relationship between rMT and perampanel dose, with center (SEIN or Kempenhaeghe) and current direction (preferentially activated hemisphere) as fixed effects. As random effects, we incorporated intercepts for subjects and by-outcome random

slopes for the effect of medication dose. The following formula describes the whole model:

$$rMT \sim 1 + Center + Current\ Direction + (1|subject) + (dose|response)$$

Visual inspection of residual plots did not suggest any apparent deviations from homoscedasticity or normality.

## 6.3 Results

### 6.3.1 Participants

Eighteen adults with refractory epilepsy were recruited from SEIN (n=8) and ACE Kempenhaeghe (n=10). Demographics are provided in Table 1, and a flow diagram is shown in Supplementary Fig. S1. All participants well-tolerated the TMS measurement. All underwent T0. Seventeen had T1 (one lost to follow-up), of whom nine had T2. Eight participants dropped out after T1 due to increased dizziness (n=2), fatigue (n=2), emotional state (n=1), nausea (n=1), instability (n=1), or inability to do a specific activity and a feeling that the seizures became more severe (n=1).

In most participants, perampanel was increased to a 4mg/day dose at a median of four weeks. Measurement T1 was performed at a median of seven weeks. One subject, however, reached the 4mg dose within two weeks of starting treatment with T1 measured at the end of the fourth week. Measurement T2 was performed on a 6mg dose in three, 8mg dose in four, and a 10mg dose in two.

The average seizure frequency was  $4.15 \pm 2.98$  events/month at T0,  $3.05 \pm 3.33$  events/month at T1, and  $2.50 \pm 2.57$  events/month at T2. Six subjects responded to adjuvant drug treatment (>50% seizure reduction compared to baseline) at measurement T1. Two responders stopped after T1 due to side effects.

### 6.3.2 Resting motor threshold

The rMT measured at each center for each measurement session is shown in Table 2. The results of the linear mixed effect model are shown in Table 3. There were marked differences in rMT between responders and non-responders. The

**Table 1.** Population Demographics

Case	Age (years)	Gender	Handedness	Seizure Type	Onset (Age)	ASM (n)	Seizures (events/month)			Dose (mg)	
							T0	T1	T2	T1	T2
401	47	F	R	FIA	33	1	9	7	8	4	10
402	57	M	R	FIA/fbTC	4	2	5	4	4	4	8
403	60	M	R	FIA	55	1	4	0	1	4	8
404	41	M	R	FIA	4	1	8	7	-	4	-
405	64	F	R	FIA	10	3	6	2	-	4	-
406	76	M	R	FIA/fbTC	17	2	3	1	-	4	-
407	59	M	R	FIA/fbTC	10	3	2	2	-	4	-
408	22	F	R	FIA/fbTC	8	1	8	6	-	4	-
409	20	F	L	FIA/fbTC	6	1	10	13	-	4	-
410	19	M	R	FIA	7	1	2	0	0	4	6
411	24	M	R	FIA/fbTC	7	2	1	1	-	4	-
412	51	M	R	FIA	34	2	1	1	-	4	-
413	28	M	R	FIA/fbTC	18	2	4	3	5	4	10
414	29	M	L	FIA/fbTC	30	2	2	2	3	4	8
415	32	M	R	FIA/fbTC	17	2	1	0	0	4	8
416	26	M	R	FIA/fbTC	18	2	3	1	1	4	6
417	44	F	R	FIA/fbTC	40	3	7	-	-	-	-
418	26	F	R	FA/fbTC	21	2	1	1	1	4	6

*FIA: focal with impaired awareness, fbTC: focal to bilateral tonic-clonic, T0: baseline pre-adjuvant treatment, T1: 4mg-dose measurement, T2: max effective/ tolerable dose measurement.*

rMT was significantly increased when increasing medication dose in the responder subgroup (estimate: -1.4022 %MSO/mg, p-value: <0.001, CI: -0.82813, CI+: 1.9763), but not in the in the non-responder subgroup (estimate: 0.1201, p-value: 0.591, CI: -0.322, CI+: 0.563). The fixed effect for the center was highly significant, with thresholds measured at SEIN requiring significantly

lower stimulator output compared to Kempenhaeghe (estimate: -15.238 %MSO/mg, p-value: 0.001, CI-: -24.648, CI+ -5.8275). No significant effect of the stimulated hemisphere was observed.

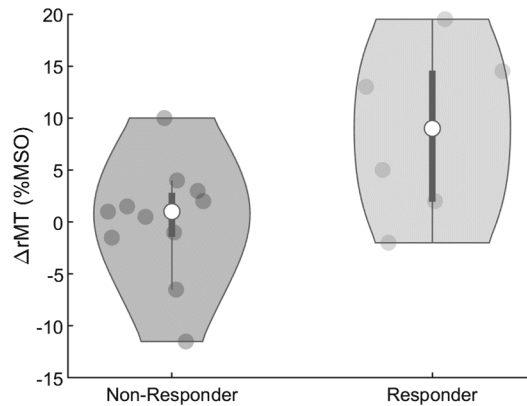


**Fig. 1.** Violin plots of the change in resting motor threshold (rMT) dichotomized by response to adjuvant perampanel administration. Depicts the change ( $\Delta$ ) in the rMT averaged across hemispheres measured at the 4mg dose measurement (T1) relative to the baseline pre-adjuvant treatment measurement (T0). The grey dots represent the individual measurements, the white circle represents the mean value, the dark grey bars represent the interquartile range, and the grey area represents the smoothed probability density. rMT: resting motor threshold, MSO: mean stimulator output.

**Table 2.** Overview of changes in resting motor threshold.

Center	Measurement	Cases (n)	Resting Motor Threshold	
			Right Hemisphere %MSO (std)	Left Hemisphere %MSO (std)
ACE Kempenhaeghe	T0	10	64.7 (11.6)	65.2 (10.6)
	T1	10	68.9 (13.4)	66.3 (12.4)
	T2	4	71 (6.6)	69.5 (9.7)
SEIN	T0	8	49.3 (8.6)	51.6 (8.3)
	T1	7	52.1 (12.7)	52.71 (11.0)
	T2	5	54.4 (15.8)	53.6 (9.7)

T0: baseline pre-adjuvant treatment, T1: 4mg-dose measurement, T2: max effective/ tolerable dose measurement, %MSO: percentage of max stimulator output, std: standard deviation.

### 6.3.3 TMS-EEG

Montecarlo cluster statistics for both spTMS and ppTMS protocols for the pre-specified TOI's are shown for 1) the baseline T0 current direction comparison (supplementary Table S1), the 4mg perampanel dose T1 versus baseline T0 comparison (supplementary Table S2), and the responder versus non-responder subgroup comparison (supplementary Table S3). No significant clusters were observed.

*Single Pulse.* The single pulse evoked responses measured at T0 and at T1 of the left hemisphere are shown in the left panel in Fig. 2. Pre-treatment TEPs and their topographical distributions were consistent with previous studies of single-pulse TMS. Current direction had no significant influence on the presence, latency and amplitude of peaks. The difference between T1 and T0 for the responder and non-responder group is shown in Fig. 3. Sham stimulation between measurements revealed no significant changes and not a single cluster between measurements averaged across subjects.

*Paired pulse intracortical facilitation.* TMS evoked potentials evoked by the paired-pulse ICF protocol, measured at T0 and T1 are shown in Fig. 2, right panel. Clusters for the P25 and P70 peaks evoked by left-hemispheric paired-pulse ICF stimulation were close to reaching significance, see supplementary table.1. There were no differences between responders and non-responders. Right hemispheric

**Table 3.** Resting motor threshold linear mixed effects model

<i>Fixed Effects</i>				
<b>Parameter Name</b>	<b>Estimate (%MSO)</b>	<b>Lower-95 (%MSO)</b>	<b>Upper-95 (%MSO)</b>	<b>p-value</b>
Intercept	64.35%	58.16%	70.54%	<0.001
Center	-15.17%	-24.57%	-5.78%	0.002
Handedness	0.91%	-1.07%	2.89%	0.364
<i>Random Effects</i>				
<b>Parameter Name</b>	<b>Estimate (%MSO)</b>	<b>Lower-95 (%MSO)</b>	<b>Upper-95 (%MSO)</b>	<b>p-value</b>
Intercept   Subject	9.35%	6.56%	13.34%	18 levels
Dose   Responders	1.41%/mg	0.84%/mg	1.97%/mg	<0.001
Dose   Non-responders	0.15%/mg	-0.25%/mg	0.55%/mg	0.452

%MSO: percentage of max stimulator output.

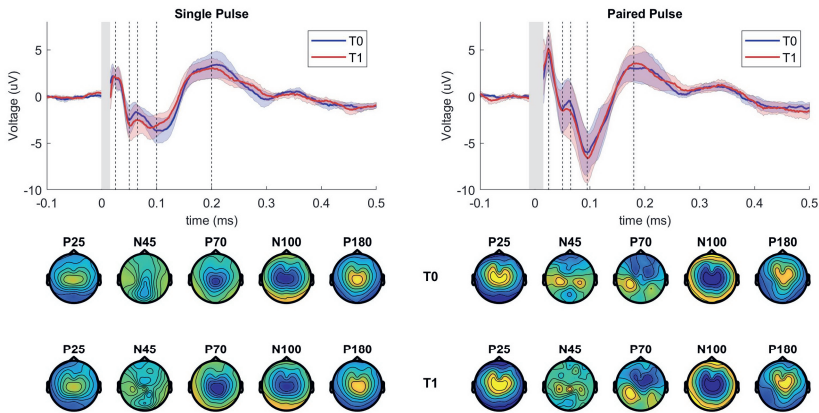


**Fig. 2.** Group average of TEPs evoked by single and paired-pulse TMS of the left hemisphere before and at 4mg perampanel dose. Upper panel shows pretreatment baseline (T0) and fixed 4mg perampanel dose (T1) TEPs averaged across all subjects for the central electrode cluster (Cz and neighboring electrodes with distance  $<2$ ). The grey area reflects the segmented window impacted by the TMS pulse artefact. The dotted lines indicate the location of the TEP peaks (P25, N45, P70, N100 and P180). The bottom panels show pretreatment baseline T0 and T1 topographic distributions of the peaks averaged across subjects. Each topography was obtained by averaging the signal in the respective TOI (P25:15-30ms, N45: 31-55ms, P70: 56-70ms, N100: 71-135ms, P180: 136-250ms).

stimulation with spTMS and ppTMS protocols resulted in clusters at every TOI, but no significance was reached for any cluster. Left hemispheric single-pulse stimulation also resulted in non-significant clusters found at P25, P70, N100 and P180. No clusters were found for TOI's for right hemispheric stimulation.

## 6.4 Discussion

We investigated the effect of long-term adjuvant AMPA-receptor antagonist treatment on TMS-evoked EMG and EEG potentials in adults with pharmaco-resistant epilepsy. Perampanel treatment had no significant effects on TEP peak amplitudes or latencies. We found no significant modulation of TEP's and the peak time of interest windows for either hemisphere or stimulation protocols. After introducing perampanel, rMT increased significantly in the responder subgroup, but not in the non-responder subgroup. The physiology and mechanisms underlying TMS-evoked EEG peaks and amplitudes remain controversial.<sup>19</sup> Previous pharmaco-TMS-EEG studies have shown that single

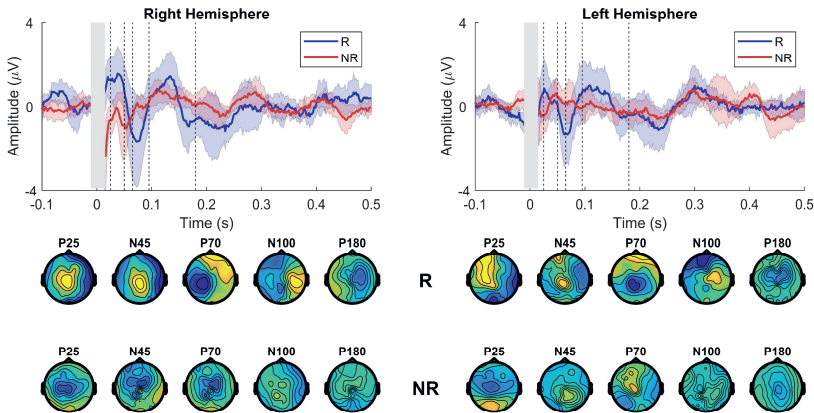


**Fig. 3.** The difference waveforms between 4mg fixed dose measurement T1 and baseline T0 TEPs averaged across responders and non-responders. Upper panel shows the difference curves between T1 and T0 for the central electrode cluster (Cz and neighbouring electrodes with distance  $<2$ ) averaged across responders and non-responders. The grey area reflects the segmented window impacted by the TMS pulse artefact. The dotted lines indicate the location of the TEP peaks (P25, N45, P70, N100 and P180). The bottom panels show the corresponding topographic distributions of the peaks averaged across responders and non-responders. Each topography was obtained by averaging the signal in the respective TOI (P25:15-30, N45: 31-55ms, P70: 56-70ms, N100: 71-135ms, P180: 136-250ms).

oral doses of various ASMs can modulate specific peaks in the TEP.<sup>17,18</sup> We found no modulation of TMS-evoked potentials between pretreatment baseline and the long-term fixed 4mg dose measurement in response to spTMS or ppTMS paradigms when averaged across all subjects or groups. This contrasts with a recent study that compared two glutamate-mediated receptor antagonists and found that perampanel reduced the P60 amplitude in the non-stimulated hemisphere in healthy subjects.<sup>20</sup> They speculate that this modulation may be related to inter-hemispheric inhibition mediated by perampanel. We could not re-confirm these findings in individuals with epilepsy starting long-term adjuvant treatment. We also did not find significant modulation of any of the peaks following the ppTMS ICF protocol. No previous work utilised TMS-EEG in conjunction with ppTMS protocols to explore AMPA-receptor agonist peak modulation. Previous pharmacological studies with TMS-EMG have demonstrated that NMDA antagonist dextromethorphan and AMPA-type glutamate receptor antagonist memantine decreased ICF,<sup>21,22</sup> while GABA<sub>A</sub> agonist lorazepam also decreased ICF.<sup>27</sup> It is thus surprising that we do not find

any peak modulation after long-term use of perampanel for spTMS and ppTMS readouts. One explanation for the null results for spTMS en ppTMS protocols could be the small sample size, yet, the monte-carlo permutation based statistics we used are robust even in small samples. Another explanation could be the rMT changes we measured. Stimulation intensity for spTMS and ppTMS is set at a fixed percentage relative to the measured rMT. Considering the significant differences in rMT within subjects, this may have normalized TEP changes. Another possibility is that, in contrast with single oral dose pharmaco-EEG studies, long-term use of medication does not modulate TEPs to a significant degree. Whilst single-dose studies investigating various ASMs have demonstrated modulation of specific peaks in the evoked response, long-term use of ASMs could potentially return evoked responses to pre-treatment baseline. There is little evidence at present to answer these questions as there are few longitudinal TMS-EEG studies investigating long-term administration of ASMs.

Resting Motor threshold is thought to reflect membrane excitability and is thus affected by agents that either directly or indirectly influence the membrane potential.<sup>28,29</sup> Voltage-gated sodium channel blockers have increased rMT compared to drug-naïve people with epilepsy and people without epilepsy. We found that people with epilepsy starting perampanel who respond to treatment have a significant increase in rMT, suggesting a reduction in cortical excitability. Non-responders, in contrast, had no significant change in rMT in response to adjuvant treatment. A pharmacological single-dose study has shown similar increases in rMT after administration of perampanel in healthy subjects, suggestive of a contribution of AMPA-receptors and their fast kinetics to corticospinal excitability.<sup>20</sup> The observed long-term increase in rMT in responders to perampanel treatment suggests that efficacy might be reflected in the corticospinal excitability, whilst those with no significant changes in seizure frequency showed no such lasting changes. Besides the demonstrated dose effect, a significant difference was observed between the two measurement locations. This difference may be attributed to the difference in stimulation strength output of the TMS equipment used and the difference in coil diameter.<sup>30</sup>

Our study has limitations. Firstly, concomitant medications may have potential confounding effects on rMT and ICF. Care was taken to schedule measurements

at fixed times to minimize the effects of drug intake and/or daily fluctuations in cortical excitability. Blood levels of ASMs change depend on the timing of drug intake relative to the measurement time. Perampanel is prescribed to be taken before bedtime to mitigate the peak effects. Perampanel interacts with other ASMs, which may have contributed to the stability of the TEP readouts and the relatively stable response in rMT in non-responders. Secondly, we did not use an auditory noise-masking procedure during the experiments. There may have been some potential effect of the somatosensory response associated with the click generated by the coil. A recent study found that non-transcranial multisensory co-stimulation significantly contributes to components often interpreted as the direct brain's response.<sup>19</sup> At the stage of off-line analysis, we compared test TMS protocols that had nearly identical somatosensory inputs associated with the TMS-clicks within subjects. In addition, between-subject comparisons were made through the difference curve between T1 and T0. As a result, this potential confounding was limited. Lastly, the dichotomization of the participants in responders and non-responders is contentious. The <50% reduction in seizure frequency would classify as ILAE class 4, which is not typically regarded as a favourable outcome. Generally, complete remission of seizures is warranted and is seen as a favourable outcome. We performed measurements in people with refractory epilepsy, thus severely limiting the chance of seizure freedom after starting adjuvant administration with perampanel.

## **6.5 Concluding statements and future perspective**

We demonstrated that long-term effects of perampanel treatment in people with epilepsy do not lead to significant modulation of any of the TMS evoked potential peaks. This contrasts with the more basic EMG rMT measure, which showed a significant reduction in corticospinal excitability in the responder subgroup. In individual cases, changes in rMT may be monitored or used as a promising biomarker to evaluate lasting changes in overall (motor) cortical excitability, treatment adjustments and outcome. Future research should be focused on exploring the effect of long-term use of ASMs and the effect on TMS-EMG/EEG measures as potential biomarkers for treatment outcome.

## References

1. Jefferys, J. G. R. Advances in understanding basic mechanisms of epilepsy and seizures. *Seizure* **19**, 638–646 (2010).
2. Avoli, M. & de Curtis, M. GABAergic synchronization in the limbic system and its role in the generation of epileptiform activity. *Progress in Neurobiology* vol. 95 104–132 (2011).
3. Rogawski, M. A. Common pathophysiologic mechanisms in migraine and epilepsy. *Arch. Neurol.* **65**, 709–714 (2008).
4. Mantegazza, M. & Cestè, S. Pathophysiological mechanisms of migraine and epilepsy: Similarities and differences. *Neuroscience Letters* vol. 667 92–102 (2018).
5. Rogasch, N. C. & Fitzgerald, P. B. Assessing cortical network properties using TMS-EEG. *Hum. Brain Mapp.* **34**, 1652–1669 (2013).
6. Suffczynski, P., Kalitzin, S. & Lopes Da Silva, F. H. Dynamics of non-convulsive epileptic phenomena modeled by a bistable neuronal network. *Neuroscience* **126**, 467–484 (2004).
7. Bauer, P. R., Kalitzin, S., Zijlmans, M., Sander, J. W. & Visser, G. H. Cortical excitability as a potential clinical marker of epilepsy: A review of the clinical application of transcranial magnetic stimulation. *Int. J. Neural Syst.* **24**, 1430001 (2014).
8. Traynelis, S. F. *et al.* Glutamate receptor ion channels: Structure, regulation, and function. *Pharmacol. Rev.* **62**, 405–496 (2010).
9. Rogawski, M. A. Revisiting AMPA receptors as an antiepileptic drug target. *Epilepsy Curr.* **11**, 56–63 (2011).
10. Hanada, T. & Hanada, T. The AMPA receptor as a therapeutic target in epilepsy: Preclinical and clinical evidence. *J. Receptor. Ligand Channel Res.* **7**, 39–50 (2014).
11. Hanada, T. *et al.* Perampanel: A novel, orally active, noncompetitive AMPA-receptor antagonist that reduces seizure activity in rodent models of epilepsy. *Epilepsia* **52**, 1331–1340 (2011).
12. French, J. A. *et al.* Perampanel for tonic-clonic seizures in idiopathic generalized epilepsy. *Neurology* **85**, 950–957 (2015).
13. Barker, A. T., Jalinous, R. & Freeston, I. L. Non-Invasive Magnetic Stimulation of Human Motor Cortex. *The Lancet* vol. 325 1106–1107 (1985).
14. Lee, H. W., Seo, H. J., Cohen, L. G., Bagic, A. & Theodore, W. H. Cortical excitability during prolonged antiepileptic drug treatment and drug withdrawal. in *Clinical Neurophysiology* vol. 116 1105–1112 (2005).
15. Helling, R. M. *et al.* Tracking cortical excitability dynamics with transcranial magnetic

- stimulation in focal epilepsy. *Ann. Clin. Transl. Neurol.* **9**, 540–551 (2022).
16. Ilmoniemi, R. J. *et al.* Neuronal responses to magnetic stimulation reveal cortical reactivity and connectivity. *Neuroreport* **8**, 3537–3540 (1997).
  17. Ziemann, U. *et al.* TMS and drugs revisited 2014. *Clin. Neurophysiol.* **126**, 1847–1868 (2015).
  18. Premoli, I. *et al.* TMS-EEG signatures of GABAergic neurotransmission in the human cortex. *J. Neurosci.* **34**, 5603–5612 (2014).
  19. Conde, V. *et al.* The non-transcranial TMS-evoked potential is an inherent source of ambiguity in TMS-EEG studies. *Neuroimage* **185**, 300–312 (2019).
  20. Belardinelli, P. *et al.* TMS-EEG signatures of glutamatergic neurotransmission in human cortex. *Sci. Rep.* **11**, (2021).
  21. Ziemann, U., Chen, R., Cohen, L. G. & Hallett, M. Dextromethorphan decreases the excitability of the human motor cortex. *Neurology* **51**, 1320–1324 (1998).
  22. Schwenkreis, P. *et al.* Influence of the N-methyl-D-aspartate antagonist memantine on human motor cortex excitability. *Neurosci. Lett.* **270**, 137–140 (1999).
  23. Cohen, L. G. *et al.* Effects of coil design on delivery of focal magnetic stimulation. Technical considerations. *Electroencephalogr. Clin. Neurophysiol.* **75**, 350–357 (1990).
  24. Rossini, P. M. *et al.* Non-invasive electrical and magnetic stimulation of the brain, spinal cord, roots and peripheral nerves: Basic principles and procedures for routine clinical and research application: An updated report from an I.F.C.N. Committee. *Clin. Neurophysiol.* **126**, 1071–1107 (2015).
  25. Oostenveld, R., Fries, P., Maris, E. & Schoffelen, J. M. FieldTrip: Open source software for advanced analysis of MEG, EEG, and invasive electrophysiological data. *Comput. Intell. Neurosci.* **2011**, (2011).
  26. Maris, E. & Oostenveld, R. Nonparametric statistical testing of EEG- and MEG-data. *J. Neurosci. Methods* **164**, 177–190 (2007).
  27. Ziemann, U., Lönnecker, S., Steinhoff, B. J. & Paulus, W. The effect of lorazepam on the motor cortical excitability in man. *Exp. Brain Res.* **109**, 127–135 (1996).
  28. Theodore, W. H. Transcranial Magnetic Stimulation in Epilepsy. *Epilepsy Curr.* **3**, 191–197 (2003).
  29. Tsuboyama, M., Lee Kaye, H. & Rotenberg, A. Biomarkers Obtained by Transcranial Magnetic Stimulation of the Motor Cortex in Epilepsy. *Frontiers in Integrative Neuroscience* vol. 13 (2019).
  30. Rossi, S. *et al.* Safety, ethical considerations, and application guidelines for the use of transcranial magnetic stimulation in clinical practice and research. *Clin. Neurophysiol.* **120**, 2008–2039 (2009).

## Supplementary information

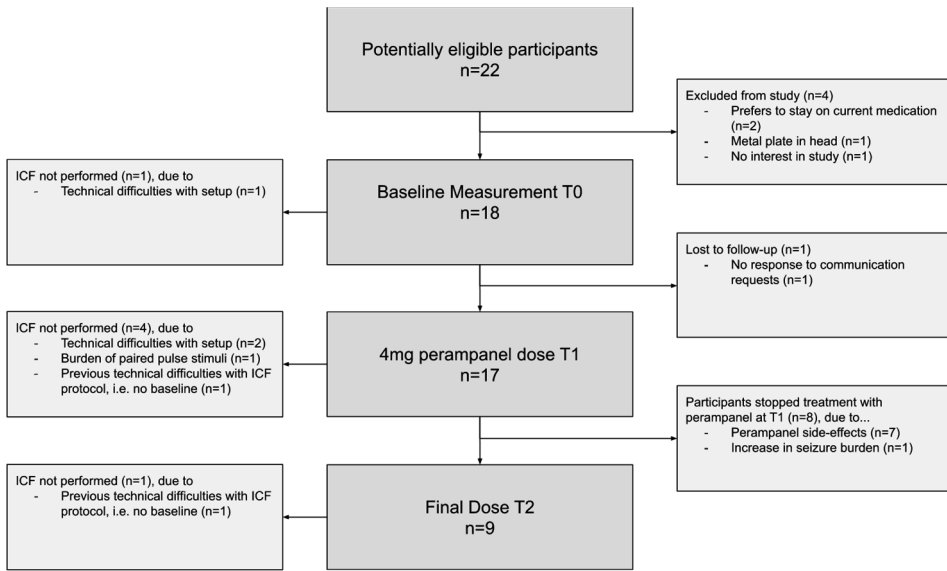


Fig. S1. Study flow-chart.

**Table S1. Cluster statistics for TMS-evoked EEG peaks for the clockwise versus counterclockwise current direction at baseline.**

Prot	P25		N45		P70		N100		P180		
	n	p	n	p	n	p	n	p	n	p	
SP	- / -	- / -	- / -	- / -	- / -	- / -	- / -	- / -	- / -	- / -	- / -
ICF	1 / 1	0.44 / 0.47	- / -	- / -	- / -	- / -	- / -	- / -	- / -	- / -	- / -

For each comparison we show the number of found positive and/or negative clusters (n of 1 / 2 means a single positive and two negative clusters were found) and corresponding p-value statistics for the cluster with highest summed T-values. Sham results are not shown because not a single cluster was found.

**Table S2. Cluster statistics for TMS-evoked EEG peaks for the measurement at 4mg perampanel (T1) in comparison to baseline (T0).**

Prot	Hemi	P25		N45		P70		N100		P180	
		n	p	n	p	n	p	n	p	n	p
SP	Right	- / -	- / -	- / -	- / -	- / -	- / -	- / 1	- / 0.213	1 / 3	0.329 / 0.304
	Left	- / -	- / -	- / -	- / -	- / -	- / -	- / -	- / -	2 / 4	0.205 / 0.533
ICF	Right	- / -	- / -	- / -	- / -	- / -	- / -	- / -	- / -	1 / 2	0.32 / 0.410
	Left	1 / -	0.089 / -	- / -	- / -	2 / -	0.064 / -	1 / 1	0.226 / 0.412	- / 2	- / 0.284

For each comparison we show the number of found positive and/or negative clusters (n of 1 / 2 means a single positive and two negative clusters were found) and corresponding p-value statistics for the cluster with highest summed T-values. Sham results are not shown because not a single cluster was found.

**Table S3. Cluster statistics for TMS-evoked EEG peaks for the responders non-responder comparison.**

Prot	Hemi	P25		N45		P70		N100		P180	
		n	p	n	p	n	p	n	p	n	p
SP	Right	1 / 2	0.112 / 0.119	- / 1	- / 0.130	1 / 1	0.118 / 0.368	1 / -	0.295 / -	2 / 4	0.511 / 0.630
	Left	1 / -	0.432 / -	- / -	- / -	1 / -	0.151 / -	- / 1	- / 0.491	2 / 6	0.304 / 0.324
ICF	Right	1 / -	0.226 / -	1 / -	0.089 / -	2 / -	0.146 / -	1 / 1	0.412 / 0.402	1 / 1	0.268 / 0.123
	Left	- / -	- / -	- / -	- / -	- / -	- / -	- / 1	- / 0.266	1 / 1	0.177 / 0.076

For each comparison we show the number of found positive and/or negative clusters (n of 1 / 2 means a single positive and two negative clusters were found) and corresponding p-value statistics for the cluster with highest summed T-values. Sham results are not shown because not a single cluster was found.

# Chapter 7

## Tracking cortical excitability dynamics with transcranial magnetic stimulation in focal epilepsy

Based on:

**Helling RM**, Shmuely S, Bauer PR, Tolner EA, Visser GH, Thijs RD. Tracking cortical excitability dynamics with transcranial magnetic stimulation in focal epilepsy. *Annals of Clinical and Translational Neurology*. 2022;9(4):540–51.

DOI: [10.1002/acn3.51535](https://doi.org/10.1002/acn3.51535)

## Abstract

The lack of reliable biomarkers constrain epilepsy management. We assessed the potential of repeated transcranial magnetic stimulation with electromyography (TMS-EMG) to track dynamical changes in cortical excitability on a within-subject basis.

We recruited people with refractory focal epilepsy who underwent video-EEG monitoring and drug tapering as part of the presurgical evaluation. We performed daily TMS-EMG measurements with additional postictal assessments 1-6 hours following seizures to assess resting motor threshold (rMT), and motor evoked potentials with single- and paired-pulse protocols. Antiseizure medication regimens were recorded for the day before each measurement and expressed in proportion to the dosage before tapering. Additional measurements were performed in healthy controls to evaluate day-to-day rMT variability.

We performed 77 (58 baseline, 19 postictal) measurements in sixteen people with focal epilepsy and 35 in seven healthy controls. Controls showed minimal day-to-day rMT variation. Withdrawal of antiseizure medications was associated with a lower rMT without affecting motor evoked potentials of single- and paired-pulse TMS-EMG paradigms. Postictal measurements following focal to bilateral tonic-clonic seizures demonstrated unaltered rMT and increased short-interval intracortical inhibition, while measurements following focal seizures with impaired awareness showed decreased rMT's and reduced short and long interval intracortical inhibition.

Serial within-subject rMT measurements yielded reproducible, stable results in healthy controls. Antiseizure medication tapering and seizures had distinct effects on TMS-EMG excitability indices in people with epilepsy. Drug tapering decreased resting motor threshold, indicating increased overall corticospinal excitability, whereas seizures affected intracortical inhibition with contrasting effects between seizure types.

## 7.1 Introduction

Epilepsy is characterized by neuronal hyperexcitability and hypersynchrony involving a disturbed balance between cortical excitatory and inhibitory inputs<sup>1-3</sup>. Seizures may be difficult to control and impact the quality of life<sup>4</sup>. Biomarkers that measure disease severity and help evaluate pharmacotherapy are needed.

Transcranial magnetic stimulation with electromyography (TMS-EMG) has been utilized for the non-invasive assessment of cortical excitability<sup>5</sup>. It yields various read-outs, including the resting motor threshold (rMT) reflecting membrane excitability of neurons within the corticospinal tract, and measures reflecting the activity of excitatory and inhibitory intracortical circuits<sup>6-8</sup>. The rMT is determined with single-pulse TMS (spTMS) while paired-pulse TMS (ppTMS) paradigms are used to determine short interval cortical inhibition (SICI), a marker for GABA<sub>A</sub>-receptor-mediated inhibition<sup>9</sup> and the long interval cortical inhibition (LICI) a measure of GABA<sub>B</sub>-receptor-mediated inhibition<sup>10</sup>. Clinical studies demonstrated that various antiseizure medications (ASM) influence rMT<sup>7,11-16</sup>. SICI and LICI have been used to investigate the GABAergic properties of pharmacological compounds<sup>17-19</sup> and investigate aberrant inhibition in epilepsy<sup>2,20,21</sup>. For instance, a TMS-EMG study in people with Dravet syndrome reported facilitation, rather than suppression, of the response with short-interval ppTMS, indicating reduced recruitment of inhibitory neurons by the conditioning pulse<sup>21</sup>. Combining spTMS and ppTMS may help assess the different aspects of cortical motor excitability.

The use of TMS to differentiate between people with epilepsy and healthy controls proved inadequate because of high inter-subject variability<sup>22,23</sup>. Serial within-subject TMS measurements, however, may potentially trace the cortical excitation:inhibition balance within individuals over time. Accordingly, a longitudinal study in twenty healthy controls demonstrated that the use of carbamazepine and lamotrigine exerts a dose-dependent effect on the rMT<sup>14</sup>. Likewise, the initiation of a ketogenic diet in eight people with epilepsy was associated with increased attenuation following short-latency ppTMS, indicating increased GABA-mediated inhibition<sup>24</sup>. Serial TMS may thus be attractive to monitor treatment response. A previous study demonstrated that seizures impacted ppTMS read-outs with more attenuated conditioned responses,

indicating increased recruitment of inhibitory neurons by the conditioning stimulus after seizures<sup>20</sup>. TMS could therefore help assess cortical excitability in the postictal state, especially for seizures followed by postictal generalized EEG suppression (PGES), an EEG marker related to excessive inhibition<sup>25–27</sup>. This approach could further our understanding of seizure termination mechanisms in focal impaired awareness (FIA) and focal to bilateral tonic-clonic (fbTC) seizures.

We aimed to explore the potential of TMS-EMG measures to assess the impact of ASM tapering and seizures on cortical excitability measures. We performed daily, and postictal assessments in people admitted for seizure recordings as part of a presurgical evaluation at the epilepsy monitoring unit (EMU)<sup>28</sup>. We hypothesized that ASM tapering would result in increased TMS-EMG measures of excitatory control, while the occurrence of a seizure would increase TMS-EMG measures reflecting inhibitory control.

## 7.2 Methods

### 7.2.1 Participants

Adults admitted to the EMU for presurgical evaluation were consecutively included between May 2017 and July 2019 if they had (1) a history of fbTC seizures and (2)  $\geq 1$  fbTC seizures in the year before admission. Healthy controls were recruited among employees of the institution. Cases and controls were excluded in case of contraindications to TMS other than epilepsy, including pregnancy, inability to follow the experimental protocol, and in case of any medication changes other than the ASM scheduled during the trial period. The study was approved by the ethics committee of Leiden University Medical Center. All participants provided written informed consent before entry.

### 7.2.2 Experimental design

Daily records were kept of seizures (based on video-EEG) and drug regimens. Clinical observation included continuous video-EEG and ECG, recordings. On the day of admission, a baseline TMS-EMG measurement was performed at approximately 1:30 P.M. Subsequent TMS-EMG measurements were performed daily around 8:00 A.M. Postictal measurements were performed 1–6

hours after the end of any fbTC or FIA seizure. Each individual underwent a maximum of three postictal measurements of their most common seizure type. In the case of two distinct seizure types, we limited the postictal measurements to a single assessment if we had already obtained three postictal measurements for another seizure type. Each control underwent five consecutive daily rMT assessments performed at approximately the same time.

### *7.2.3 Measurement setup and protocol*

Magnetic stimulation was performed using a Magpro X100 Magnetic stimulator (Magventure, Denmark) using a large 140-mm diameter circular coil (MMC-140) centred above the vertex (Cz-EEG electrodeposition)<sup>29</sup>. The circular coil allows for a diffuse stimulation of the cortex, minimizes the impact of small changes in coil position, and reduces the length of a measurement session, as motor hotspot determination is not needed<sup>29</sup>. The muscle response was recorded using disposable self-adhesive pre-gelled (16 x 20) mm rectangular Ag/AgCl surface electrodes. The EMG signal was acquired with a 16k Hz sampling frequency using the Nicolet Viking EMG system (Carefusion, San Diego, CA), connected to a computer running MATLAB (version 2018a, MathWorks, USA).

Participants were seated in a comfortable chair. Muscle activity was recorded bilaterally using a belly-tendon montage of the thenar muscles. They were asked to relax and were provided with foam ear-inserts. Participants were asked to keep their eyes open during the TMS-evaluation, including during postictal measurements. If the person closed their eyes they were reinstructed to keep their eyes open. Each measurement started by assessing left and right rMT, determined as the minimal mean stimulator output (MSO) required to evoke motor responses above 50  $\mu$ V in 5 out of 10 trials. Next, for each current direction, the following stimulations were given: spTMS (50 trials, 110% rMT, 5-second intertrial interval), short-latency ppTMS to assess SICI (30 trials, 80% rMT conditioning stimulus, 110% rMT test stimulus, 5 ms inter-stimulus interval, 5 seconds in between trials), and long latency ppTMS to assess LICI (30 trials, 110% rMT conditioning, 110% rMT test stimulus, 100 ms interstimulus interval, 5 seconds in between trials). Each measurement session lasted approximately 30 minutes.

### 7.2.4 Data processing and motor evoked potential analysis

EMG signals were extracted starting 20 ms before and ending 50 ms after TMS pulses. Trials with significant pre-activation ( $>20\mu\text{V}$  amplitude) of the abductor polices brevis muscle in the 20 ms window before stimulation were discarded from the analysis. For each trial, the peak-to-peak amplitude of the motor evoked potentials (MEPs) was determined in the window starting 15 ms after and ending 50 ms after the stimulus trigger. For ppTMS the conditioned peak-to-peak MEP amplitude was divided by the unconditioned peak-to-peak amplitude. Values below 1 thus indicate suppression of the response, whilst values above 1 indicate facilitation.

### 7.2.5 Medication effects

To investigate the effect of ASM dosage on TMS indices we normalized the summed dosage for each ASM type 24 hours prior to measurement and divided this value by the 24-hour summed medication taken at home. Next, to calculate a combined normalized ASM load, we summed the normalized values per ASM type and divided this by the total number of ASMs. Consider  $\mathcal{S}$  as the set containing all the ASM types an individual with epilepsy takes, then we can estimate the overall ASM load  $L$  at measurement  $m$  as follows:

$$L(m) = \frac{1}{N} \sum_{x \in \mathcal{S}} \frac{x_{24}(m)}{x_h}$$

Where for every type of ASM  $x \in \mathcal{S}$ ,  $x_{24}$  is the summed dosage of ASM  $x$  in the 24 hours prior to measurement  $m$ ,  $x_h$  is the summed daily at home dosage of ASM  $x$  and  $N$  is the total number of elements in set  $\mathcal{S}$ .

### 7.2.6 Statistical analysis

We used regression analysis to determine correlations between TMS-EMG indices and ASM dosage and investigate the impact of single seizures on the TMS-EMG indices. For rMT a linear mixed effects model was used with fixed effects for the intercept, ASM load, handedness, lateralization of the epileptic focus (according to the ictal EEG onset and/or clinical semiology or interictal epileptiform EEG activity), seizure occurrence before measurement and type (none, FIA, fbTC), and random intercept by-subject (to account for high between-subject variation in baseline rMT). For MEP, SICI and LICI we used a

linear mixed-effect model with ASM load and seizure type entered as fixed effects, and a random effect model for intercept by-subject. The best linear unbiased predictor estimates and corresponding 95% confidence interval (CI) for each predictor are presented.

We calculated the intraclass correlation coefficient (ICC) to estimate the agreement between repeated sessions within healthy controls. ICC varies between 0 and 1, where 1 represents perfect repeatability.

## **7.2 Results**

### *7.2.1 Population characteristics*

Characteristics of participants are summarised in Table 1 and an overview of the ASMs for each individual with epilepsy is given in Table 2. In total, 77 measurements (58 baseline and 19 postictal) were performed in sixteen people with epilepsy (mean age 32 years, range: 19-51 years; 9 male, 7 female), and 35 in seven controls (mean age 34 years, range 19-57 years; 3 male, 4 female). Two individuals with epilepsy terminated the study prematurely; one due to a self-reported high emotional burden of the TMS measurement in combination with the presurgical evaluation, the second due to fear of seizure induction by TMS. The remaining fourteen tolerated the TMS-EMG procedures well. One was rejected from analysis due to insufficient TMS-EMG data as evaluation was terminated after two days.

A total of 34 seizures (range 1-9) were recorded in nine people, including nine fbTC seizures in four people. In four, no seizures occurred. Postictal generalized EEG suppression was observed in the EEG for four out nine fbTC seizures (mean postictal generalized EEG suppression duration 40 seconds, range: 14-59 seconds). The remaining 25 seizures in seven people were FIA seizures.

Post-ictal TMS-EMG measurements were performed for six out of nine fbTC seizures and 13 out of 25 FIA seizures. All participants were awake, able and willing to undergo the postictal evaluations and had their eyes open during the measurement. Postictal measurements were not performed following the remaining 15 seizures due to either the occurrence of seizure clusters (n=11),

Table 1. Population demographics

Case	Sex	Age	Epi dur	Handedness	Epilepsy Lateralisation			MRI findings	Seizures		
					Interictal EEG	Ictal onset EEG	Semiology		FIA	fbTC	M
301	M	37	20	Left	Left	Left	Left	MTS left.	8	1	2
302	M	51	45	Right	Left	Left	Left	MTS left.	4	-	1
303	F	19	16	Left	-	-	Left	-	-	-	-
304	F	45	13	Right	Bilat.	-	Right	bilat. white-matter abnormalities.	-	-	-
305	M	29	6	Left	-	-	-	MTS left.	-	-	-
306	M	20	13	Right	Bilat. (R>L)	Right	Right	-	-	2	1
308	M	34	13	Right	-	Left	-	Left sided DVA with cavernoma temporal lobe.	3	-	3
309	F	30	18	Right	-	-	Right	-	-	-	-
310	M	41	27	Right	Left	Left	-	MAP abnormality left.	3	-	3
311	M	23	8	Right	Right	Right	Right	-	1	3	3
312	M	24	5	Right	Bilat. (R>L)	Right	Right	-	-	3	2
313	F	34	10	Right	Left	-	-	MTS left.	1	-	1
316	M	38	11	Right	Bilat. (L>R)	Left	Left	MTS left.	5	-	2

*Subj: Subject, F: female, M: male, Epi dur: years living with epilepsy, Bilat: bilateral, R: right, L: left, MTS: mesiotemporal sclerosis, DVA: developmental venous anomaly, MAP: morphometric analysis program*

presence of at least three previous postictal recordings following the same seizure type (n=3), or general fatigue/exhaustion (n=1). Examples of serial TMS-EMG measurements in a case with fbTC seizures and a case with FIA seizures are shown in Fig. 1 and Fig. 2, respectively.

**Table 2.** Antiseizure medication per individual with epilepsy

Subj	Medication type (mg)								Total number of ASM types per subject
	CBZ	CLB	LCM	LTG	LEV	OCB	TPM	VPA	
301	1600				3000				2
302	1600	10						2250	3
303	1200								1
304					1500	900			2
305			150						1
306			350			1500			2
308			200					1250	2
309		20		450					2
310			300		1000		150	2000	4
311		15			2000	1299			3
312	1000				2500			2250	3
313				300					1
316	1400	10							2
<b>Total number of subjects on ASM</b>	5	4	4	2	5	3	1	4	

ASM: antiseizure medication, N: number of ASMs, CBZ: carbamazepine, LEV: levetiracetam, VPA: valproic acid, CLB: clobazepam, OCB: oxcarbamazepine, LCM: lacosamide, LTG: lamotrigine, TPM: topiramate, FLA: focal impaired awareness, fbTC: focal to tonic-clonic, Meas: measurement.

### 7.3.2 TMS-EMG parameter changes

A schematic overview of the results is shown in Table 3. The difference in the spTMS and ppTMS-EMG parameters in the postictal evaluations relative to the previous baseline measurement are shown per seizure type in Fig. 3.

### 7.3.3 Resting motor threshold changes

Intersession reproducibility of the rMT across the different testing days in the healthy controls was high (ICC: 0.996). The changes in rMT as a function of normalized ASM load, including the model's significant curve fits and their corresponding confidence intervals, are shown for the individual subjects in Fig. 4. Decreasing ASM load in people with epilepsy was associated with lower rMT

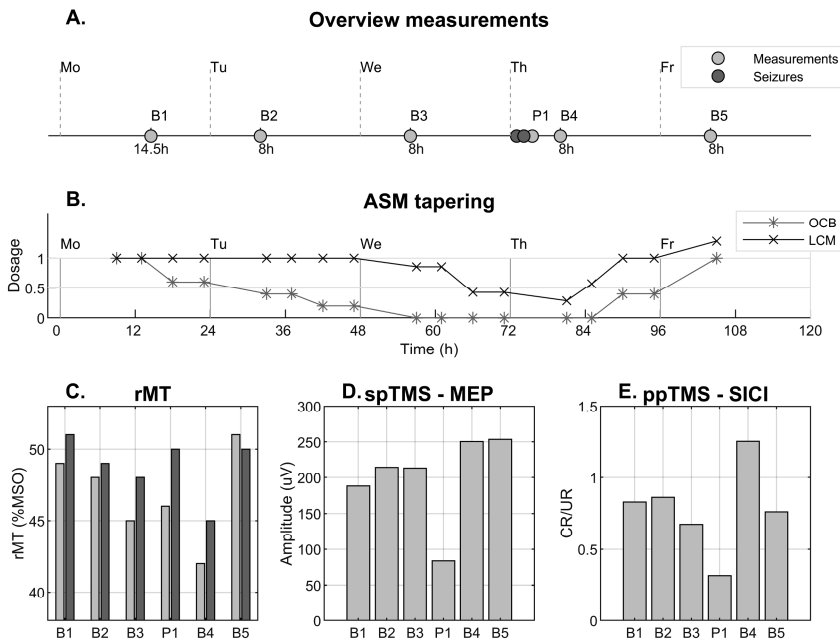


**Fig. 1.** Case 306 with multiple focal to bilateral tonic clonic seizures with right hemispheric onset. Panel (a) provides an overview of the timing of the TMS-EMG measurements (open blue circles indicated as B1-B5 for baseline evaluations and P1 for the postictal evaluation) and detected focal to bilateral tonic clonic (fbTC) seizures (red circles). Panel (b) displays the ASM regimen changes during tapering, as expressed by the normalised dosage (i.e. the summed dosage over the 24 hours prior to each measurement timepoint, divided by the standard at-home dosage summed over 24 hours); changes of individual ASMs are depicted with separate lines. Panels (c-e) show the cortical excitability indices for all measurements that showed significant ASM- and seizure-related changes in the postictal phase. The individual left-hand (light grey) and right-hand (dark grey) rMT values are shown in panel (c). Note that the rMT shows a gradual reduction with a reduction in medication dosage. The postictal P1 measurements demonstrated an increased rMT when compared to the surrounding baseline measurements. MEP amplitude for single-pulse TMS, measured at 110% rMT (d) was significantly reduced for the postictal measurement when compared to surrounding baseline measurements. The measure of short interval ppTMS (SICI; CR/UR) showed a diminished postictal ratio (e), suggesting an increase in GABAA-mediated inhibition in the postictal phase. Measures of long interval ppTMS (LICI) were not significant for fbTC seizures and are not shown. *ASM: antiseizure medication, OCB: oxcarbazepine, LCM: lacosamide, rMT: resting motor threshold, MSO: mean stimulator output, MEP: motor evoked potential, spTMS: single-pulse TMS, ppTMS: paired pulse TMS, SICI: short interval cortical inhibition, CR: conditioned response, UR: unconditioned response*

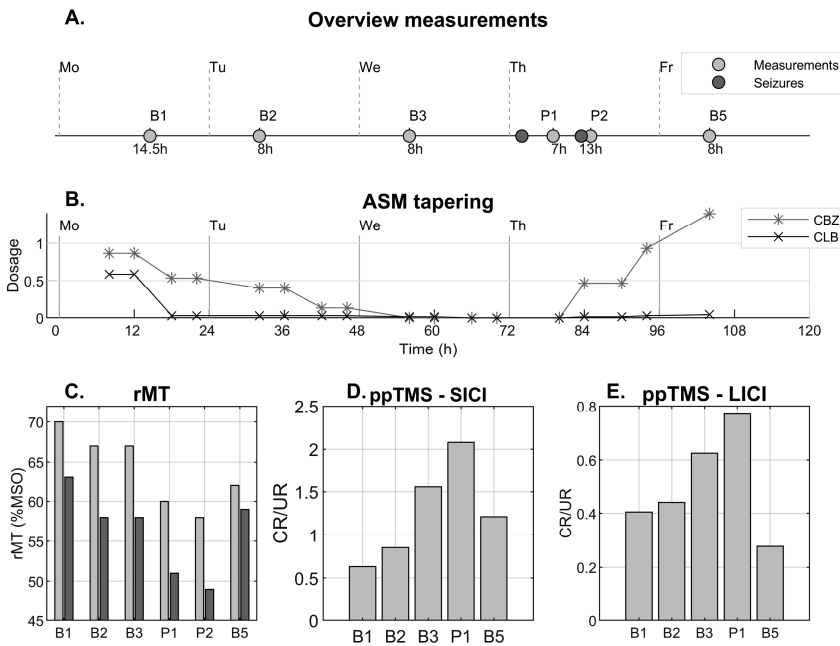


**Fig. 2.** Case 316 with multiple focal impaired awareness seizures with left hemispheric onset. Panel (a) provides an overview of the serial TMS-EMG measurements (open blue circles indicated as B1-B5 for baseline evaluations and P1-P2 for the postictal evaluations) and detected focal impaired awareness (FIA) seizures (red circles). Note that P1 coincided with the planned baseline measurement B4 for this case and thus replaced B4. Panel (b) displays the ASM regimen changes during tapering, as expressed by the normalised dosage (i.e. the summed dosage over the 24 hours prior to each measurement timepoint, divided by the standard at-home dosage summed over 24 hours); changes of individual ASMs are depicted with separate lines. Panels (c-e) show the cortical excitability indices that showed significant ASM- and seizure-related changes in the postictal phase. The individual left-hand (light grey) and right-hand (dark grey) rMT values are shown in panel (c). Note that the rMT was further reduced in the postictal evaluations relative to the baseline measurements, while SICI and LICI (panel d-e) both showed increased conditioned to unconditioned response ratios, suggesting reduced GABA<sub>A</sub>-mediated inhibition in the postictal phase. Note that after the second seizure, no ppTMS paradigms were performed. The spTMS MEP responses at 110% rMT were not significant for FIA seizures and are not shown. *ASM*: antiseizure medication, *CBZ*: carbamazepine, *CLB*: clobazam, *rMT*: resting motor threshold, *MSO*: mean stimulator output, *ppTMS*: paired pulse TMS, *SICI*: short interval cortical inhibition, *LICI*: long interval cortical inhibition, *CR*: conditioned response, *UR*: unconditioned response.

values (5.3% MSO, 95%CI: 3.1 to 7.4% MSO). The occurrence of fbTC seizures did not have a significant effect on rMT (estimate: -0.2% MSO, 95%CI: -2.4 to 2.0% MSO). Conversely, following FIA seizures a decrease in rMT was found (estimate: -2.2% MSO, 95%CI: -3.7 to -0.6% MSO). Both handedness and lateralization of the seizure onset zone had an effect on the rMT with lowervalues for the dominant hemisphere (estimate: 1.2% MSO, 95%CI: 0.2 to 2.3% MSO) and the hemisphere ipsilateral to the seizure onset zone (estimate: 1.6% MSO, 95%CI: 0.6 to 2.7% MSO).

#### 7.3.4 *Single and paired pulse motor evoked potential changes*

Single pulse MEP amplitudes did not correlate with the normalized ASM load  $L$  (estimate: -3.4 uV, 95%CI: -74.1 to 67.1 uV). Post-ictal measurements showed a reduction in MEP amplitude measured at 110% rMT after fbTC seizures (estimate: -106.8 uV, 95%CI: -181.6 to -32.1 uV), but not following FIA seizures (estimate: -9.3 uV, 95%CI: -64.5 to 45.8 uV).

The change in ppTMS SICI and LICI as a function of normalized ASM load, including the model's significant curve fits and corresponding confidence intervals, are shown in Supplementary Fig.1 and Supplementary Fig.2 respectively.

Short interval ppTMS evoked responses did not correlate with the normalized ASM load  $L$  (estimate: -0.3, 95%CI: -0.7 to 0.1). Post-ictal short-interval measurements performed after fbTC seizures showed a decrease in the SICI CR/UR-ratio (estimate: -0.5, 95%CI: -1.0 to -0.1), whereas a significant increase in the SICI measure was observed following FIA seizures (estimate: 0.8, 95%CI: 0.4 to 1.1).

Long interval paired-pulse evoked responses did not correlate with the normalized ASM load  $L$  (estimate: 0.2, 95%CI: -0.3 to 0.6), or fbTC seizures (estimate: -0.2, 95%CI: -0.9 to 0.6). Similar as for the SICI measure, after FIA seizures the LICI CR/UR-ratio was increased (estimate: 0.8, 95%CI: 0.3 to 1.4).

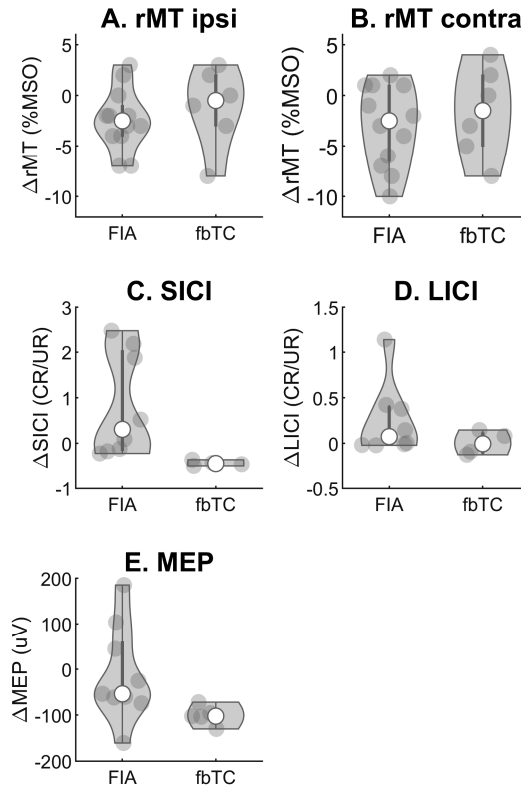


**Fig.3.** Violin plots of the postictal change in TMS-EMG parameters per seizure type. Each panel depicts the change ( $\Delta$ ) in the postictal TMS-EMG parameters compared to the baseline evaluation. The grey dots represent the individual measurements, the white circle represents the median value, the dark grey bars represent the interquartile range, and the grey area represents the smoothed probability density. Panels (a) and (b) show the postictal change in resting motor threshold for the hemisphere ipsilateral and contralateral to the seizure onset zone; panels (c) and (d) display the postictal paired pulse TMS-EMG changes related to short and long interval cortical inhibition; panel (e) shows the postictal change in the MEP measured at 110% resting motor threshold. *FIA*: focal seizures with impaired awareness, *fbTC*: focal to bilateral tonic-clonic seizures, *rMT*: resting motor threshold, *MSO*: mean stimulator output, *SICI*: short interval cortical inhibition, *LICI*: long interval cortical inhibition, *CR*: conditioned response, *UR*: unconditioned response.

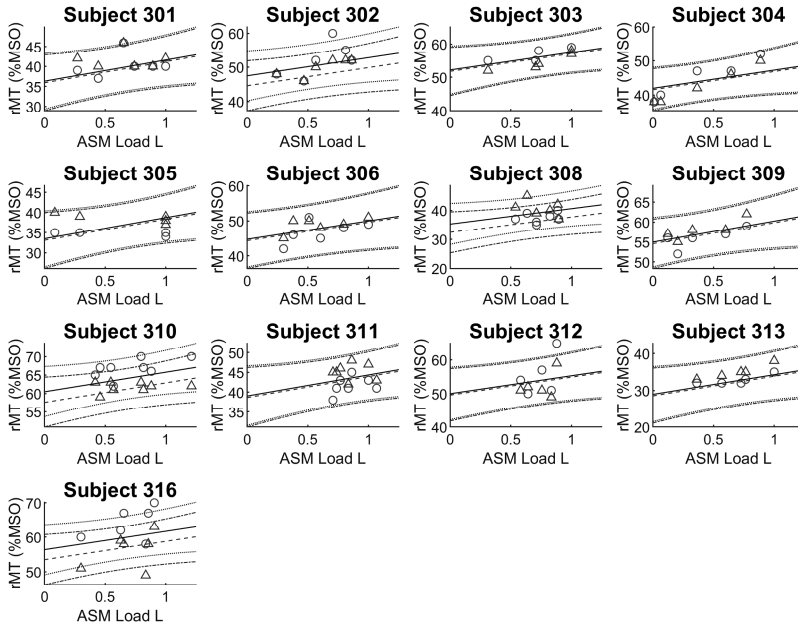


**Fig. 4.** Resting motor threshold as function of normalized antiseizure medication dose for all individuals with epilepsy. For each case the seizures types that occurred during their admittance to the epilepsy monitoring unit are shown within the parenthesis. The circles depict the resting motor threshold measurements ipsilateral to the hemisphere of the seizure onset zone, while the triangles display the contralateral hemisphere measurements. The solid lines show the significant curve fits for the ipsilateral measurements with the corresponding confidence interval shown by the dotted line. Similarly, the dashed lines shows the significant curve fit for the contralateral measurements with the corresponding confidence interval shown by the dash-dotted lines. *ASM*: antiseizure medication, *rMT*: resting motor threshold, *MSO*: mean stimulator output.

## 7.4 Discussion

We demonstrated that ASM tapering and seizures impact motor cortex excitability with distinct effects on TMS-EMG based excitability measures. Drug tapering resulted in decreased rMT, suggestive of increased corticospinal excitability. Seizures affected intracortical inhibition with contrasting effects between fbTC and FIA seizure types. Postictal TMS evaluations following fbTC seizures were associated with increased cortical inhibition (presumptively mediated by altered GABAA-mediated mechanisms). Conversely, FIA seizures

were associated with reduced cortical inhibition and elevated corticospinal excitability.

#### *7.4.1 Limitations*

The EMU offered an ideal environment to study peri-ictal and ASM dose-response effects on cortical excitability, but the setting also limited our analysis in several ways. The heterogeneity of drug regimens and tapering schemes did not allow us to assess the effects of each drug individually. Instead, we used normalized medication levels to estimate the overall ASM load. We could not account for the pharmacokinetic contrasts between ASMs, but we found a clear correlation between various ASM regimes drug load. Previous TMS-EEG studies suggested specific fingerprints per ASM type<sup>7,8</sup>. Further studies are needed to explore the individual ASM effects on the rMT.

The sample of postictal measurements after fbTC seizures (6 measurements in 3 people) was low, increasing the probability of a type-II error. Nevertheless, we found effects of ASM tapering and seizure occurrence and type with small confidence intervals suggesting that these effects were robust.

We also assessed TMS-EEG, but we did not include these measurements in the final analysis as the EEG contained too many artifacts for low-density EEG recordings with the limited number of trials used in this study. TMS-EEG measures could provide a valuable addition<sup>30</sup>, but would in retrospect, require more extensive EEG coverage and extended measurement sessions with more trials per protocol to allow for better post-processing of the recordings.

The spTMS and ppTMS protocols were performed at the lowest rMT of both hemispheres to compare clockwise versus counter-clockwise stimulation directly. This resulted in subthreshold stimulation intensities for the hemisphere with higher rMT. TMS-EMG measures thus were only compared for the hemisphere with the lowest within-subject rMT. We did not repeat TMS protocols at different stimulation intensities to limit the study burden.

#### *7.4.2 Changes in antiseizure medications*

ASM tapering strongly correlated with lower rMT thresholds, suggesting increased corticospinal excitability. Previous pharmacological studies showed dose-response effects with an increased rMT (i.e. indicating reduced excitability)

following a single ASM dose<sup>7,11-16</sup>. One study performed multiple TMS measurements over eight weeks to evaluate the effect of carbamazepine and lamotrigine on rMT in healthy volunteers<sup>14</sup>. While the increase in ASM blood levels following ASM initiation correlated with higher rMT values, a weaker correlation was found between ASM blood levels and rMT in the TMS trials one to three days following acute withdrawal. This indicates that recovery of the rMT to baseline values is slower than the recovery of the ASM blood levels. Following ASM withdrawal, we found a reduction in rMT thresholds, indicating enhanced corticospinal excitability and an increase in rMT when medication returned back to at-home levels. While our experiment was not designed to compare the up-titration and tapering period directly, no significant differences were observed in posthoc analysis. We speculate that pharmacokinetic and pharmacodynamic factors may differ between people on chronic drug regimens and those starting with medication. ASM tapering did not impact the read-outs of the ppTMS paradigms. This is in agreement with previous single-dose studies of several ASMs, where no direct effect on the ppTMS read-outs was found<sup>2,7,8,31</sup>.

#### 7.4.3 Postictal measurements

Postictal measurements following fbTC seizures showed marked SICI enhancement with increased response attenuation. SICI increase after fbTC seizures is congruent with a previous study where a similar enhancement of SICI was found up to 24 hours after seizure onset<sup>28</sup>. Postictal MEPs measured at 110% rMT were significantly reduced in amplitude compared to baseline measurements, suggesting a reduction in the input-output recruitment slope of the motor system after fbTC seizures. A single-dose study of lorazepam, a GABA<sub>A</sub>-receptor agonist, demonstrated depressed input-output curves following administration and decreased MEP amplitudes, especially in the high-intensity part of the input-output curve<sup>32</sup>. Therefore, we speculate that our finding of SICI enhancement and MEP amplitude decrease following fbTC seizures reflects increased GABA<sub>A</sub>-mediated inhibition. We found no significant effect on rMT or LICI, which has been demonstrated to involve mainly GABA<sub>B</sub> rather than GABA<sub>A</sub>-mediated inhibition<sup>9</sup>. This suggests that enhanced postictal inhibition after fbTC seizures is primarily mediated by GABA<sub>A</sub>-receptors.

Post-ictal TMS-EMG measures following FIA seizures, in contrast, showed signs of increased excitability due to reduced inhibition. rMT following FIA

seizures was lower, and SICI and LICI read-outs showed signs of reduced inhibition causing increased excitability, reflected in facilitation of the MEP conditioned response relative to the unconditioned response. We speculate that increased excitability after FIA seizures may reflect an ictal focus to be more excitable (less inhibited) following a first seizure, thus lowering the threshold for a seizure cluster. Seizure clusters are common in refractory epilepsy and imply impaired seizure termination or increased cortical excitability<sup>33</sup>. Both are potential consequences of secondary alterations from an initial seizure that promotes a second seizure or excess seizure-promoting factors<sup>34</sup>. Our finding of increased excitability following FIA seizures contrasts with a previous study, where postictal SICI and LICI both were enhanced, i.e. more attenuated conditioned responses, for almost all interstimulus intervals in focal and generalized epilepsy<sup>28</sup>. They all had newly-diagnosed epilepsy, thus contrasting with our population of refractory focal epilepsy. We speculate that in people with refractory epilepsy, there may be aberrant inhibition in the postictal state, resulting in an increased tendency for seizure clusters and secondary fbTC seizures. However, another important difference is the contrasts in the timing of the TMS measurements. We performed measurements on average 2.25 hours (range: 1-7 hours) after seizures, while the referred study performed measurements on average 17 hours after seizure occurrence. We postulate that measurements performed with significant time lag between the seizure and the TMS evaluation will miss the pro-ictal state changes observed in our study.

#### *7.4.4 Interhemispheric differences*

Handedness is the most outward example of motor laterality. When accounting for various other factors, we found that handedness was correlated with slightly lower thresholds in the hemisphere corresponding to the dominant hand. Similarly, lateralization of the seizure onset zone was associated with lower rMT in the ipsilateral hemisphere relative to the contralateral hemisphere. This may reflect increased excitability of the hemisphere ipsilateral to the seizure focus (due to reduced inhibition or increased excitation) or decreased excitability of the contralateral hemisphere. Considering that epilepsy is generally regarded as a condition with an aberrant excitation:inhibition balance, we find the prior explanation more likely. Previous rMT studies on the lateralization of handedness<sup>35-38</sup> and seizure onset zone<sup>20,39,40</sup> yielded mixed results. Our study differs from the above report in three significant aspects: coil type, serial

measurements and the EMU setting. We employed round-coil TMS in contrast to figure-of-eight coils commonly used in TMS-EMG studies. We speculate that more broad activation of the cortex by round coil TMS results in more widespread activation patterns of inhibitory and excitatory networks resulting in different downstream effects than expected with a figure-of-eight coil with effects on rTMS and MEP features. We used serial measurements within individuals to demonstrate the group-level fixed effects. Single TMS measurements not taking into account physiological fluctuations in cortical excitability may lack sufficient power to establish the observed effect. Lastly, we performed measurements in a setting where the balance between excitation and inhibition fluctuated due to ASM load changes and a relative high seizure burden. Our findings suggest that these fluctuations affect the interhemispheric rMT differences over time. The interhemispheric rMT differences and the relation with lateralization of handedness and seizure onset zone is, however, anything but straightforward and more research is needed to further explore the observed effects.

#### 7.4.5 *Safety of TMS in people with epilepsy*

Seizure induction is the most severe complication of TMS<sup>41</sup>. In our study, where participants were inpatients for seizure recordings, induced seizures were not considered adverse events provided that the provoked seizure in an individual had similar semiology to unprovoked seizures. Two seizures occurred during a TMS evaluation; in one case, seizure onset occurred during a single-pulse TMS session. In the second, it was within one minute after rMT determination. Seizure semiology for TMS-related seizures was similar to their unprovoked seizures. The provoked seizures occurred within a seizure cluster of multiple FIA seizures for both cases. It, therefore, remains questionable whether these two clusters were started by the TMS session or were coincidental.

## 7.5 **Concluding statements and future perspectives**

We demonstrated that serial TMS-EMG evaluations, using various spTMS and ppTMS EMG parameters, can be used to monitor changes in motor cortex excitability in the context of epilepsy. Longitudinal measurements can be applied to unveil effects related to changes in ASM regiment changes and effects related

to the occurrence of seizures that can be distinct per seizure type. The observation of increased excitability after FIA seizures, that could be due to a period of reduced inhibition, may play a role in the occurrence of seizure clusters, thus reflecting a pro-ictal state. Conversely, the finding of increased inhibition after fbTC seizures suggests a shift of the excitation:inhibition-axis towards a condition of increased inhibition or reduced excitation. We postulate that the PGES seen after some fbTCs may be a phenomenon related to such a shift. However, more research is needed to better understand the mechanism behind seizure clusters and PGES. Studies using within-subject designs may help elucidate the role of aberrant inhibition or excitation levels in the peri-ictal state and relate these to clinical outcome. Another yet underexplored prospect of serial TMS evaluations is to predict the individual treatment response.

## References

1. Avoli, M. & de Curtis, M. GABAergic synchronization in the limbic system and its role in the generation of epileptiform activity. *Progress in Neurobiology* vol. 95 104–132 (2011).
2. Bauer, P. R. *et al.* Long-interval intracortical inhibition as biomarker for epilepsy: A transcranial magnetic stimulation study. *Brain* **141**, 409–421 (2018).
3. Jefferys, J. G. R. Advances in understanding basic mechanisms of epilepsy and seizures. *Seizure* **19**, 638–646 (2010).
4. Thijs, R. D., Surges, R., O'Brien, T. J. & Sander, J. W. Epilepsy in adults. *The Lancet* vol. 393 689–701 (2019).
5. Barker, A. T., Jalinous, R. & Freeston, I. L. Non-Invasive Magnetic Stimulation of Human Motor Cortex. *The Lancet* vol. 325 1106–1107 (1985).
6. Theodore, W. H. Transcranial Magnetic Stimulation in Epilepsy. *Epilepsy Curr.* **3**, 191–197 (2003).
7. Ziemann, U. *et al.* TMS and drugs revisited 2014. *Clin. Neurophysiol.* **126**, 1847–1868 (2015).
8. Tsuboyama, M., Lee Kaye, H. & Rotenberg, A. Biomarkers Obtained by Transcranial Magnetic Stimulation of the Motor Cortex in Epilepsy. *Frontiers in Integrative Neuroscience* vol. 13 (2019).
9. Sanger, T. D., Garg, R. R. & Chen, R. Interactions between two different inhibitory systems in the human motor cortex. *J. Physiol.* **530**, 307–317 (2001).
10. Fitzgerald, P. B., Maller, J. J., Hoy, K., Farzan, F. & Daskalakis, Z. J. GABA and cortical inhibition in motor and non-motor regions using combined TMS-EEG: A time analysis. *Clin. Neurophysiol.* **120**, 1706–1710 (2009).
11. Chen, R., Samii, A., Caños, M., Wassermann, E. M. & Hallett, M. Effects of phenytoin on cortical excitability in humans. *Neurology* **49**, 881–883 (1997).
12. Manganotti, P., Bongiovanni, L. G., Zanette, G., Turazzini, M. & Fiaschi, A. Cortical excitability in patients after loading doses of lamotrigine: A study with magnetic brain stimulation. *Epilepsia* **40**, 316–321 (1999).
13. Kimiskidis, V. K. *et al.* Lorazepam-induced effects on silent period and corticomotor excitability. *Exp. Brain Res.* **173**, 603–611 (2006).
14. Lee, H. W., Seo, H. J., Cohen, L. G., Bagic, A. & Theodore, W. H. Cortical excitability during prolonged antiepileptic drug treatment and drug withdrawal. in *Clinical Neurophysiology* vol. 116 1105–1112 (2005).
15. Li, X. *et al.* Lamotrigine and valproic acid have different effects on motorcortical

- neuronal excitability. *J. Neural Transm.* **116**, 423–429 (2009).
16. Lang, N., Rothkegel, H., Peckolt, H. & Deuschl, G. Effects of lacosamide and carbamazepine on human motor cortex excitability: A double-blind, placebo-controlled transcranial magnetic stimulation study. *Seizure* **22**, 726–730 (2013).
  17. Gersner, R., Ekstein, D., Dhamne, S. C., Schachter, S. C. & Rotenberg, A. Huperzine A prophylaxis against pentylenetetrazole-induced seizures in rats is associated with increased cortical inhibition. *Epilepsy Res.* **117**, 97–103 (2015).
  18. Ossemann, M., de Fays, K., Bihin, B. & Vandermeeren, Y. Effect of a single dose of retigabine in cortical excitability parameters: A cross-over, double-blind placebo-controlled TMS study. *Epilepsy Res.* **126**, 78–82 (2016).
  19. Premoli, I. *et al.* TMS-EEG and TMS-EMG to assess the pharmacodynamic profile of a novel potassium channel opener (XEN1101) on human cortical excitability. *Brain Stimul.* **12**, 459 (2019).
  20. Badawy, R. A. B., Curatolo, J. M., Newton, M., Berkovic, S. F. & Macdonell, R. A. L. Changes in cortical excitability differentiate generalized and focal epilepsy. *Ann. Neurol.* **61**, 324–331 (2007).
  21. Stern, W. M., Sander, J. W., Rothwell, J. C. & Sisodiya, S. M. Impaired intracortical inhibition demonstrated in vivo in people with Dravet syndrome. *Neurology* **88**, 1659–1665 (2017).
  22. Du, X., Summerfelt, A., Chiappelli, J., Holcomb, H. H. & Hong, L. E. Individualized brain inhibition and excitation profile in response to paired-pulse TMS. *J. Mot. Behav.* **46**, 39–48 (2014).
  23. Wassermann, E. M. Variation in the response to transcranial magnetic brain stimulation in the general population. *Clin. Neurophysiol.* **113**, 1165–1171 (2002).
  24. Cantello, R. *et al.* Ketogenic diet: Electrophysiological effects on the normal human cortex. *Epilepsia* **48**, 1756–1763 (2007).
  25. Boido, D., Gnatkovsky, V., Uva, L., Francione, S. & De Curtis, M. Simultaneous enhancement of excitation and postburst inhibition at the end of focal seizures. *Ann. Neurol.* **76**, 826–836 (2014).
  26. Žiburkus, J., Cressman, J. R. & Schiff, S. J. Seizures as imbalanced up states: Excitatory and inhibitory conductances during seizure-like events. *J. Neurophysiol.* **109**, 1296–1306 (2013).
  27. Pottkämper, J. C. M., Hofmeijer, J., van Waarde, J. A. & van Putten, M. J. A. M. The postictal state — What do we know? *Epilepsia* vol. 61 1045–1061 (2020).
  28. Badawy, R., MacDonell, R., Jackson, G. & Berkovic, S. The peri-ictal state: Cortical excitability changes within 24 h of a seizure. *Brain* **132**, 1013–1021 (2009).
  29. Rossini, P. M. *et al.* Non-invasive electrical and magnetic stimulation of the brain,

- spinal cord, roots and peripheral nerves: Basic principles and procedures for routine clinical and research application: An updated report from an I.F.C.N. Committee. *Clin. Neurophysiol.* **126**, 1071–1107 (2015).
30. Bauer, P. R. *et al.* Phase clustering in transcranial magnetic stimulation-evoked EEG responses in genetic generalized epilepsy and migraine. *Epilepsy Behav.* **93**, 102–112 (2019).
  31. de Goede, A. A. & van Putten, M. J. A. M. Repeatability of long intracortical inhibition in healthy subjects. *Clin. Neurophysiol. Pract.* **2**, 26–34 (2016).
  32. Di Lazzaro, V. *et al.* GABAA receptor subtype specific enhancement of inhibition in human motor cortex. *J. Physiol.* **575**, 721–726 (2006).
  33. Jafarpour, S., Hirsch, L. J., Gaínza-Lein, M., Kellinghaus, C. & Detyniecki, K. Seizure cluster: Definition, prevalence, consequences, and management. *Seizure* vol. 68 9–15 (2019).
  34. Taubøll, E., Lundervold, A. & Gjerstad, L. Temporal distribution of seizures in epilepsy. *Epilepsy Res.* **8**, 153–165 (1991).
  35. Livingston, S. C., Goodkin, H. P. & Ingersoll, C. D. The influence of gender, hand dominance, and upper extremity length on motor evoked potentials. *J. Clin. Monit. Comput.* **24**, 427–436 (2010).
  36. Davidson, T. & Tremblay, F. Hemispheric Differences in Corticospinal Excitability and in Transcallosal Inhibition in Relation to Degree of Handedness. *PLoS One* **8**, (2013).
  37. Bäumer, T. *et al.* Laterality of interhemispheric inhibition depends on handedness. *Exp. Brain Res.* **180**, 195–203 (2007).
  38. Daligadu, J., Murphy, B., Brown, J., Rae, B. & Yilder, P. TMS stimulus-response asymmetry in left- and right-handed individuals. *Exp. Brain Res.* **224**, 411–416 (2013).
  39. Hamer, H. M. *et al.* Motor cortex excitability in focal epilepsies not including the primary motor area - A TMS study. *Brain* **128**, 811–818 (2005).
  40. Varrasi, C. *et al.* Cortical excitability in drug-naive patients with partial epilepsy: A cross-sectional study. *Neurology* **63**, 2051–2055 (2004).
  41. Bae, E. H. *et al.* Safety and tolerability of repetitive transcranial magnetic stimulation in patients with epilepsy: a review of the literature. *Epilepsy and Behavior* vol. 10 521–528 (2007).

## Supplementary Information

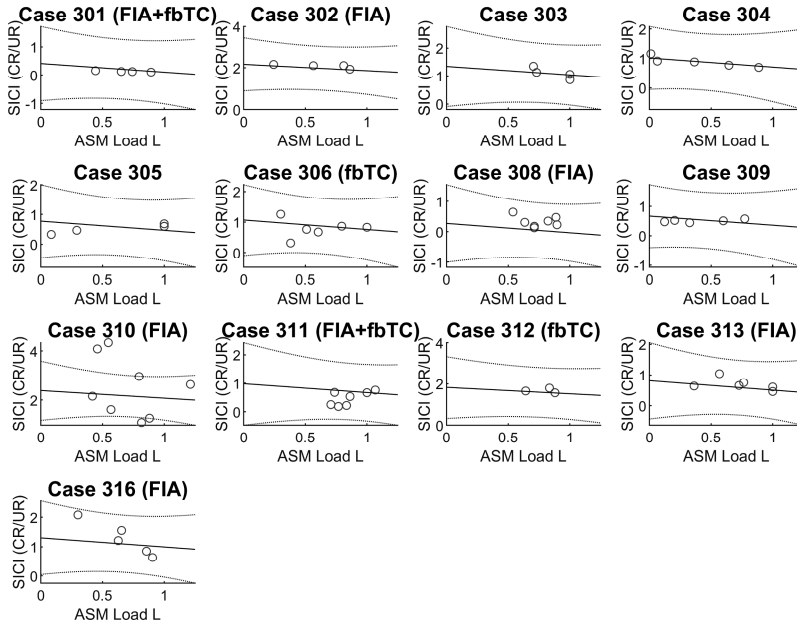


**Fig. S1.** Short interval cortical inhibition as function of normalized antiseizure medication dose for all epilepsy subjects. For each case the seizure types that occurred during their admittance to the epilepsy monitoring unit are shown within the parenthesis. The circles depict the measurements. The solid line shows the curve fit with the corresponding confidence interval shown by the dotted line. *ASM*: anti-seizure medication, *SICI*: short interval cortical inhibition, *M<sub>SO</sub>*: mean stimulator output, *CR*: conditioned response, *UR*: unconditioned response.

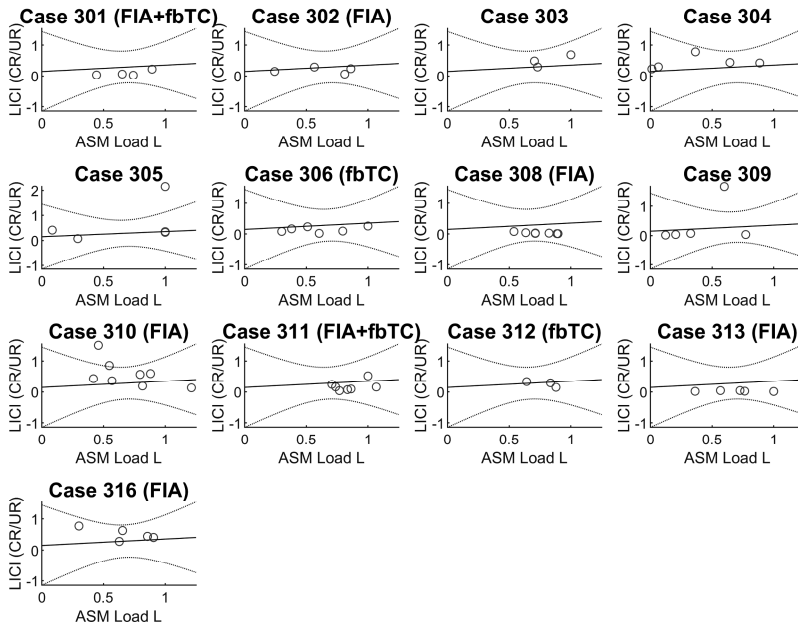


**Fig. S2.** Long interval cortical inhibition as function of normalized antiseizure medication dose for all epilepsy subjects. For each case the seizure types that occurred during their admittance to the epilepsy monitoring unit are shown within the parenthesis. The circles depict the measurements. The solid line shows the curve fit with the corresponding confidence interval shown by the dotted line. *ASM*: anti-seizure medication, *LICI*: long interval cortical inhibition, *MSO*: mean stimulator output, *CR*: conditioned response, *UR*: unconditioned response.

# Chapter 8

General discussion

## **8.1 General discussion**

The repeated and yet unpredictable occurrence of seizures has a major impact on quality of life in people with epilepsy. The transient nature of seizures makes epilepsy a dynamic disease where periods of normal brain function are intermittently interrupted by seizures that impair partial- or whole- brain function. In this thesis, we have looked for new biomarkers for diagnosis and to evaluate or follow the treatment response of people with epilepsy. To do this, we conducted various exploratory studies and used computational models to identify biomarkers that are associated with cortical excitability and epileptogenicity, or the likelihood of seizures, based on resting state or perturbation-based EEG recordings. We then took a more proactive approach by giving stimuli to disrupt brain dynamics in people with epilepsy and migraines, using transcranial magnetic stimulation (TMS) and light flash stimuli while recording responses with EEG and EMG.

## **8.2 Biomarkers in epilepsy care**

Multimodal TMS can be used to effectively measure cortical excitability using EMG and EEG measures of excitability.<sup>1</sup> There is no lack of studies demonstrating group-level differences between people with various types of epilepsy and/or healthy controls.<sup>2-7</sup> These results are useful for understanding trends or patterns within the group, but they may not necessarily apply to or accurately predict the outcomes for an individual within the group. There are many reasons why group results may not help individual cases. The individuals within a group may have different characteristics and circumstances that can affect the outcome, or there may be overlap between the distributions of the measure between the studied populations resulting in indeterminate results. For biomarkers of cortical excitability and epileptogenicity to have clinical utility in patient care they should provide useful information which improves or evaluates patient outcomes on a case-by-case basis. Conceptually such a biomarker should have high precision (repeatability) and trueness (establish that the marker actually measures the intended analyte).<sup>8</sup> For clinical validation a high level of

clinical accuracy (sensitivity and specificity) in the intended patient population is required, with a low level of failure rate and/or indeterminate results.

### 8.2.1 *Diagnostic biomarkers*

*High frequency oscillations and Epilepsy.* In **Chapter 2**, we show how high frequency oscillations (HFOs) and epileptic seizures are intrinsically linked to increased local connectivity by gap-junctions in a cascade of models. In the microscopic compartmental model, we simulated a network of axons connected by gap junctions, and observed that when one neuron depolarized and fired, the neighbouring neurons were activated through the gap junctions. Highly connected neuronal networks through gap junctions demonstrate that HFOs emerge when gap-junction density is increased and that HFOs are superimposed on a slow-wave carrier component. This phenomenon was an emergent property of the model due to desynchronous firing of the highly connected network. Interestingly, this phenomenon has recently been confirmed, showing that HFO's are typically observed during the upwards slope of interictal discharges.<sup>9</sup> Although HFOs have been proposed as a potential biomarker for the epileptogenic zone, their clinical feasibility as a biomarker is still being evaluated.<sup>10</sup> We also used ad-hoc testing with the autoregressive residual (ARR) and the relative phase clustering index (rPCI) to evaluate the microscale population network response.<sup>11,12</sup> Both measures were correlated with the increase in connectivity, but the ARR seemed to better distinguish between different levels of connectivity in the network. A recent study employed a ground-truth model,<sup>13</sup> where many uni- and bivariate measures were compared in pre- and post-resection intracranial EEG recordings for regions to be resected and brain tissue which remained untouched (and was considered healthy considering patient outcome). They showed that there was no one-size-fits-all biomarker to assess epileptogenicity within all patients, but rather that each patient requires a different approach and likely has a specific biomarker applicable to their situation.

*TMS-evoked EEG potentials.* In **Chapter 4 and 5**, we demonstrated group level differences in TMS evoked EEG potential (TEP) waveforms between people with juvenile myoclonic epilepsy (JME), migraine and controls. On a subject level there was large variability in TEP readouts between subjects of the same group. Similar findings have been described elsewhere.<sup>5,14,15</sup> Pharmacology-EEG

studies are used to explore drug-specific modulation of the various TEP-peaks.<sup>16–19</sup> They can be useful to determine the mechanisms that drive modulation of various peaks. In **Chapter 4**, we demonstrated decreased frontal and occipital N100 peak amplitudes in people with migraine with aura relative to controls. Several lines of evidence support the hypothesis that the larger N100 peak in epilepsy is a result of enhanced gamma-aminobutyric acid (GABA) mediated activity. Studies have shown that the N100 peak is larger in individuals with epilepsy relative to healthy controls.<sup>7</sup> Additionally, the N100 peak has been shown to be modulated by manipulations of GABAergic activity in healthy controls.<sup>16,20</sup> These findings suggests that the decreased N100 observed in the migraine with aura subgroup in our study may indicate decreased cortical inhibition. This opens up possibilities for similar TMS studies in subjects without aura or with exclusive aura, and for longitudinal TMS-EEG studies during the migraine cycle. Such studies could strengthen the specificity of our observed findings for migraine with aura, and provide insight in changes of cortical excitability related to the onset of a migraine attack. In **Chapter 5**, we observed an exaggerated P60 in a post-hoc analysis of the JME subgroup when compared to controls. A recent pharmaco-EEG study with perampanel showed decreased P60 amplitudes after a single dose, indicating that perhaps the P60 component is related to glutamatergic neurotransmission.<sup>19</sup> However, the underlying physiological underpinnings of these changes in evoked responses remain a topic of much debate. Interpreting TEP waveforms is further complicated by the somatosensory component.<sup>21,22</sup> A recent study demonstrated that ‘realistic’ sham stimulation, mimicking the TMS related somatosensory and auditory response, showed similar evoked potential waveforms as observed with real TMS.<sup>21</sup> This suggests a large contribution of the somatosensory (and auditory component) in previously assumed direct TMS induced cortical activity and the averaged TEP waveforms. Studies that have shown modulation of TEP readouts need to carefully consider their observed results with regard to the somatosensory component. While we provided subjects with ear-plugs to dampen the TMS-related click, we did not perform realistic sham measurements. Early TMS components seem to be unaffected and likely reflect ‘real’ TMS induced cortical activity.<sup>23</sup> While later peaks likely to some extent still reflect cortical activation related to TMS, they are mixed with the somatosensory activation patterns. In light of this development, the N100 peak differences in the migraine with aura

group may also be explained by differences in somatosensory processing relative to controls. Considering the highly complex measurement setup and the time-consuming protocols that need to be implemented to guarantee reproducibility of measurements without contamination with unwanted somatosensory activation, the clinical feasibility for TEP peaks as diagnostic biomarkers seems limited. Furthermore, the large between-subject variability in evoked TEP waveforms indicate that beyond group statistics, peak analysis has no place as a diagnostic biomarker.

*Quantitative TEP and photic response analysis.* In **Chapter 5**, we used a novel way of assessing cortical excitability by determining the uniformity of phase angles across trials using the relative PCI. The rPCI is a measure of the difference between phase clustering on higher order frequencies (commonly beta- or gamma-band clustering) to the clustering of the base frequency (determined by the epoch length, but in our work around the alpha band frequency of 10Hz).<sup>11</sup> We evaluated changes in cortical excitability assessed by the rPCI and the related phase clustering neural network excitability index (NNEI) measure<sup>24</sup> between JME, migraine with aura and healthy controls. Higher order gamma-band clustering is likely related to excitatory recurrent intracortical populations. An increase in phase clustering in the gamma band indicates increased propensity to synchronization and entrainment of recurrent neural populations to repeated stimuli, indicative of increased intracortical excitability. We demonstrated that the rPCI had clinical utility as a measure of cortical excitability in people with JME, with JME showing increased levels of excitability with elevated rPCI when compared to healthy controls for both TMS and photic stimulation modalities. Z-scores of the rPCI in all JME cases were a minimum of one standard deviation from the mean of the healthy controls, indicating diagnostic potential of the rPCI. No elevated rPCI, but rather an increase in NNEI was found for the migraine with aura group, suggesting that increased recurrent connectivity in JME and reduced GABA-ergic inhibition in migraine with aura may set migraine and epilepsy apart. The ‘trueness’ of the rPCI as a biomarker for increased cortical excitability in JME is still unclear. Attempts to use the rPCI and NNEI measures in focal epilepsy groups were unfruitful and were subsequently not pursued. A recent modelling study demonstrated that the rPCI may be a surrogate measure for critical slowing down, which is directly related to the closeness of transition to an epileptic seizure.<sup>25</sup> From a system dynamics

perspective there are however more direct measures to capture this phenomenon. The authors propose and validate another index, the retention, as a more direct measure of critical slowing down. While retrospective analysis on our datasets show some potential for this measure as a biomarker of seizure susceptibility, validation of the measure through a prospective trial is necessary.

### 8.2.2 *Therapeutic effect biomarkers*

Therapeutic biomarkers are biological indicators that can be used to guide treatment decisions. In the context of seizures, therapeutic biomarkers may refer to various types of biomarkers that can be used to determine the likelihood of seizures occurring in a given individual, as well as the likelihood that a particular treatment will be effective in reducing or preventing seizures. Therapeutic biomarkers that reflect seizure susceptibility within subjects can be used to identify individuals who are at higher risk for experiencing seizures and to tailor treatment strategies accordingly. For example, if an individual has a high level of a certain biomarker that has been linked to increased seizure susceptibility, they may be more likely to benefit from a particular seizure medication or other treatment approach.

*Resting state EEG.* In **Chapter 3**, we utilized a computational neural mass model (NMM) of coupled oscillators to simulate EEG. The connectivity strength and the local node properties were used as the varying control parameters within the model. The mean functional connectivity (MFC) of the simulated resting state EEG data segments were strongly associated with the time that each node spent in limit cycle type of behaviour, irrespective of whether fluctuations in MFC were driven by changes in connectivity strength or by changes in the local node properties. A critical component for this positive finding was the use of a nonlinear association index  $h^2$  as the synchrony measure after Hilbert transforming the data.<sup>26</sup> Using various other correlation measures between the original EEG signals did not provide similar results. The results are in agreement with the connotation that the aggregated global connectivity between brain areas (expressed in amplitude correlations rather than an acute neuronal synchronization) is connected with the epileptic state. We proposed an expert system for optimal dose-finding based on this measure, however this proof of concept study needs to be validated in a larger cohort.

*TMS-EMG.* In the TMS studies discussed in **Chapter 6 and 7**, we focused on within-subject measurements across multiple sessions to evaluate the feasibility of TMS biomarkers to track and monitor patients starting adjuvant therapy or during tapering of anti-seizure medication (ASM). In **Chapter 6**, we monitored a cohort of refractory epilepsy patients starting with adjuvant perampanel treatment. In the measurement sessions performed two months after introduction with perampanel we observed a significant increase in right hemispheric resting motor threshold (rMT). Subgroup analysis revealed that the rMT increased bilaterally in the responder subgroup – defined as a minimal seizure frequency reduction of 50% - with no significant differences in the non-responder subgroup. We demonstrated that the rMT – the most straightforward EMG measure of global motor cortical excitability - showed promise in tracking responsiveness to adjuvant therapy. Responders to adjuvant perampanel therapy (outcome assessed at the 6-month interval) showed a clear bilateral increase in rMT measured at the 4mg dose TMS evaluation performed two months after the start with adjuvant perampanel therapy. Conversely, no such increase was observed in the non-responder subgroup. The observed difference suggests that the rMT has potential as a biomarker to evaluate treatment in patients starting perampanel. The observed rMT changes were significant; however, there was some overlap in the distribution of the rMT change between responders and non-responders, which may limit the clinical feasibility of the rMT as a therapeutic biomarker due to indeterminate results in a subset of patients. Similar changes in rMT were described in people with new onset epilepsy.<sup>27</sup> In **Chapter 7**, we evaluated motor cortex excitability daily in people with epilepsy admitted to the presurgical evaluation tapering medication. In general, changes in rMT were highly correlated with tapering of ASMs, with a significant effect of seizure events on TMS measures of motor cortex excitability. A prospective randomized controlled trial is warranted to further study rMT changes in a larger sample of patients starting treatment to validate the observed results and to investigate the clinical accuracy of rMT changes in relation to treatment success.

*Post-ictal Evaluations.* In **Chapter 7**, we evaluated motor cortex excitability within 1-3 hours after seizures. Post ictal measurements performed after focal to bilateral tonic clonic (FBTC) seizures showed a significant attenuation of the paired-pulse TMS (ppTMS) response, suggestive of an increase in inhibition of the local tissue. The single pulse TMS (spTMS) induced motor evoked potential

(MEP) amplitudes were significantly reduced in amplitude, but no significant differences in rMT or long interval intracortical inhibition (LICI) were observed. Together this suggests an increased GABA-mediated inhibition which we speculate may be related to the phenomenon of generalized EEG-suppression, which is an marked EEG-flattening often seen after fbTCs.<sup>28–30</sup> Measurements performed after focal impaired awareness (FIA) seizures however showed different effects with signs of increased excitability – as a decrease in rMT was observed and both ppTMS paradigms showed signs of elevated responses. This implies that the observed increased excitability after FIA seizures are indicative that an ictal focus may be more excitable, or less inhibited, following a first seizure, which can potentially lead to a seizure cluster.<sup>31</sup> In contrast to a previous study,<sup>32</sup> our research found that excitability increased after FIA seizures, while in the previous study, postictal short interval intracortical inhibition (SICI) and LICI were both enhanced (meaning there were more attenuated conditioned responses) for almost all interstimulus intervals in both focal and generalized epilepsy. However, they included individuals with newly diagnosed epilepsy, while our study included individuals with refractory focal epilepsy. This suggests that in people with refractory epilepsy, there may be abnormal inhibition in the postictal state, leading to a higher likelihood of seizure clusters and secondary fbTC seizures.

*TMS-evoked Potentials.* In contrast to the observed rMT changes, TEP waveform analysis for both spTMS and SICI did not reveal significant differences between the pre- and 4mg dose TMS evaluations. This is in contrast with pharmaco-EEG studies that showed P60 modulation after a single dose of perampnel.<sup>19</sup> These results may indicate that the TEP changes that generally occur in single-dose studies are short-lasting, with the TEP waveform eventually returning to pre-treatment baseline. A further complicating factor is that ASM studies such as discussed in these chapters are conducted in refractory patients resistant to mono- or polytherapy. Treatment success in epilepsy care is dependent on achieving seizure freedom, the ultimate goal of epilepsy treatment. In this cohort complete seizure control is not a realistic expectation.

### 8.3 Circular-coil versus figure-of-eight coil

For TMS research circular coils and figure-of-eight coils can be used. Circular coils and figure-of-eight coils have their own set of advantages and disadvantages. The type of TMS coil used in TMS-EEG studies can affect the depth and specificity of the brain regions that are stimulated. Circular coil TMS may stimulate a more superficial brain region and produce a wider spread of activation, while figure-of-eight coil TMS may be more effective at stimulating deeper brain structures and produce more focused activation. Both types of TMS coils can be used in TMS-EEG studies, and the choice of coil depends on the specific research question being addressed. For example, if the goal is to investigate the effects of TMS on a specific brain region, a figure-of-eight coil may be used to more precisely target that region. On the other hand, if the goal is to investigate the broader network of brain regions involved in a particular task or process, a circular coil may be used to stimulate a wider area. The more diffuse stimulation pattern of circular coil-TMS minimizes the impact of small changes in coil position, and reduces the length of a measurement session, as motor hotspot determination is not needed.<sup>33</sup> This benefits the reproducibility of the measurements within-subjects, especially when there is no neuronavigation equipment. In the TMS-EEG literature, the broad-activation characteristics of the circular coil are underutilised.

In this thesis, we made a deliberate choice to focus on TMS protocols with the intended goal of eventual clinical implementation. Our exploratory studies often had no specific cortical area-of-interest, but rather broad activations were preferred to explore the TEP over all electrodes in both epilepsy and migraine with aura. Moreover, the reduced time commitment for patient preparation (no need for hotspot determination), and increased reproducibility (more lenient with small differences in coil position) made the circular coil the preferred option.

### 8.4 Safety of TMS in epilepsy

Stimulating the brain with TMS is not without risk.<sup>34</sup> The primary concern when using TMS is the induction of seizures. Safety guidelines were implemented to

mitigate some of the risk associated with TMS and limit the occurrence of seizures in healthy volunteers.<sup>35</sup> As a result the occurrence of seizures in healthy controls became very rare indeed, with few remaining cases often due to stimulation protocols exceeding the safety guidelines. However, epilepsy patients are at increased risk of seizures when compared to healthy controls. A review of the safety and tolerability of repetitive TMS (rTMS) – which has increased risk compared to spTMS or ppTMS for seizure induction - reported an estimated risk of 1.4% (95% CI: 0.04–2.82) for seizure induction among a cohort of 280 epilepsy cases.<sup>36</sup> A more recent study found a crude risk of 2.9% (95% CI: 1.3-4.5) in epilepsy which is almost twice as high as the previous study.<sup>34</sup>

In this thesis, we measured the response to TMS in 38 epilepsy patients with an aggregate 150 TMS evaluations. In total two seizure events happened, one occurred during a TMS evaluation and one within five minutes after a TMS session. Both seizures occurred as part of a seizure cluster in patients with refractory epilepsy admitted to the EMU, where there is increased risk of recurrent seizures. Seizure semiology for both TMS-related seizures was similar to the habitual spontaneous seizure semiology of those subjects. Considering the subsequent course, it remains unclear if these particular seizures were provoked by the TMS session, or should be seen as spontaneous events that accidentally coincided with - or shortly after - a TMS session. In light of the nature of our data and patient population, stochastically seizure events were likely to happen in some cases during the TMS evaluations. Generally, TMS in epilepsy can be considered safe when following the safety guidelines.<sup>34</sup> However, a small risk on seizure induction remains and monitoring of cases by a physician during the evaluation is still recommended.

## 8.5 Future directions

In this thesis, we performed several studies to explore the dynamics of cortical activation patterns ‘in silico’ and ‘in vivo’ in healthy participants and in those suffering from epilepsy and migraine. Effective treatment in people with epilepsy should show a decrease of excitability, or increase in inhibition, while moving away from the proximity of a critical transition point to a seizure state. Predicting the effectiveness of an ASM with a short measurement of resting-state or

perturbation-based EEG is warranted on several levels. It may be used for expedient dose-finding on an individual basis, or may be used to make more rational choices for the type of anti-seizure medication. It may provide objective measurements to evaluate treatment-response, with no need to rely on feedback through seizure diaries.

The most promising biomarker related to evoked EEG-responses was the rPCI in people with JME. More research is needed to validate this biomarker for diagnosing people with JME, and potentially other generalized epilepsies, and monitoring treatment response. However, the time-intensive measurements and the highly complex measurement setup required for recording TMS-evoked EEG potentials may all prove to be too big of a hurdle to overcome for clinical implementation beyond research studies. One interesting recent development is the utilization of within-subject group level independent component analysis,<sup>23,37</sup> which may be used to combine trials of multiple intensities to construct an input-output curve of evoked potentials. This would allow for shorter lasting protocols with only few trials per intensity without significant loss of fidelity per intensity when compared to longer lasting protocols with many trials. Input-output curves with many stimulation intensity steps could be recorded though which a wealth of extra parameters could be extracted, such as the slope and inflection point of the sigmoidal activation curve of peak amplitudes, but also the (non-)linear rates of change in various peak amplitudes. Notwithstanding this development, there are still many open-standing questions regarding biological fluctuations in excitability, optimal measurement protocols and standardization of measurements within the field of TMS.<sup>38</sup> There is still large variation in experimental design, which is probably an indicator of currently unsatisfactory measurement setup prone to artefacts. These problems may in the end hamper successful implementation of TMS in the daily clinical practice.

The TMS-EMG-based measures that reflect corticospinal excitability may have potential as a tool to evaluate treatment outcome. In future studies hemisphere specific TMS-EMG protocols should help elucidate the role of lateralization of the epileptic focus on hemispheric differences in measures of excitability. Neuronavigation may be used in combination with more focal TMS using figure-of-eight coils to assure intersession reproducibility within subjects at the cost of

increasing the time commitment required for the measurement sessions. There was however, some overlap in distributions of the various EMG-measures, which may hamper their use as biomarkers. Biological fluctuations of cortical excitability is one of the underlying mechanisms, including but not limited to differences in hormonal balance, hours of sleep, intake of caffeine or other neuroactive substances, and stress level at the time of measurement which all impact cortical excitability.<sup>39</sup> These biological sources of variability remain a major issue that just as with TMS-EEG, may cause the EMG measures to give indeterminate results. Overall, both fields are still developing and new methods for assessing the evoked potentials may give rise to better and more discriminate biomarkers.

## References

1. Cantello, R. *et al.* Ketogenic diet: Electrophysiological effects on the normal human cortex. *Epilepsia* **48**, 1756–1763 (2007).
2. Badawy, R. A. B., Curatolo, J. M., Newton, M., Berkovic, S. F. & Macdonell, R. A. L. Changes in cortical excitability differentiate generalized and focal epilepsy. *Ann. Neurol.* **61**, 324–331 (2007).
3. Badawy, R. A. B., Jackson, G. D., Berkovic, S. F. & MacDonell, R. A. L. Cortical excitability and refractory epilepsy: A three-year longitudinal transcranial magnetic stimulation study. *Int. J. Neural Syst.* **23**, (2013).
4. ter Braack, E. M., Koopman, A. W. E. & van Putten, M. J. A. M. Early TMS evoked potentials in epilepsy: A pilot study. *Clin. Neurophysiol.* **127**, 3025–3032 (2016).
5. de Goede, A. A., ter Braack, E. M. & van Putten, M. J. A. M. Single and paired pulse transcranial magnetic stimulation in drug naïve epilepsy. *Clin. Neurophysiol.* **127**, 3140–3155 (2016).
6. Kimiskidis, V. K., Kugiumtzis, D., Papagiannopoulos, S. & Vlaikidis, N. Transcranial magnetic stimulation (TMS) modulates epileptiform discharges in patients with frontal lobe epilepsy: A preliminary EEG-TMS study. *Int. J. Neural Syst.* **23**, 121102031948003 (2013).
7. Kimiskidis, V. K. *et al.* TMS combined with EEG in genetic generalized epilepsy: A phase II diagnostic accuracy study. *Clin. Neurophysiol.* **128**, 367–381 (2017).
8. Holland, R. L. What makes a good biomarker? *Adv. Precis. Med.* **1**, 66 (2016).
9. Guth, T. A. *et al.* Interictal spikes with and without high-frequency oscillation have different single-neuron correlates. *Brain* **144**, 3078–3088 (2021).
10. Zweiphenning, W. *et al.* Intraoperative electrocorticography using high-frequency oscillations or spikes to tailor epilepsy surgery in the Netherlands (the HFO trial): a randomised, single-blind, adaptive non-inferiority trial. *Lancet Neurol.* **21**, 982–993 (2022).
11. Parra, J. *et al.* Gamma-band phase clustering and photosensitivity: Is there an underlying mechanism common to photosensitive epilepsy and visual perception? *Brain* **126**, 1164–1172 (2003).
12. Geertsema, E. E. *et al.* Automated Seizure Onset Zone Approximation Based on Nonharmonic High-Frequency Oscillations in Human Interictal Intracranial EEGs. *Int. J. Neural Syst.* **25**, 1550015 (2015).
13. Demuru, M. *et al.* The value of intra-operative electrographic biomarkers for tailoring during epilepsy surgery: from group-level to patient-level analysis. *Sci. Rep.* **10**, (2020).
14. Wassermann, E. M. Variation in the response to transcranial magnetic brain

- stimulation in the general population. *Clin. Neurophysiol.* **113**, 1165–1171 (2002).
15. Du, X., Summerfelt, A., Chiappelli, J., Holcomb, H. H. & Hong, L. E. Individualized brain inhibition and excitation profile in response to paired-pulse TMS. *J. Mot. Behav.* **46**, 39–48 (2014).
  16. Premoli, I. *et al.* TMS-EEG signatures of GABAergic neurotransmission in the human cortex. *J. Neurosci.* **34**, 5603–5612 (2014).
  17. Premoli, I. *et al.* Characterization of GABAB-receptor mediated neurotransmission in the human cortex by paired-pulse TMS-EEG. *Neuroimage* **103**, 152–162 (2014).
  18. Premoli, I. *et al.* The impact of GABAergic drugs on TMS-induced brain oscillations in human motor cortex. *Neuroimage* **163**, 1–12 (2017).
  19. Belardinelli, P. *et al.* TMS-EEG signatures of glutamatergic neurotransmission in human cortex. *Sci. Rep.* **11**, (2021).
  20. Ziemann, U. *et al.* TMS and drugs revisited 2014. *Clin. Neurophysiol.* **126**, 1847–1868 (2015).
  21. Conde, V. *et al.* The non-transcranial TMS-evoked potential is an inherent source of ambiguity in TMS-EEG studies. *Neuroimage* **185**, 300–312 (2019).
  22. Gordon, P. C. *et al.* Recording brain responses to TMS of primary motor cortex by EEG – utility of an optimized sham procedure. *Neuroimage* **245**, (2021).
  23. Raffin, E. *et al.* Probing regional cortical excitability via input–output properties using transcranial magnetic stimulation and electroencephalography coupling. *Hum. Brain Mapp.* **41**, 2741–2761 (2020).
  24. Wendling, F. *et al.* Brain (Hyper)Excitability Revealed by Optimal Electrical Stimulation of GABAergic Interneurons. *Brain Stimul.* **9**, 919–932 (2016).
  25. Kalitzin, S. *et al.* Epilepsy as a manifestation of a multistate network of oscillatory systems. *Neurobiology of Disease* vol. 130 (2019).
  26. Kalitzin, S. *et al.* Quantification of spontaneous and evoked HFO's in SEEG recording and prospective for pre-surgical diagnostics. Case study. in *Proceedings of the Annual International Conference of the IEEE Engineering in Medicine and Biology Society, EMBS* vol. 6 1024–1027 (2012).
  27. Badawy, R. A. B., Macdonell, R. A. L., Berkovic, S. F., Newton, M. R. & Jackson, G. D. Predicting seizure control: Cortical excitability and antiepileptic medication. *Ann. Neurol.* **67**, 64–73 (2010).
  28. Boido, D., Gnatkovsky, V., Uva, L., Francione, S. & De Curtis, M. Simultaneous enhancement of excitation and postburst inhibition at the end of focal seizures. *Ann. Neurol.* **76**, 826–836 (2014).
  29. Žiburkus, J., Cressman, J. R. & Schiff, S. J. Seizures as imbalanced up states: Excitatory

- and inhibitory conductances during seizure-like events. *J. Neurophysiol.* **109**, 1296–1306 (2013).
30. Pottkämper, J. C. M., Hofmeijer, J., van Waarde, J. A. & van Putten, M. J. A. M. The postictal state — What do we know? *Epilepsia* vol. 61 1045–1061 (2020).
  31. Taubøll, E., Lundervold, A. & Gjerstad, L. Temporal distribution of seizures in epilepsy. *Epilepsy Res.* **8**, 153–165 (1991).
  32. Badawy, R., MacDonell, R., Jackson, G. & Berkovic, S. The peri-ictal state: Cortical excitability changes within 24 h of a seizure. *Brain* **132**, 1013–1021 (2009).
  33. Rossini, P. M. *et al.* Non-invasive electrical and magnetic stimulation of the brain, spinal cord, roots and peripheral nerves: Basic principles and procedures for routine clinical and research application: An updated report from an I.F.C.N. Committee. *Clin. Neurophysiol.* **126**, 1071–1107 (2015).
  34. Pereira, L. S., Müller, V. T., da Mota Gomes, M., Rotenberg, A. & Fregni, F. Safety of repetitive transcranial magnetic stimulation in patients with epilepsy: A systematic review. *Epilepsy Behav.* **57**, 167–176 (2016).
  35. Rossi, S. *et al.* Safety, ethical considerations, and application guidelines for the use of transcranial magnetic stimulation in clinical practice and research. *Clin. Neurophysiol.* **120**, 2008–2039 (2009).
  36. Bae, E. H. *et al.* Safety and tolerability of repetitive transcranial magnetic stimulation in patients with epilepsy: a review of the literature. *Epilepsy and Behavior* vol. 10 521–528 (2007).
  37. Du, Y. *et al.* Artifact removal in the context of group ICA: A comparison of single-subject and group approaches. *Hum. Brain Mapp.* (2016) doi:10.1002/hbm.23086.
  38. Julkunen, P., Kimiskidis, V. K. & Belardinelli, P. Bridging the gap: TMS-EEG from lab to clinic. *J. Neurosci. Methods* (2022) doi:10.1016/j.jneumeth.2022.109482.
  39. Badawy, R. A. B., Freestone, D. R., Lai, A. & Cook, M. J. Epilepsy: Ever-changing states of cortical excitability. *Neuroscience* **222**, 89–99 (2012).

# List of acronyms

AMPA	amino-3-hydroxyl-5-methyl-4-isoxazole-propionate
AR	autoregressive
ARR	autoregressive residual
ASM	anti-seizure medication
BNI	brain network ictogenicity
CBZ	carbamazepine
CCW	counterclockwise
CI	confidence interval
CLB	clobazam
CR	conditioned response
CW	clockwise
DLPFC	dorsolateral pre-frontal cortex
DVA	developmental venous anomaly
ECG	electrocardiogram
ECoG	electrocorticography
EEG	electroencephalography
E:I	excitation to inhibition
EMG	electromyogram
EMU	epilepsy monitoring unit
FBTC	focal to bilateral tonic clonic seizure
FC	functional connectivity

FIA	focal impaired awareness
GABA	gamma-aminobutyric acid
GMFP	global mean field power
HFO	High frequency oscillations
ICA	independent component analysis
ICC	intraclass correlation coefficient
ICF	intracortical facilitation
IED	interictal epileptiform discharge
IN	interneuron
ISI	interstimulus interval
JME	juvenile myoclonic epilepsy
LC	limit cycle
LCM	lacosamide
LEV	leveteracitam
LICI	long interval cortical inhibition
LTG	lamotrigine
LTP	long-term potentiation
MAP	morphometric analysis program
MEG	magnetoencephalography
MEP	motor evoked potential
MFC	mean functional connectivity
MRI	magnetic resonance imaging
MSO	maximum stimulator output
MTS	mesial temporal sclerosis

| *List of acronyms*

NMDA	N-methyl-D-aspartate
NMM	neural mass model
NNEI	neural network excitability index
OCB	oxcarbamazepine
ppTMS	paired pulse TMS
PC	polarity compensated
PY	pyramidal neurons
PCI	phase clustering index
PGES	postictal generalized EEG suppression
rMT	resting motor threshold
rPCI	relative phase clustering index
RS	resting state
rTMS	repetitive TMS
SD	standard deviation
SEEG	stereoelectroencephalography
SICI	short-interval intracortical inhibition
SOZ	seizure onset zone
spTMS	single pulse TMS
TC	tonic clonic
TEP	TMS-evoked EEG potential
TF	time-frequency
TMS	transcranial magnetic stimulation
TMS-EEG	transcranial magnetic stimulation with electroencephalography
TMS-EMG	transcranial magnetic stimulation with electromyography

TOI	time of interest
TPM	topiromate
UR	unconditioned response
VPA	valproatic acid

# List of definitions

biomarker	Any measurable characteristic in the body that provides information about a biological process, condition, or response to a treatment.
bistability	In a dynamical system, bistability describes a system that has two stable equilibrium states.
conditioned response	Response observed after paired pulse, where a secondary test stimulus was combined with an initial conditioning stimulus.
control parameter	Model variable in the governing equations of a computational model that may vary throughout the domain, space or time.
computational model	Computer simulations of complex dynamical systems using mathematics and physics.
cortical excitability	Responsiveness of the cerebral cortex, i.e. the ease with which neurons in the cortex can generate electrical impulses and transmit signals.
cortical silent period	TMS protocol which elicits a temporary interruption of sustained EMG activity following a motor evoked potential triggered by TMS.
critical slowing down	Cortical slowing down occurs near critical transitions when systems undergo phase transitions, which is manifested by the slowing down of the recovery of the dynamical system to its original state after perturbations
critical transition	Abrupt shifts in the state of a complex dynamical system that may occur when changing conditions pass a critical (bifurcation) point. Recovery of such shifts may require more than a simple return to the conditions at which the transition occurred (e.g. hysteresis).
epileptogenicity	Capacity or property of brain tissue to generate or promote the development of seizures.
excitation	Process by which neurons become more active and generate electrical impulses or action potentials. It promotes the generation of an action potential, leading to an increase in neuronal activity and the transmission of information.

excitation:inhibition balance	The balance between inhibition and excitation that controls cortical excitability in many brain circuits.
functional connectivity	The statistical relationship between specific (patho)physiological signals in time and is considered a measure of how regions of the brain interact with each other.
high frequency oscillations	Brain activity observed in the intracranial EEG in frequency ranges between 80-500 Hz.
ictal	State or period during which a seizure occurs.
ictality	Index that is used to quantify the likelihood to seizure within a computation model based on the auto-covariance peaks.
ictogenicity	Probability of spontaneous seizures or the capability to provoke or trigger seizures in individuals who are already susceptible to them.
inhibition	Process by which neurons become less active or suppressed, reducing the likelihood of the neuron generating an action potential, dampening neuronal activity and preventing excessive or uncontrolled excitatory activity.
interictal	Period between seizures.
intracortical facilitation	Enhanced (increased) response after paired pulse TMS (with a conditioning and test stimulus) relative to the unconditioned test response, which typically occurs between interstimulus intervals between 1 and 5-10ms.
limit cycle	Isolated closed trajectory in a phase space in non-linear systems. Stable limit cycles exhibit self-sustained oscillations i.e. systems that oscillate even in absence of an external driving force.
long interval cortical inhibition	Paired pulse TMS technique where a suprathreshold primary conditioning and secondary test stimulus are combined with a relatively long interval (50-200ms) between them, typically resulting in attenuated responses relative to the unconditioned test stimulus.
mean functional connectivity	Averaged node connectivity of all existing connections between pairs of nodes in a reconstructed functional network.
motor evoked potential	Electrical signals recorded from the muscles following stimulation of motor pathways within the brain.
multistability	Ability of a system to achieve multiple steady states under the same external conditions.

## | *List of definitions*

neural network epileptogenicity index	Biomarker of excitability that is assessed by computing the phase clustering of EEG responses at the alpha band.
paired pulse TMS	Stimulation paradigm in which a conditioning and test stimulation are combined to assess the excitatory and inhibitory interactions in the motor cortex.
paroxysmal	Sudden or abrupt increase of symptoms that occurs, quiets down, and occurs again and again.
perturbation	Disturbance of the state of equilibrium of a complex dynamical system.
phase clustering	Uniformity of phase angles across trials in EEG responses.
phosphene	Luminous floating shapes in the visual field that occur without light entering the eye.
postictal generalized EEG suppression	Diffuse suppression of EEG activity lasting up to several minutes which may follow generalized tonic clonic seizures.
relative phase clustering index	Biomarker of excitability computed as the phase clustering of the higher order frequency bands relative to the alpha-band.
resting state	Baseline neurophysiological activity of a participant, typically recorded in a relaxed position with eyes closed for multiple minutes.
resting motor threshold	Minimal TMS intensity at which MEPs (>50uV) are registered in 50% of trials.
seizure onset zone	Area of the cortex from which seizures originate.
sham measurement	Control measurement in which an investigator goes through the motions of an experiment, without the actual intervention.
short interval cortical inhibition	Paired pulse TMS technique in which a low intensity subthreshold conditioning stimulus is used combined with a secondary suprathreshold test stimulus with an ISI of 5-20ms, typically resulting in attenuated responses relative to the unconditioned test response.
single pulse TMS	TMS stimulation paradigms involving responses to single stimuli typically averaged across many trials.
steady state	State of a complex dynamical system that changes negligibly over time and is considered in a state of equilibrium.

tipping point	Critical point in a complex dynamical system beyond which an unstoppable change takes place.
transient	Momentary variation in current, voltage or frequency.
TMS evoked EEG potentials	Averaged EEG response that consists of a series of positive and negative deflections measured after TMS stimulation.
unconditioned response	The measured EMG response after only the test stimulus of the paired pulse stimulation paradigms.



## Summary and Appendices

## Summary

Epilepsy is a chronic condition characterized by recurrent and unpredictable seizures. The transient nature of seizures makes epilepsy a dynamic disease where periods of normal brain function are intermittently interrupted by seizures that impair partial- or whole- brain function. These seizures can have a significant impact on the quality of life of people with epilepsy. Cortical excitability refers to the ability of brain cells (neurons) to generate and transmit electrical signals. In people with epilepsy, there may be abnormal levels of cortical excitability, which can contribute to the development of seizures. Quantifying cortical excitability through with excitability measures in people with epilepsy may help inform the development of new treatments and therapies for this condition.

Diagnostic biomarkers are markers that can be used to identify a particular health condition or disease. They can be used to diagnose a condition, assess its severity, or predict the likelihood of developing a particular condition. Some examples of diagnostic biomarkers include low nerve conduction velocities in carpal tunnel syndrome, cancer biomarkers such as tumour markers or genetic mutations. Therapeutic biomarkers, on the other hand, are used to predict or monitor the response to a particular treatment or therapy. They can help physicians determine the most appropriate treatment for a particular patient and assess its effectiveness. Some examples of therapeutic biomarkers include markers of inflammation for autoimmune diseases, markers of bone density for osteoporosis, and markers of drug metabolism for certain medications. Both diagnostic and therapeutic biomarkers are important tools in medicine and can help inform treatment decisions, improve patient outcomes, and personalize care. In this thesis, we aimed to identify biomarkers for diagnosis and treatment evaluation in people with epilepsy.

One diagnostic biomarker for epilepsy is the presence of high-frequency oscillations (HFOs), which are short oscillations recorded in the intracranial

EEG. While they are currently used as a biomarker to determine resection extent during surgical procedures in patients with difficult to treat epilepsy, there was not yet a causal link between the occurrence of HFO's and epileptic seizures. In **Chapter 2**, we showed in a cascade of computation models with two levels of complexity that HFOs are induced by increased gap-junction connectivity between neurons in the microscopic model, which in turn is associated with an increase in seizure susceptibility in the higher level model. These models were linked through their population firing rate. We also tested two indices that are used to detect HFOs, the autoregressive residual (ARR) and the relative phase clustering index (rPCI), which were correlated with increased connectivity of gap-junctions. However, the clinical applicability of HFOs as a biomarker is still being evaluated.

In **Chapter 3**, we focused on measuring the epileptogenicity from resting-state EEG only, before moving on to evoked responses in later chapters. We used a computational model to find a good measure that reflects the epileptogenicity, and subsequently used 'in vivo' EEG segments of patients to evaluate the measure as a proof of concept. In the simulated data, we can reconstruct the exact time the model spends in a seizure state for various node-parameters and connectivity strengths between nodes within the model. In the following step, we used the resting-state EEG only (periods without seizures) and found that the mean functional connectivity (MFC) of the reconstructed functional networks of these EEG segments correlated well with the amount of time the network spend in a seizure state. The 'in vivo' dataset consisted of resting-state EEG measurements in people with epilepsy that started medication, including responders, non-responders, and negative responders. We demonstrated that the responders indeed showed a significant decrease in MFC with the increasing antiseizure medication dose, the negative responders showed a significant increase in MFC, and the non-responders had indeterminate results. More research is needed to validate this approach in a larger dataset.

In the following chapters, we utilised a more proactive perturbation-based approach to investigate cortical excitability changes in paroxysmal disorders. In **Chapter 4 and 5**, we evaluated how TMS-evoked EEG potentials (TEP) are different between people with juvenile myoclonic epilepsy (JME), migraine with aura and healthy controls. Migraine is of interest because it is a comorbid disease

of epilepsy with paroxysmal events that are likely also related to changes in cortical excitability. The TEP is an averaged response over many trials that has a distinct pattern of positive and negative deflections between 10-400ms after the stimulus. In **Chapter 4**, we observed that people with migraine with aura had a decreased negative deflection at 100 ms, the so-called N100-peak. The reduction in this peak is suggestive of reduced inhibition in the migraine with aura group. In **Chapter 5**, we observed an exaggerated positive deflection at around 60 ms in the JME group without medication when compared to controls in a post-hoc analysis. There are, however, many factors that can influence TEP peaks, thus making it unlikely that these observed TEP changes can be used as an effective biomarker. We continued with a more analytic approach, where we used the rPCI to quantify the responses to both TMS and photic stimulation modalities. We found a clear increase in rPCI for both stimulation modulations for the JME group when compared to healthy controls. This effect disappeared in the JME group on medication. Moreover, we found a clear inversely correlated dose-response effect for the rPCI in one of the patients with JME starting with medication in over five measurements, indicating that rPCI might be a good measure for monitoring cortical excitability in generalized epilepsy. In migraine with aura, the rPCI did not differ from controls. More research is needed to validate this biomarker for diagnosing people with JME and other types of generalized epilepsy and determine its value for monitoring treatment response.

In **Chapter 6**, we continued with this approach and explored the TEP within-subject over multiple measurement sessions in people with refractory focal epilepsy starting with adjuvant treatment with perampanel. Perampanel is a relatively new anti-seizure medication that targets the AMPA-receptor. We did a baseline measurement before starting perampanel, a second measurement at a 4mg/day dose and finally a third measurement at the maximum tolerated or effective dose. We observed that TEPs remained stable between the different measurement sessions. This contrasts with a previous single-dose study where differences in early peak amplitude were observed. We speculate that long-term use of medication eventually results in a normalized TEP back to baseline. In addition to the TEP analysis, we also tried the rPCI to monitor changes in excitability in these focal epilepsy patients, however the results were disappointing and we did not further pursue this approach in people with focal

epilepsy. More interesting findings were observed with the electromyography (EMG)-based measures of excitability. There we saw that the resting motor threshold (rMT) increased with increasing perampanel dose, suggesting decreased motor cortical excitability. When we did a subgroup analysis of responders and non-responders to perampanel, dichotomized by a more than 50% reduction in seizure frequency, we observed a significant and relatively large increase in rMT in the responder subgroup. No significant changes were seen in the non-responder subgroup. This indicates that there may be potential for the rMT as a biomarker for treatment response and adjustments by measuring lasting changes in corticospinal excitability.

In **Chapter 7**, to further validate the potential for TMS-EMG-based measures we tracked corticospinal excitability in people with refractory epilepsy admitted to the epilepsy monitoring unit in SEIN. Typically, anti-seizure medication is tapered to increase the probably on seizures. This is an ideal setting to see whether TMS-EMG markers can track the dynamic changes in excitability in patients due to changes in antiseizure medication during their admission. We again observed a significant dose-response effect in rMT with a significant reduction after tapering antiseizure medication. Moreover, we observed changes in excitability in postictal evaluations recorded shortly after seizures, with distinct effects per seizure type. Focal impaired awareness seizures were generally followed by an increase in excitation which we speculate might be indicative of a pro-ictal state. Conversely, focal to bilateral tonic-clonic seizures showed a reduction in excitability, reflecting a more inhibited brain. Future research should be focused on exploring the effect of long-term use of ASMs and the effect on TMS-EMG measures as potential biomarkers for treatment outcome.

In these studies, we have demonstrated how various EEG, TMS-EMG, and TMS-EEG based measures can be used to quantify cortical excitability and epileptogenicity in people with epilepsy. Due to the varied types of epilepsy and underlying causes, it is likely that different approaches will be needed for different patients, with each patient or epilepsy type potentially requiring a specific biomarker that is relevant to their particular case.

# Nederlandse samenvatting

Epilepsie is een chronische aandoening die gekenmerkt wordt door terugkerende en toch onvoorspelbare aanvallen. De paroxismale aard van aanvallen maakt epilepsie een dynamische ziekte waarbij periodes van normale hersenfunctie met tussenpozen worden onderbroken door aanvallen die gedeeltelijk of volledig de hersenfunctie beïnvloeden. Deze aanvallen kunnen een significante impact hebben op de kwaliteit van leven van mensen met epilepsie. Corticale exciteerbaarheid verwijst naar het gemak waarmee hersencellen (neuronen) elektrische signalen genereren en doorsturen. Bij mensen met epilepsie kunnen er verhoogde niveaus van corticale exciteerbaarheid zijn, wat door het gebrek aan voldoende remming kan onttaarden in epileptische aanvallen. Het kwantitatief kunnen meten van corticale exciteerbaarheid bij mensen met epilepsie kan helpen bij het ontwikkelen van nieuwe behandelingen en therapieën voor deze aandoening.

Diagnostische biomarkers zijn markers (indicatoren) die gebruikt kunnen worden om een bepaalde gezondheidstoestand of ziekte te identificeren. Ze kunnen gebruikt worden om een aandoening te diagnosticeren, de ernst ervan te beoordelen of de kans op het ontwikkelen van een bepaalde aandoening te voorspellen. Voorbeelden van diagnostische biomarkers zijn bijvoorbeeld de verlaagde conductiesnelheid van de nervus medianus bij carpaletunnelsyndroom en kankerbiomarkers zoals tumormarkers of genetische mutaties. Therapeutische biomarkers worden daarentegen gebruikt om de reactie op een bepaalde behandeling of therapie te voorspellen of te monitoren. Ze kunnen artsen helpen om de meest geschikte behandeling voor een bepaalde patiënt te bepalen en de effectiviteit ervan te beoordelen. Voorbeelden van therapeutische biomarkers zijn markers van ontsteking bij auto-immuun aandoeningen, markers van botdichtheid bij osteoporose en markers van geneesmiddelmetabolisme voor bepaalde medicijnen. Zowel diagnostische als therapeutische biomarkers zijn belangrijke hulpmiddelen in de geneeskunde en kunnen bijdragen aan het nemen van behandelbeslissingen, het verbeteren van patiëntuitkomsten en het personaliseren van zorg. In deze thesis hebben wij ons ten doel gesteld om

biomarkers te identificeren voor diagnose en behandelbevaluatie bij mensen met epilepsie.

Een diagnostische biomarker voor epilepsie is de aanwezigheid van hoogfrequente oscillaties (HFO's), dit zijn korte oscillaties die worden geobserveerd in het intracraniale EEG. Hoewel ze momenteel worden gebruikt als biomarker om de extensie van de resectie te bepalen tijdens chirurgische ingrepen bij mensen met moeilijk behandelbare epilepsie, was er nog geen causale link tussen het voorkomen van HFO's en epileptische aanvallen. In **Hoofdstuk 2** hebben wij twee computationele modellen gebruikt op verschillende niveaus van complexiteit (schaal), waarmee wij laten zien dat HFO's worden veroorzaakt door een toename van de gap-junction connectiviteit tussen neuronen in het microscopische model, wat op zijn beurt geassocieerd is met een toename van de aanvalsgevoeligheid in het hogere niveau model. Deze twee modellen waren verbonden via de vuurfrequentie van de neuronale populatie. Wij hebben ook twee indices getest die worden gebruikt om HFO's te detecteren, de autoregressive residual (ARR) en de relative phase clustering index (rPCI), die beide gecorreleerd waren met een toegenomen connectiviteit van gap-junctions. De klinische toepasbaarheid van HFO's als biomarker wordt echter nog steeds onderzocht.

In **Hoofdstuk 3** hebben wij ons gericht op het meten van de epileptogeniciteit door middel van resting-state EEG segmenten, waarna wij in de latere hoofdstukken de uitgelokte responsies in het EEG onderzoeken. Wij hebben een computationeel model gebruikt om een goede maat te vinden die de epileptogeniciteit meet, om vervolgens in 'in vivo' EEG segmenten van patiënten de maat te testen als een proof of concept. In de gesimuleerde data kunnen wij de exacte tijd reconstrueren die het model doorbrengt in een (epileptische) aanvalstoestand voor verschillende parameters van de verschillende neuronale populaties (nodes) en de verbindingsterktes tussen nodes binnen het model. In de volgende analyse stap hebben wij alleen de resting-state EEG segmenten gebruikt (perioden zonder aanvallen) en gevonden dat de mean functional connectivity (MFC) van de gereconstrueerde functionele netwerken van deze EEG segmenten goed correleerde met de tijd die het netwerk doorbracht in een aanvalstoestand. Wij hebben vervolgens een 'in vivo' dataset gebruikt bestaande uit resting-state EEG segmenten bij mensen met

epilepsie die begonnen met medicatie om de MFC in de praktijk te testen, inclusief responders, non-responders en negatieve responders. Wij hebben aangetoond dat de responders inderdaad een significante afname in MFC lieten zien met opbouw van medicatie, de negatieve responders lieten een significante toename in MFC zien en de non-responders zaten hier tussenin. Meer onderzoek is nodig om deze proof of concept aanpak te valideren.

In de volgende hoofdstukken hebben we de meer proactieve op perturbatie gebaseerde meetmethodes onderzocht om veranderingen in de corticale exciteerbaarheid in paroxismale stoornissen vast te leggen. In **Hoofdstuk 4 en 5** hebben wij geëvalueerd hoe door TMS opgewekte EEG potentialen (TEP's) verschillen tussen mensen met juveniele myoclonie epilepsie (JME), migraine met aura en gezonde controles. Migraine is interessant omdat het een comorbide aandoening is van epilepsie, die ook gekenmerkt wordt door paroxismale gebeurtenissen met daaraan ten grondslag naar alle waarschijnlijkheid ook veranderingen in de corticale exciteerbaarheid. De TEP is een gemiddelde respons over vele stimuli met een duidelijk patroon van positieve en negatieve deflexies tussen 10 en 400 ms na de stimulus. In **Hoofdstuk 4** hebben wij geobserveerd dat mensen met migraine met aura een afname van de negatieve deflexie lieten zien op 100 ms, de zogenaamde N100-piek. De reductie van deze piek duidt op een verminderde inhibitie in de migraine-met-aura-groep. In **Hoofdstuk 5** hebben wij in een post hoc analyse een verhoogde positieve deflexie rond de 60 ms waargenomen in de JME-groep zonder medicatie, in vergelijking met de controles. Er zijn echter veel factoren die invloed kunnen hebben op de TEP piekamplitudes, waardoor deze geobserveerde effecten waarschijnlijk niet effectief kunnen worden ingezet als biomarker. Vervolgens gingen wij in **Hoofdstuk 5** verder met een meer analytische aanpak waarbij wij de rPCI gebruikten om de respons op zowel TMS- als lichtflitsstimulatie modaliteiten te kwantificeren. Er was een duidelijke toename van de rPCI voor zowel TMS- als lichtflits stimulatie voor de JME-groep in vergelijking met de gezonde controles. Dit effect verdween in de JME-groep met medicatie. Bovendien liet één van de patiënten met JME die begon met medicatie in de loop van vijf metingen een duidelijk omgekeerd evenredig dosis-respons-effect zien voor de rPCI, wat erop duidt dat de rPCI een goede maat kan zijn om de corticale exciteerbaarheid in JME te monitoren. Bij migraine met aura verschilde de rPCI niet van de controles. Er is meer onderzoek nodig om deze biomarker

te valideren voor het diagnosticeren van mensen met JME en andere gegeneraliseerde vormen van epilepsie en of hij gebruikt kan worden voor het monitoren van de behandeling respons.

In **Hoofdstuk 6** zetten wij door met deze aanpak en hebben wij de TEP binnen de proefpersoon over meerdere meetsessies onderzocht bij mensen met refractaire focale epilepsie die begonnen met aanvullende behandeling met perampanel. Perampanel is een relatief nieuw anti-epilepticum dat zich richt op de AMPA-receptor. Wij begonnen met een basismeting voorafgaand aan ophoging, een tweede meting bij een dosis van 4 mg/dag en uiteindelijk een derde meting bij de maximale tolereerbare of effectieve dosis. Daar zagen wij dat de TEP's tussen de verschillende metingsessies stabiel bleven. Dit staat in contrast met een eerdere studie met één dosis waarbij verschillen in amplitudes van vroege pieken werden waargenomen. Wij speculeren dat langdurig gebruik van medicatie uiteindelijk leidt tot normalisatie van de TEP terug naar het baseline-niveau. Naast de TEP analyse hebben wij ook geprobeerd om de rPCI te gebruiken om veranderingen in exciteerbaarheid bij deze focale epilepsie patiënten te monitoren. De resultaten vielen echter tegen en daarom hebben wij deze niet verder ingezet bij dergelijke focale epilepsie patiënten. Daarentegen zagen wij bij de op electromyografie (EMG) gebaseerde maten van exciteerbaarheid betere resultaten. Daar zagen wij dat de resting motor threshold (rMT) sterk correleerde met een verhoging in perampanel, wat suggestief is voor een verlaging van de motor cortex exciteerbaarheid. Bij een subgroep analyse van responders en non-responders, ingedeeld op basis van een reductie van aanvalsfrequentie van 50% of meer, werd er een significante en relatief sterke verhoging van rMT gezien in de responders. Er werden geen significante verschillen gezien in de non-responders. Dit laat een mogelijke rol zien voor de rMT als biomarker voor het evalueren en monitoren van behandelingsuitkomst via langdurige veranderingen in corticospinale exciteerbaarheid.

Om deze op TMS-EMG gebaseerde maat verder te bestuderen hebben wij in **Hoofdstuk 7** de corticospinale exciteerbaarheid gemeten bij mensen met refractaire epilepsie die werden opgenomen in de epilepsie monitoring unit in SEIN. Typisch wordt anti-epileptica afgebouwd om de kans op aanvallen te vergroten. Dit is een ideale setting om te zien of TMS-EMG markers de dynamische veranderingen in exciteerbaarheid ten gevolge van de

medicatieveranderingen tijdens hun opname kunnen volgen. Er was wederom een significant dosis-respons effect van rMT met een significante vermindering in rMT bij het afbouwen van de medicatie. Bovendien hebben wij veranderingen in exciteerbaarheid gemeten in de postictale evaluaties kort na het optreden van aanvallen, met specifieke effecten per aanvalstype. Focale aanvallen met verminderde gewaarwording werden over het algemeen gevolgd door een toename in excitatie, wat mogelijk een indicatie is van een verhoogde aanvalsgevoeligheid. Daarentegen lieten focale tot bilaterale tonic-clonische aanvallen een reductie in exciteerbaarheid zien, wat een meer geïnhibeerd brein suggereert. Toekomstig onderzoek moet zich richten op het verkennen van TMS-EMG exciteerbaarheidsmaten bij het chronisch gebruik van verschillende anti-epileptica, en de potentiële rol die ze zouden kunnen spelen als therapeutische biomarkers.

In deze studies hebben wij aangetoond hoe verschillende op EEG-, TMS-EMG- en TMS-EEG-gebaseerde maten kunnen worden gebruikt om de corticale exciteerbaarheid en epileptogeniciteit te kwantificeren bij mensen met epilepsie. Door de verschillende vormen van epilepsie en onderliggende oorzaken is het waarschijnlijk dat verschillende methodes nodig zullen zijn voor verschillende patiënten, waarbij elke patiënt of elk type epilepsie mogelijk een specifieke biomarkers vereist die relevant zijn voor hun specifieke geval.

# List of publications

## Published papers

Gefferie SR, Jiménez-Jiménez D, Visser GH, **Helling RM**, Sander JW, Balestrini S, Thijs RD. Transcranial magnetic stimulation-evoked electroencephalography responses as biomarkers for epilepsy: A review of study design and outcomes. *Human Brain Mapping*. 2023; 44(8): 3446-60.

**Helling RM\***, Perenboom MJL\*, Bauer PR, Carpay JA, Sander JW, Ferrari MD, Visser GH1#, Tolner EA#. TMS-evoked EEG potentials demonstrate altered cortical excitability in migraine with aura. *Brain Topography*. 2023;36(2):269-81.

**Helling RM**, Shmuely S, Bauer PR, Tolner EA, Visser GH, Thijs RD. Tracking cortical excitability dynamics with transcranial magnetic stimulation in focal epilepsy. *Annals of Clinical and Translational Neurology*. 2022;9(4):540–51.

Shmuely S, Surges R, **Helling RM**, Gunning WB, Brilstra EH, Verhoeven JS, Cross JH, Sisodiya SM, Tan HL, Sander JW, Thijs RD. Cardiac arrhythmias in Dravet syndrome: an observational multicenter study. *Annals of Clinical and Translational Neurology*. 2020;7(4):462-73.

**Helling R**, Visser G, Thijs RD, Tolner E, Jansen N. Transcraniële magnetische stimulatie bij patiënten met epilepsie. *Epilepsie, Periodiek voor professionals*. 2020.

Bauer PR\*, **Helling RM\***, Perenboom MJL, Lopes da Silva FH, Tolner EA, Ferrari MD, Sander JW, Visser GH, Kalitzin SN. Phase clustering in transcranial magnetic stimulation-evoked EEG responses in genetic generalized epilepsy and migraine. *Epilepsy & Behaviour*. 2019;93:102–12.

**Helling RM**, Petkov GH, Kalitzin SN. Expert system for pharmacological epilepsy treatment prognosis and optimal medication dose prescription. In *Proceedings of the 2nd International Conference on Applications of Intelligent Systems*. 2019. 1-6.

Bauer PR, De Goede AA, Stern WM, Pawley AD, Chowdhury FA, **Helling RM**, Bouet R, Kalitzin SN, Visser GH, Sisodiya SM, Rothwell JC, Richardson MP, Van Putten MJAM, Sander JW. Long-interval intracortical inhibition as biomarker for epilepsy: A transcranial magnetic stimulation study. *Brain*. 2018;141(2):409–21.

**Helling RM**, Koppert MMJ, Visser GH, Kalitzin SN. Gap junctions as common cause of high-frequency oscillations and epileptic seizures in a computational cascade of neuronal mass and compartmental modeling. *International Journal of Neural Systems*. 2015;25(6):1550021.

Bauer PR, **Helling R**, Kalitzin S, Visser GH. Transcraniële magnetische stimulatie: diagnostische en therapeutische opties voor epilepsie. *Epilepsie, Periodiek voor professionals*. 2014;12(4):28–31.

### **Submitted papers**

**Helling RM**, van Dijk JP, Bauer PR, Thijs RD, Sander JW, Zwarts M, Visser GH. Cortical excitability before and after long-term perampanel treatment for epilepsy.

\*/# *Authors contributed equally.*

# Dankwoord

Allereerst wil ik mijn oprechte waardering uitspreken voor de personen die bereid waren deel te nemen aan mijn onderzoek. Zonder hun bereidwilligheid en tijd zou dit onderzoek niet mogelijk zijn geweest, en ik ben hen daarvoor enorm dankbaar.

Daarnaast wil ik mijn dank uitspreken aan mijn (co-)promotor(en). Max, uw toewijding aan mijn academische ontwikkeling en het bewaken van de voortgang hebben tot dit eindproduct geleid. Ik ben vereerd dat ik onder uw begeleiding heb mogen werken. Gerhard, onze langdurige gesprekken tijdens onze carpool-sessies gedurende mijn stageperiode, die tot op de dag van vandaag voortduren tijdens onze wandelingen, zullen mij altijd bijblijven. Jouw vermogen om vrij te associëren en je altijd enthousiaste benadering van potentiële nieuwe wetenschappelijke vraagstukken blijven een constante bron van inspiratie. Stiliyan, jouw kritische denkwijze, brede kennis, gecombineerd met jouw vermogen om voor elke context een passende metafoor of oneliner te vinden, heeft me altijd verbaasd doen staan.

Graag wil ik ook mijn dank betuigen aan mijn collega's bij Research gedurende deze jaren. Ley, als het fundament van de afdeling en meesterlijke verhalenverteller, Roland, de bruggenbouwer met een duidelijke visie, Prisca, mijn waardevolle leermeester, Evelien, mijn lotgenoot waarmee ik SEIN heb leren kennen, Sharon, als bron van doorzettingsvermogen en daadkracht, Mark, George en Matteo, mijn partners in crime van Universal Labs, Marije, clinicus in hart en nieren, Anouk, de creatieve denker, Hanneke, de paardenliefhebber en Trusjen, het hart van de afdeling. Daarnaast ook veel dank aan de nieuwe lichter van onderzoekers, Silvano en Arthur, die het werk zullen voortzetten. Jullie gezamenlijke inzet, steun en samenwerking hebben mijn ervaring bij Research buitengewoon waardevol gemaakt, en ik ben dankbaar voor de bijzondere band die we hebben opgebouwd tijdens onze gezamenlijke inspanningen.

Een aantal hoofdstukken in dit proefschrift zijn tot stand gekomen door openhartige samenwerkingen met de migraine-onderzoeksgroep binnen het LUMC en de afdeling KNF binnen het Academisch Centrum voor Epilepsie

Kempenhaeghe. Else, jouw ben ik bijzonder dankbaar voor het neerleggen van een hoge standaard, wat heeft geleid tot publicaties van hoog niveau. Thijs, jouw bijdrage heeft me veel waardevolle en boeiende discussies opgeleverd, zowel binnen als buiten ons eigen vakgebied. Hans, dankzij jouw gemoedelijke uitstraling voelde ik me direct welkom en gewaardeerd. Machiel, ik wil je bedanken voor je inzet en het mogelijk maken van deze samenwerking tussen SEIN en Kempenhaeghe.

Het afronden van dit proefschrift is daarnaast ook mogelijk door de ruimte die ik heb gekregen van mijn collega's bij de afdeling KNF binnen SEIN. Jullie vertrouwen en aansporing om dit tot een goed einde te brengen wordt enorm gewaardeerd.

Familie en vrienden, jullie zijn mijn onuitputtelijke bron van energie en inspiratie. Papa en mama, jullie brengen mij immense vreugde, kracht en rust. Ik heb niks anders dan ontzag voor jullie daadkracht, doortastendheid en onvoorwaardelijke steun.

Lieve Maïke, jouw aanwezigheid is onmisbaar geweest op mijn levensreis. Jouw steun en liefde hebben mijn leven verrijkt op manieren die ik nooit voor mogelijk had gehouden. Dank je wel voor alles wat je voor mij betekent. Samen met onze dochter Sofia vormen we een prachtig gezin waar ik ontzettend trots op ben.

# Biography

Robert Martijn Helling was born on November 23th, 1988 in Amsterdam, The Netherlands. After finishing his pre-university education (VWO) in 2007 at Brokdele in Breukelen, he moved to Enschede to study Applied Mathematics at the University of Twente. After one year, he decided to switch to the bachelor program of Technical Medicine. He obtained his Bachelor's Degree in 2011, after which he continued with the Medical Signal Analysis master track of Technical Medicine. One of his internships led to his master's thesis research at Stichting Epilepsie Instellingen Nederland (SEIN). During this one-year graduation internship, he worked on computational models to investigate the relationship between a specific intracranial EEG abnormality and epileptic seizures. This internship resulted in a peer-reviewed scientific publication, and sparked his interest for further work in the academic world. He obtained his master's degree in Technical Medicine in 2014. In 2014, he assisted and contributed to the transcranial magnetic stimulation measurement setup at the research department of SEIN as a clinical technologist. Starting from 2016, he began his PhD project at SEIN as an external PhD candidate of Utrecht University's Graduate School of Life Sciences, under guidance of prof. dr. ir. M.A. Viergever, dr. G.H. Visser, and dr. S.N. Kalitzin. The findings of this project are presented in this thesis. As of 2021, he is working as a clinical technologist at the clinical neurophysiology department of SEIN.

